# The hepatoprotective effects of *Moringa oleifera* against antiretroviral-induced cytotoxicity in $HepG_2$ cells

by

MBASAKAZI SAKI

Submitted in fulfillment of the requirements for the degree of

Master of Medical Science (Physiology)

in the

Department of Basic Medical Sciences

School of Biomedical Sciences

Faculty of Health Sciences

University of the Free State

Supervisor: Dr Charlette Tiloke

Co-supervisors: Dr Claudia Ntsapi and Dr Helena De Villiers

**Submitted on the 26th of July 2023**

## Declaration

I hereby declare that this work, submitted for the degree of Master of Medical Science (Physiology) at the University of the Free State, is my original work and has not previously been submitted to any other institution of higher learning for degree purposes or otherwise. I further declare that all sources cited or quoted are indicated and acknowledged by means of a comprehensive list of references. Copyright hereby cedes to the University of the Free State.

| | |
|---|---|
| Mbasakazi Saki | 26 – 07 – 2023 |
| ---------- | ---------- |
| Name and Surname | Date |

**Dedication**

***I dedicate this thesis to myself,***

Mbasakazi Saki

***Proud of all your hard work, dedication, and perseverance.***

## Table of Contents

## Acknowledgements

First and above all, praise God, the Almighty, for providing me with this opportunity and granting me the capability to proceed successfully.

**To my supervisor and co-supervisors:**

Dr Charlette Tiloke, Dr Claudia Ntsapi, and Dr Helena De Villiers. Working with you has been a great pleasure. Words cannot begin to describe how grateful I am for all the kindness, guidance, support, and unwavering encouragement throughout this study.

**My "People":**

Matlola Bopape, Songezo Vazi, and Malebogo Moremane, you took the meaning of teamwork to a whole new level. I am blessed to have worked with such a smart, driven group of people.

**My parents:**

Thank you for believing in me and for the sacrifices you made for me to achieve my goals.

I would also like to acknowledge the University of the Free State, the Faculty of Health Sciences, and the Department of Basic Medical Sciences for evaluating this research study and providing valuable and constructive suggestions during the planning and development of this research work. National Research Foundation, University of the Free State Faculty Research Funding, and Avacare bursary that provided financial support for the completion of this degree.

## Publication

Saki, M., De Villiers, H., Ntsapi, C. and Tiloke, C., 2023. The Hepatoprotective Effects of *Moringa oleifera* against Antiretroviral-Induced Cytotoxicity in $HepG_2$ Cells: A Review. *Plants*, *12*(18), p.3235.

## Presentations

Research study title: The hepatoprotective effects of *Moringa oleifera* against antiretroviral-induced cytotoxicity in $HepG_2$ cells presented at the following:

1) The Three Schools of Medicine Research and Postgraduate Evaluation Committee, University of the Free State, Faculty of Health sciences. 29 July 2021.
2) Medical Talks (MedTx) presentation at the University of the Free State, Department of Basic Medical Sciences, Faculty of Health Sciences. 22 July 2022.
3) M.Med.Sc Project presentations at the University of the Free State, Department of Haematology and Molecular Cell Biology, Faculty of Health Sciences. 25 July 2023.
4) Faculty of Health Sciences Research Forum at the University of the Free State. Scheduled for 24 – 25 August 2023.
5) MedTx presentation at the University of the Free State, Department of Basic Medical Sciences, Faculty of Health Sciences. Scheduled for 25 August 2023.

## List of Figures

## List of Tables

## List of Abbreviations

| | |
|---|---|
| AIDS | Acquired immunodeficiency syndrome |
| AP | African potato |
| ARE | Antioxidant response element |
| ART | Antiretroviral therapy |
| ARVs | Antiretrovirals |
| ATMs | African traditional medicines |
| ATP | Adenosine triphosphate |
| AZT | Zidovudine |
| GHT | Butylated toluene |
| BSA | Bovine serum albumin |
| CAT | Catalase |
| CCM | Complete culture medium |
| cDNA | Complementary deoxyribonucleic acid |
| Ctrl | Control |
| Cu/Zn-SOD | Copper-zinc-superoxide dismutase |
| CYP3A4 | Cytochrome P450 3A4 |
| dATP | Deoxyadenosine-5’-triphosphate |
| dCTP | Deoxycytidine triphosphate |

| | |
|---|---|
| DMSO | Dimethyl sulfoxide |
| DNA | Deoxyribonucleic acid |
| DTG | Dolutegravir |
| ELISA | Enzyme-linked immunosorbent assay |
| EMEM | Eagle’s minimum essential medium |
| ER | Endoplasmic reticulum |
| ETC | Electron transport chain |
| Fe-SOD | Iron superoxide dismutase |
| FHS | Faculty of Health Sciences |
| GAPDH | Glyceraldehyde 3-phosphate dehydrogenase |
| GCL | Glutamate cysteine ligase |
| GCLC | Glutamate cysteine ligase catalytic subunit |
| GCLM | Glutamate cysteine ligase modifier subunit |
| GPx-1 | Glutathione peroxide-1 |
| GR | Glutathione reductase |
| GSH | Glutathione |
| GSSG | Glutathione disulphide |
| GST | Glutathione S-transferase |
| $H_2O_2$ | Hydrogen peroxide |

| | |
|---|---|
| $H_3PO_4$ | Phosphoric acid |
| HBV | Hepatitis B virus |
| HC | High control |
| HCl | Hydrochloric acid |
| HIV-1 and HIV-2 | Human immunodeficiency virus 1 and 2 |
| HOCl | Hypochlorous acid |
| HO | Hydroxyl radical |
| $HO_2$ | Hydroperoxyl radical |
| HRP | Horseradish peroxidase |
| HSV | Herpes simplex virus |
| $IC_{50}$ | Half-maximal inhibitory concentration |
| InSTIs | Integrase strand transfer inhibitors |
| Keap1 | Kelch-like ECH-associated protein |
| LPO | Lipid peroxidation |
| M | Mitochondria |
| MDA | Malondialdehyde |
| MHC | Major histocompatibility complex |
| Mn-SOD | Manganese-dependent superoxide dismutase |
| MO | *Moringa oleifera* |

| | |
|---|---|
| mRNA | Messenger ribonucleic acid |
| mtDNA | Mitochondrial deoxyribonucleic acid |
| MTT | 3-(4, 5-Dimethyl-2-thiazolyl)-2, 5-diphenyl-2H-tetrazolium bromide |
| MTX | Methotrexate |
| NADPH | Nicotinamide adenine dinucleotide phosphate |
| N | Nucleus |
| NaOH | Sodium hydroxide |
| NC | Nitrocellulose |
| Nrf2 | Nuclear factor erythroid 2-related factor 2 |
| NNRTIs | Non-nucleoside reverse transcriptase inhibitors |
| NRTIs | Nucleoside reverse transcriptase inhibitors |
| $O_2$ | Oxygen |
| $O_2^-$ | Superoxide |
| OD | Optical density |
| OS | Oxidative stress |
| PBS | Phosphate buffered saline |
| PI’s | Protease inhibitors |
| PLHIV | People living with HIV/AIDS |

| | |
|---|---|
| p-NRF2 | NRF2 (Phospho S40) |
| qPCR | Quantitative polymerase chain reaction |
| pp | Page number. |
| RLU | Relative light units |
| RNS | Reactive nitrogen species |
| RO | Alkoxyl radical |
| $RO_2$ | Peroxyl radical |
| ROS | Reactive oxygen species |
| R-T | Room temperature |
| RT | Reverse transcriptase |
| RT-qPCR | Reverse transcription polymerase chain reaction |
| SA | South Africa |
| SDS-PAGE | Sodium dodecyl sulfate-polyacrylamide gel electrophoresis |
| Sec | Selenocysteine |
| SEM | Standard error of mean |
| SOD | Superoxide dismutase |
| SOD2 | Superoxide dismutase-2 |
| TBA | Thiobarbituric acid |
| TBARS | Thiobarbituric acid reactive substances |

| | |
|---|---|
| TDF | Tenofovir disoproxil fumarate |
| TLD | Tenofovir-Lamivudine-dolutegravir |
| TLE | Tenofovir-Lamivudine-Efavirenz |
| TMB | 3,3′,5,5′-Tetramethylbenzidine |
| TTBS | Tris-tween buffered saline |
| UFS | University of the Free State |
| UGT | Uridine 5'-diphospho-glucuronosyltransferase |
| UNAIDS | Joint United Nations Programme on HIV/AIDS |
| USA | United States of America |
| UTT | Universal Test and Treat |
| XO | Xanthine oxidase |
| 3’-OH | 3’-hydroxy group |
| 3TC | Lamivudine |
| 3TC-TP | Lamivudine triphosphate |
| 4-HNE | 4-Hydroxynonenal |
| γ-GC | γ-glutamylcysteine |

## ABSTRACT

Introduction: The untreated human immunodeficiency virus (HIV), a lentivirus species that attacks immune cells, causes acquired immunodeficiency syndrome (AIDS). HIV/AIDS is managed by Antiretroviral therapy (ART). The ART regimen contains nucleoside reverse transcriptase inhibitors (NRTIs) associated with oxidative stress. Medicinal plants are often combined with ART to diminish the side effects of ART use. The *Moringa oleifera* (MO) tree extracts have been shown to contain bioactive compounds with antioxidant effects.

Aim: This *in vitro* study evaluated the cytotoxicity of an NRTI (tenofovir) and its potential amelioration by MO leaf extract.

Methods: $HepG_2$ cells were exposed to tenofovir, MO, and combination (tenofovir and MO) treatment groups for 24 and 120 hours. MO aqueous leaf extract was prepared, and cytotoxicity was assessed. Markers for oxidative stress and antioxidant response were assessed using spectrophotometry, luminometry, ELISA, qPCR, and western blotting experimental techniques.

Results: At 24 hours, tenofovir decreased MDA, *NRF2*, *SOD2*, *CAT* mRNA, and NRF2, SOD2, and CAT protein expression. It then increased GSH, *GCLC* mRNA and p-NRF2 protein expression. MO decreased GSH levels, *NRF2*, *GCLC*, and *SOD2* mRNA expression and increased *CAT* mRNA, as well as NRF2, p-NRF2, SOD2, and CAT protein expression. At 120 hours, tenofovir increased MDA, *NRF2* mRNA, NRF2, p-NRF2, and SOD2 protein

expression. It then decreased GSH levels, *GCLC*, *SOD2*, *CAT* mRNA and CAT protein expression. MO decreased MDA and GSH levels, NRF2 and CAT protein expression. It then increased *NRF2*, *GCLC*, *SOD2*, *CAT* mRNA, p-NRF2, and SOD2 protein expression. The combination treatment group downregulated MDA and upregulated the expression of *NRF2*, *GCLC*, *SOD2*, *CAT* mRNA and NRF2, p-NRF2, SOD2, and CAT proteins.

Conclusion: Adding MO to tenofovir downregulates reactive oxygen species by upregulating the NRF2-antioxidant pathway to reduce oxidative stress. Therefore, MO has the potential to ameliorate toxicity induced by tenofovir.

**Keywords:** HIV/AIDS, tenofovir, reactive oxygen species, antioxidants, *Moringa oleifera*, human $HepG_2$ liver cells

## Arrangement of the thesis

Chapter 1: This chapter included the introduction, problem statement, study rationale, aim and objectives of the research study, as well as an overview of the methodology. The purpose of this chapter was to provide a brief overview of the research topic, a background of the problem that the research study aims to investigate and highlight the importance of this research study.

Chapter 2: This chapter consists of the literature review. The literature review aims to discuss current information, place this research study within the context of existing literature, and provide strong motivation for why further research is needed.

Chapter 3 consists of the study materials, procedures, and equipment used to conduct this research.

Chapter 4: This chapter consists of the experimental results. This chapter aims to report the findings generated from this research study by presenting the results/findings using figures and tables.

Chapter 5: This chapter consists of a discussion of the results. The purpose of this chapter is to interpret and describe the significance of the results/findings in relation to existing literature. It elaborates on any new understanding that may have emerged from conducting the research study.

Chapter 6: This chapter includes the study conclusion, limitations, and future recommendations. The purpose of this chapter is to present the conclusion drawn from the results, the potential study limitations, as well as future study recommendations for similar research studies that might be conducted in the future.

# Chapter 1

## 1.1. Introduction

Acquired Immune Deficiency Syndrome (AIDS), caused by Human Immunodeficiency Virus (HIV), is a highly communicable disease that continues to impose a significant burden on national healthcare systems across the world but specifically in sub-Saharan Africa (Pillaye et al., 2020). Globally, more than 30 million HIV-positive people have lost their lives following the identification of the first HIV-positive patient (Eilami et al., 2019). However, since the availability of antiretroviral therapy (ART) in the mid-1990s, the number of HIV/AIDS-related deaths has steadily declined (Spach, 2020).

In South Africa (SA), the accepted standard of care in HIV treatment includes using a combination of three active drugs: Tenofovir-Lamivudine-Dolutegravir (TLD) (Waters et al., 2021). The TLD treatment provides rapid viral suppression and a high genetic barrier to drug resistance (Dumitrescu et al., 2020). Consequently, the use of TLD treatment has shifted HIV infection from a terminal illness to a long-term, manageable chronic infection, with PLHIV having a life expectancy similar to that of HIV-negative individuals (Umar et al., 2020). Unfortunately, some patients receiving ART may develop severe side effects such as drug-induced liver injury (Pillaye et al., 2020). Due to the side effects associated with ART, PLHIV, especially in the rural areas of SA, tend to use traditional remedies such as medicinal trees/plants to ameliorate the side effects associated with ART (Biswas et al., 2019).

*Moringa oleifera* (MO), one such example of a medicinal plant, has been used for centuries in traditional medicine (Salami et al., 2021). The MO tree is widely used due to its high

concentration of phytochemicals which work synergistically to induce their medicinal effects (Salami et al., 2021). Scientifically, MO proved to have anti-inflammatory, antihypertensive, antimicrobial, antioxidant, anti-diabetic, and antiviral effects (Stohs and Hartman, 2015). In addition, MO has been shown to improve renal and hepatic functions (Ren et al., 2018). Various parts of the MO tree (i.e., flowers, seeds, roots, and leaves) contain various bioactive compounds, including flavonoids and phenolic acids (Vergara-Jimenez et al., 2017). However, the leaves contain the most considerable amounts of bioactive compounds and therefore have a wide range of medicinal properties (Vergara-Jimenez et al., 2017; Nizioł-ŁUkaszewska et al., 2020). Even though there is evidence to support the health benefits associated with MO treatment, little is known about using the MO leaf extracts amongst HIV/AIDS patients receiving ART in SA and its effect on patient compliance and outcomes. Thus, this research study explored the potential hepatoprotective effect of MO leaf extract following the exposure of human $HepG_2$ liver cells to ART (tenofovir) *in vitro*.

### 1.2. Problem statement

HIV-related morbidity and mortality rates have been considerably reduced since the introduction of ART in the late 1990s (Mocroft and Lundgren, 2004). Although ART regimens have significant antiretroviral activity, viral suppression is often limited due to a variety of factors, including drug toxicity, which can compromise the adherence that is required to maintain the efficacy of ART (Nadkar and Bajpai, 2009; Carr and Cooper, 2010). Mitochondrial toxicity is one of the side effects of ART use, resulting in ART-induced oxidative stress. Uncontrolled oxidative stress can be responsible for the induction of several diseases, both chronic and degenerative (Pizzino et al., 2017). Addressing this shortcoming could lead to the discovery of less toxic remedies that may help to ameliorate the ART-related

toxicological effects. Medicinal plants have great potential to produce new remedies and are currently used in traditional medicine to treat chronic and infectious diseases (Street and Prinsloo, 2013). These medicinal plants contain a variety of phytochemicals (secondary metabolites) that may act individually or synergistically in treating illnesses such as rheumatism and type 2 diabetes mellitus (Tanga et al., 2018; Street and Prinsloo, 2013). The MO plant is one such example used to treat various ailments such as headaches, skin wounds, insect bites, bacterial or fungal infections, gastric ulceration, diarrhoea, joint pain, and liver injury (Reinert, 2013). The MO leaves have several biological activities, including antioxidant, anti-inflammatory, anticancer, anti-atherosclerotic effects, including the improvement of the immune system (Salami et al., 2021). These activities can be attributed to proteins, β-carotene, vitamins A, B, C, and E, steroids, minerals, alkaloids, quercetin, and kaempferol found in the MO leaves (Salami et al., 2021). Various parts of the MO tree have been reported to have a variety of biological activities. However, no in vitro studies have assessed the hepatoprotective effects of MO aqueous leaf extract against tenofovir-induced oxidative stress in human $HepG_2$ liver cells.

### 1.3. Research Rationale

Various clinical disorders such as lipodystrophy, pancreatitis, myopathy, hepatic steatosis, and lactic acidosis have been found in HIV-positive patients on ART, containing nucleoside reverse transcriptase inhibitors (NRTIs) (Chhatwani et al., 2016). These side effects, which generally occur due to prolonged treatment, are associated with mitochondrial toxicity, as evidenced in several *in vitro* and *in vivo* studies with different NRTIs (Venhoff et al., 2007; Nagiah et al., 2015; Mallon et al., 2005; Kohler et al., 2009). Therefore, it is important to assess drugs from the NRTI class for their ability to cause mitochondrial toxicity and oxidative stress. Tenofovir

is used in the first-line treatment of HIV in combination with lamivudine and dolutegravir (Mendelsohn and Ritchwood, 2020). It is associated with severe lactic acidosis and hepatic steatosis (Wassner et al., 2020). Nagiah and colleagues conducted a study in 2015. They found that tenofovir induces oxidative stress in human $HepG_2$ liver cells, compared to other regimens (Nagiah et al., 2015). Due to the side effects attributed to tenofovir, research studies are continuously conducted to understand this cytotoxic mechanism. Therefore, this research study aimed to broaden the understanding of the *in vitro* cytotoxicity of tenofovir by investigating its effects on human $HepG_2$ liver cells. The MO tree is one of many medicinal plants/trees that have been shown to contain bioactive compounds with anti-inflammatory and antioxidant effects (Stohs and Hartman, 2015; Salami et al., 2021). Subsequently, the flavonoids and phenolic acids found in the MO tree have a significant protective role against oxidative stress conditions. Therefore, MO aqueous leaf extract was evaluated for its potential hepatoprotective effect following exposure to tenofovir in human $HepG_2$ liver cells.

### 1.4. Aim of the study

The study aimed to investigate the effect of MO aqueous leaf extract on oxidative stress and antioxidant responses in human $HepG_2$ liver cells *in vitro*, following acute and chronic exposure to the antiretroviral drug (tenofovir).

## 1.5. Research study questions

The following overarching research questions guided this study:

1.5.1. Will acute and chronic exposure to tenofovir in human $HepG_2$ liver cells result in oxidative stress?

1.5.2. After 24-hour exposure to tenofovir, does MO have a hepatoprotective effect in human $HepG_2$ liver cells?

1.5.3. After 120-hour exposure to tenofovir, does MO have a hepatoprotective effect in human $HepG_2$ liver cells?

## 1.6. Objectives of the study

The above-stated aim was achieved by pursuing the following objectives:

- Assessment of cell viability following exposure to MO using the MTT assay.
- Assessment of reactive oxygen species (lipid peroxidation) using the TBARS assay.
- Measurement of glutathione levels using the Glutathione-Glo™ assay.
- Assessment of SOD2 activity using the Human SOD2 ELISA Kit.
- Assessment of catalase activity using the Human Catalase activity ELISA Kit.
- Using western blot analysis, evaluate the protein expression of NRF2, p-NRF2, SOD2, and catalase.
- Analysis of mRNA expression (*NRF2*, *SOD2*, *GCLC*, and *catalase*) using qPCR.

## 1.7. Methodology

The methodology chapter consists of all the procedures and laboratory techniques used to pursue the research study objectives, providing a clear explanation of the execution and analysis of the results. The study was conducted by the researcher, under the supervision of the study supervisors, using the laboratory equipment and resources available in the Department of Basic Medical Sciences, the Department of Human Molecular Biology, the Department of Haematology and Cell Biology, and the Department of Chemical Pathology at the University of the Free State. COVID-19 regulations were adhered to during laboratory procedures. These included wearing protective masks, maintaining a social distance, and routinely using sanitising stations.

## 1.8. Significance of the study

The study will be of scientific, clinical, and public value. It will contribute to the scientific knowledge pool by determining the extent to which MO may be used for medicinal purposes and its potential to reduce tenofovir-induced oxidative stress. People living with HIV often use MO with antiretrovirals to reduce the side effects. However, the use of MO and antiretrovirals is not well researched. Therefore, this research study evaluated the potential effect of MO to reduce antiretroviral-related side effects. Clinically, this study may aid in the future prevention of chronic diseases associated with oxidative stress and improve the overall health and well-being of patients. The findings from this research study will also be disseminated to benefit society and provide insight into how the bioactive compounds found in MO aqueous leaf extract may protect against tenofovir-induced oxidative stress.

# Chapter 2

## 2. Literature review

Since the introduction of ART for HIV-1, there has been a significant decline in HIV/AIDS-related mortality and morbidity (Ikekpeazu et al., 2019). Despite the positive effects of ART on improving the overall health of HIV/AIDS patients, it has also been associated with the onset of oxidative stress linked to mitochondrial toxicity (Akay et al., 2014; Ikekpeazu et al., 2019). As a result, researchers continue to investigate the medicinal use of natural remedies that may aid in reducing the side effects linked to ART use. Therefore, this chapter will describe the proposed mechanism underlying ART's ability to induce oxidative stress. Moreover, this chapter elaborates on the potential effect of medicinal trees/plants in reducing oxidative stress.

### 2.1. Prevalence of HIV/AIDS

AIDS was first discovered in patients in the United States of America (USA) in 1981 (Sharp and Hahn, 2010). It is caused by the human immunodeficiency virus 1 (HIV-1) and 2 (HIV-2) (Heeney et al., 2006). AIDS originated from two species of lentivirus (Van Heuverswyn and Peeters, 2007), which entered the human population through cross-species transmission in the early 20$^{th}$ century (De Cock et al., 2012). These viruses are spread by one of three modes of transmission: sexual, parenteral, and mother-to-child (Delpech and Gahagan, 2009).

Globally, the vast majority (~98%) of HIV infections are caused by HIV-1 (Sharp and Hahn, 2010), a variant of HIV that primarily attacks the immune system's CD4+ T cells (Ncube et al., 2018). The CD4+ T cells are thymus lymphocytes that recognise antigenic peptides in the form of MHC class II molecules (Nair et al., 2011). These cells help B cells produce antibodies

and are required to generate cytotoxic and memory CD8+ T cells that destroy infected cells (Swain et al., 2012). However, when infected by HIV, CD4+ T cells replicate the virus (Aavani and Allen, 2019). HIV thus hijacks and manipulates the transcriptional and translational machinery of CD4+ T cells to replicate itself (Kirchhoff, 2016).

Worldwide, the number of HIV-1-infected people continues to increase. There are approximately 40 million HIV-positive people in the world, with developing countries accounting for 95% of those infected (Eilami et al., 2019). Globally, SA has the largest number of HIV-1 infections (Pillay and Johnson, 2021). Since the estimated 5.3 million PLHIV reported in 2004 (Heyer and Ogunbanjo, 2006), there has been an increase in the number of HIV-1 infections in SA. There are approximately 7.5 million PLHIV, an estimated 200,000 new HIV-1 infections, and 74,000 HIV/AIDS-related mortalities reported in 2019 (Pillay and Johnson, 2021). The prevalence of HIV is approximately 19.5% among the South African adult population (Orton et al., 2021). Poverty, a lack of education about the virus and its modes of transmission, a high incidence of rape, non-disclosure of HIV-positive status to partners, and mother-to-child HIV transmission are overarching factors associated with the increasing number of HIV-1 infections in SA (Ramlagan et al., 2018; Mabaso et al., 2019).

In 2004, SA started the national rollout of ART to treat HIV-1 infections (Heyer and Ogunbanjo, 2006). Since 2005, deaths related to HIV/AIDS have decreased from 50.8% to 31.1% in 2016 (Loeliger et al., 2016). This decrease can primarily be attributed to the government's rapid scale-up of public-sector HIV resources to make ART extensively accessible (Loeliger et al., 2016). As of 2016 (see Figure 2.1), SA reportedly has the largest ART programme, with approximately 3.9 million individuals receiving antiretrovirals (ARVs) (Ncube et al., 2018). This value is four times the number of all other ART programmes globally, equating to 24% of all ART programmes worldwide (Ncube et al., 2018).

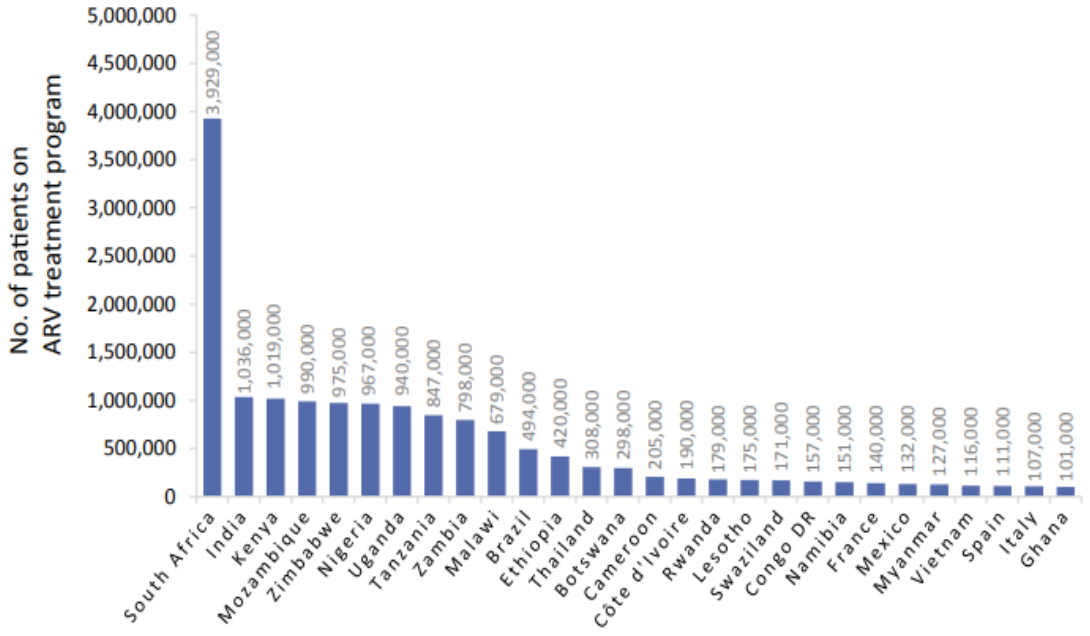


**Figure 2.1: Countries with the largest antiretroviral treatment programmes** (Ncube et al., 2018)

The programme's success is expected to increase as plans and policies initiated in 2004 have improved HIV patient outcomes and survival rates throughout the country (Loeliger et al., 2016). The plans and policies include providing ART free of charge and using community-based programmes expanding on HIV care and treatment services (Loeliger et al., 2016). At

first, only those with CD4+ T cell counts of 200 cells $\mu L^{-1}$ or less were approved for treatment (Bessong et al., 2021). A low CD4+ T cell count indicates that the immune system has been compromised by HIV and/or the disease is progressing (Torti et al., 2012). However, in 2016, SA implemented the Universal Test and Treat (UTT) programme, where all individuals who tested positive were allowed to receive treatment regardless of their CD4+ T cell count (Bessong et al., 2021).

The initiation of the UTT programme led to the Joint United Nations Programme on HIV/AIDS (UNAIDS) 90-90-90 mantra, which was adopted in 2016. In simple terms, it means that 90% of the populace should be aware of their HIV status, 90% of those who are aware of their HIV status should be on therapy, and 90% of those receiving therapy should achieve suppressed viral loads (Levi et al., 2016). According to the UNAIDS 2020 report, 92% of people in SA are aware of their HIV status, 75% receive therapy, and 92% are virally suppressed (see Figure 2.2) (Avert, 2020).


**Figure 2.2: The progress towards the 90-90-90 targets** (Avert, 2020)

In order to manage the HIV epidemic, it is critical to achieve optimum virologic suppression across key population groups (Moses et al., 2020). ART is the only proven management strategy for HIV-1 infection that has improved the quality of life in PLHIV (Sibanda et al., 2016).

## 2.2. Antiretroviral therapy

There are five ART drug categories approved by the USA Food and Drug Administration (FDA) (Spach, 2020). These ART drugs include NRTIs, non-nucleoside reverse transcriptase inhibitors (NNTRIs), integrase strand transfer inhibitors (InSTIs), protease inhibitors (PIs), and entry inhibitors (Spach, 2020). Each class targets a specific phase of the HIV-1 replication cycle (see Figure 2.3) (Ncube et al., 2018).

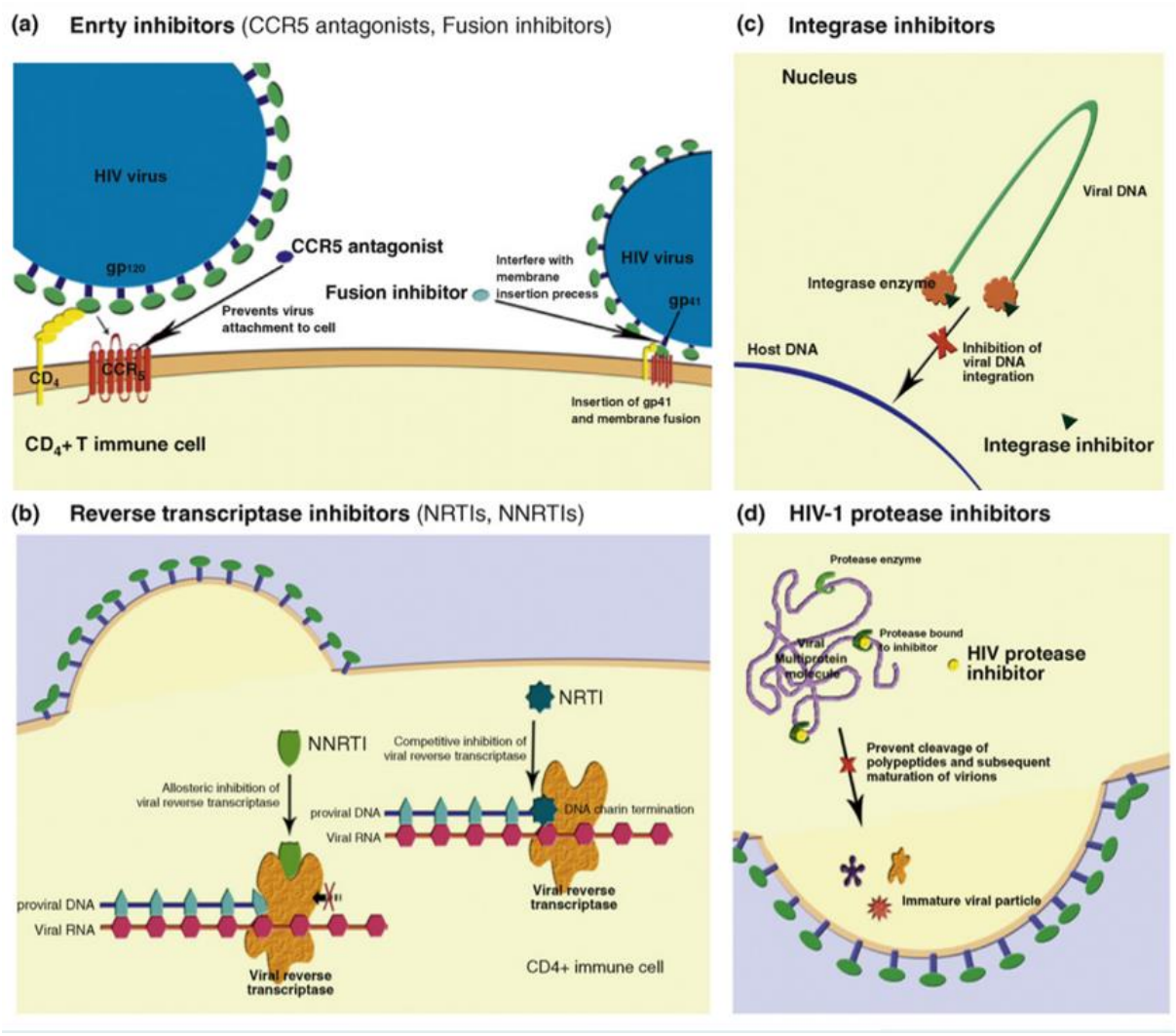


**Figure 2.3: Mechanism of action of antiretroviral therapy drugs: (a)** Entry inhibitors **(b)** Reverse transcriptase inhibitors (NRTIs, NNRTIs); **(c)** Integrase inhibitors; **(d)** HIV-1 protease inhibitors (Kis et al., 2010)

Two classes of HIV cell entry inhibitors act at different sites: i) CCR5-antagonists prevent virus attachment to the membrane receptors; and ii) fusion inhibitors interfere with membrane insertion processes (Kis et al., 2010). The NRTIs halt the elongation of the proviral deoxyribonucleic acid (DNA) strand by blocking the HIV-1 reverse transcriptase (RT) enzyme responsible for converting viral ribonucleic acid (RNA) into viral DNA (Max and Sherer, 2000; Ha et al., 2021). The NNRTIs inhibit DNA polymerase activity by inducing a conformational

change, disrupting the enzyme's catalytic site (Temesgen et al., 2006). The HIV integrase enzyme, which is responsible for integrating viral DNA into the host cell's DNA, is inhibited by InSTIs (Kis et al., 2010). The PIs inhibit HIV-1 protease, which cleaves newly synthesized polyproteins (Gag and Gag-Pol) into a mature infectious virus (Eggleton and Nagalli, 2020; Weber et al., 2021).

### 2.3. The approved standard treatment for HIV

The approved standard treatment for HIV-1 consists of a combination of three drugs from at least two different categories (Waters et al., 2021). One of the first NRTIs accepted to treat HIV-1 infection was zidovudine (AZT). Following its acceptance, several other NRTIs, such as tenofovir, were produced and used with NNRTIs or PIs (Gabazana and Sitole, 2021). Until 2018, the first-line regimen for HIV-1 treatment in many countries was the combination of Tenofovir-Lamivudine-Efavirenz (TLE); that is, two NRTIs (Tenofovir-Lamivudine) and one NNRTI (Efavirenz) (Kouanfack et al., 2019). However, TLE has a low genetic barrier to drug resistance and causes neuropsychiatric side effects (Raffi et al., 2014). Subsequently, in 2019, the South African National Department of Health changed the prescribed standard initial treatment from TLE to Tenofovir–Lamivudine–Dolutegravir (InSTI) (TLD), a fixed-dose combination (Mendelsohn and Ritchwood, 2020). The backbone for HIV-1 treatment, TLD, targets a specific phase of the HIV-1 replication cycle, aggressively suppresses viral replication, and halts the progression of HIV-1 infection (Desta et al., 2020). The TLD treatment is more tolerable and has a high genetic barrier to drug resistance (Umar et al., 2020).

## 2.4. The types of antiretroviral drugs

### 2.4.1. Tenofovir

Tenofovir is a nucleotide analogue of adenosine 5'-monophosphate (Anderson et al., 2011). It is a highly hydrophilic compound with two negative charges resulting in low intestinal membrane permeability (Geboers et al., 2015). In order to improve oral bioavailability and membrane permeability, tenofovir is commercially available as a pro-drug, tenofovir disoproxil fumarate (TDF) (Wassner et al., 2020). Following oral administration, TDF is rapidly converted to tenofovir in the intestinal walls through esterase hydrolysis (Cressey et al., 2020). Tenofovir then enters cells through organic anion transporters 1 and 3 (James et al., 2012).

Intracellularly, tenofovir is phosphorylated by adenylate kinases and subsequently phosphorylated by nucleoside diphosphate kinases into its active form, tenofovir diphosphate (Kearney et al., 2004). Tenofovir diphosphate is an analogue of deoxyadenosine-5'-triphosphate (dATP), a regular substrate for DNA polymerase. Tenofovir diphosphate terminates the viral DNA chain elongation by competing with dATP to be incorporated into viral DNA (Fernandez-Fernandez et al., 2011). The kidneys excrete Tenofovir through glomerular filtration and tubular secretion (James et al., 2012). Organic anion transporters in the basolateral membrane actively transport about 20-30% of tenofovir into renal proximal tubule cells. Subsequently, tenofovir is secreted into the tubular lumen by the apical membrane transporters, multidrug resistance proteins, MRP-4 and MRP-2 (encoded by *ABCC4* and *ABCC2* genes, respectively) (Fernandez-Fernandez et al., 2011).

### 2.4.2. Lamivudine

Lamivudine (3TC) forms part of the NRTIs; it inhibits viral DNA synthesis via RT DNA chain termination post phosphorylation (Max and Sherer, 2000). 3TC is highly soluble and rapidly absorbed, with bioavailability ranging from 82-86% for oral administration (Dumitrescu et al., 2020). Intracellularly, 3TC is metabolised to its active triphosphate form, lamivudine triphosphate (3TC-TP), through kinase phosphorylation (Taylor et al., 2020).

The 3TC-TP competes with the corresponding endogenous nucleoside triphosphate, deoxycytidine triphosphate (dCTP), for binding to the viral RT. Once incorporated into the viral DNA, chain termination results due to the absence of a 3'-hydroxy (3'-OH) group to enable the 3'-5'-phosphodiester linkages essential for DNA elongation (Else et al., 2012). The majority of 3TC is eliminated by filtration and active renal tubular secretion. Metabolism is a minor route of elimination, with only 10% of the parent drug metabolised to an inactive trans-sulfoxide metabolite that is excreted in the urine (Dumitrescu et al., 2020).

### 2.4.3. Dolutegravir

Dolutegravir (DTG), an orally bio-available integrase strand transfer inhibitor, is an efficacious, well-tolerated drug with a high barrier to drug resistance (Mohan et al., 2021). Upon oral administration, DTG binds and inhibits the active site of integrase. This HIV enzyme catalyses the integration of viral DNA into chromosomal DNA, leading to viral replication (Kandel and Walmsley, 2015). DTG is metabolised in the liver by uridine 5'-diphospho-glucuronosyltransferase (UGT) 1A1 and cytochrome P450 (CYP) 3A4 (Castellino et al., 2013).

## 2.5. Antiretroviral drugs' side effects

The most common side effects of ART TLD-based regimens include nausea, diarrhoea, hypoglycaemia, insomnia, and headaches (Kaeni, 2020). Appetite loss, vomiting, diarrhoea, and abdominal pain caused by ART use can result in malnutrition (Gambo et al., 2021). HIV and malnutrition can be detrimental to the immune system, decreasing the number of CD4+ and CD8+ T cells. A compromised immune system will subsequently increase the body's susceptibility to opportunistic infections, including pneumocystis pneumonia, cryptococcal meningitis, and mycobacterium tuberculosis (Gambo et al., 2021; Vaillant and Naik, 2021). Opportunistic infections and malnutrition can worsen disease progression and increase HIV-related mortality (Gambo et al., 2021).

Reports from preclinical and clinical-based studies have also linked ART with hepatotoxicity associated with oxidative stress (Elias et al., 2013). Hepatotoxicity is defined as a liver injury or impairment of liver function caused by exposure to xenobiotics such as drugs, alcohol, peroxidized fatty acids, environmental toxicants, and even some medicinal plants (Paniagua and Amariles, 2018). Hepatotoxicity may include hepatitis, granuloma, lactic acidosis, cholestasis, and hepatic steatosis (Sharma, 2014). The TDF regimen has been associated with severe lactic acidosis and hepatic steatosis (Wassner et al., 2020). The mechanism proposed behind TDF causing the latter complications is the inhibition of mitochondrial DNA (mtDNA) polymerase gamma (γ) (Chhatwani et al., 2016). Mitochondrial toxicity can therefore manifest as nephrotoxicity, myopathy, pancreatitis, or peripheral neuropathy, in addition to lactic acidosis, and hepatic steatosis (Chhatwani et al., 2016). Figure 2.4 illustrates the mechanism of ART-induced cytotoxicity in liver cells.

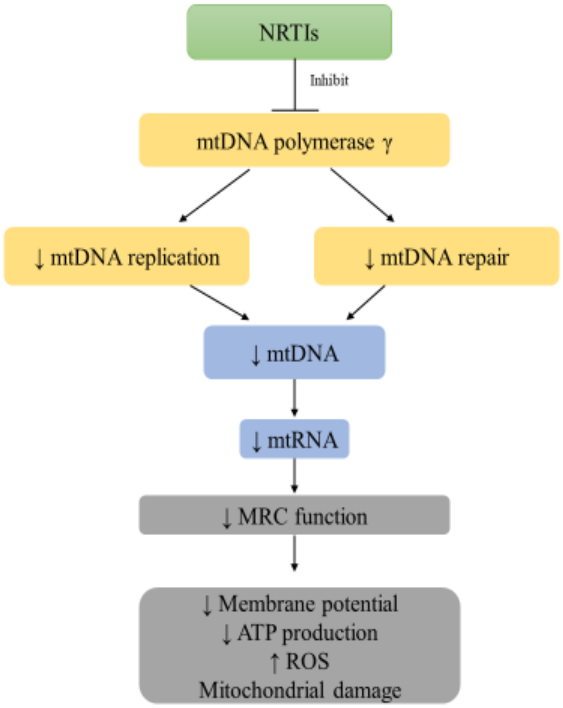


**Figure 2.4: Mechanism of ARV-drug-induced hepatotoxicity**

ATP: Adenosine triphosphate; MRC: Mitochondrial respiratory chain; ROS: Reactive oxygen species (Created by the researcher, M. Saki, in 2023 (Smith et al., 2013)).

Figure 2.4 demonstrates that ARVs such as NRTIs inhibit DNA polymerase γ, leading to decreased mtDNA, loss of mitochondrial membrane potential, and oxidative phosphorylation, precipitating as oxidative stress (Akay et al., 2014). Since NRTIs lack a 3'-OH group on their pentose rings, incorporating the nucleoside analogue prevents the subsequent phosphodiester bond formation and terminates mtDNA chain elongation (Warnke et al., 2007). As a result, mtDNA copy numbers decrease, and mitochondrial-encoded genes, which are essential components of the mitochondrial respiratory chain (MRC) function. This leads to a disrupted electron transport chain and a concomitant reduction in membrane potential and ATP production by the mitochondrion. This destruction in mitochondrial function can result in

increased ROS production and changes in mitochondrial morphology (Smith eta., 2013; Kline et al., 2009).

## 2.6. Oxidative stress

Oxidative stress is an imbalance between the excessive generation of free radicals or reactive oxygen species (ROS) and their eradication by the antioxidant defence system (Ďuračková, 2010). Free radicals are atoms that contain an unpaired electron in their outer orbital (Andrade et al., 2005). Free radicals are unstable and extremely reactive; however, they gain stability by attracting electrons from other compounds. The compound loses an electron and becomes a free radical, triggering a chain reaction cascade, ultimately damaging the living cell (Phaniendra et al., 2015). The term "reactive oxygen species" refers to any oxygen-containing molecule (radical or non-radical) capable of causing harmful reactions. These include superoxide anion ($O_2^-$), hydrogen peroxide ($H_2O_2$), hydroxyl radical (HO•), alkoxyl radical (RO), peroxyl radical ($RO_2$), hydroperoxyl radical ($HO_2$), hypochlorous acid (HOCl), and singlet oxygen ($O_2$) (Lambert and Brand, 2009).

During the oxidative stress reaction (illustrated below), the formation of superoxide results from the one-electron reduction of $O_2$, disproportionation of two superoxide molecules yields $H_2O_2$ and $O_2$, and the oxidation of ferric iron by $H_2O_2$ yields HO• and the hydroxide anion (Lambert and Brand, 2009):

$$O_2 + e^- \rightarrow O_2^- \qquad \text{(Superoxide)}$$

$$2O_2^- + 2H+ \rightarrow O_2 + H_2O_2 \qquad \text{(Hydrogen peroxide)}$$

$$Fe^2 + H_2O_2 \rightarrow Fe^3 + HO\bullet + OH^- \qquad \text{(Hydroxyl radical)}$$

As illustrated in Figure 2.5, free radicals/ROS are formed due to adenosine triphosphate (ATP) production by the mitochondria when cells utilise oxygen to produce energy (Pham-Huy et al., 2008).

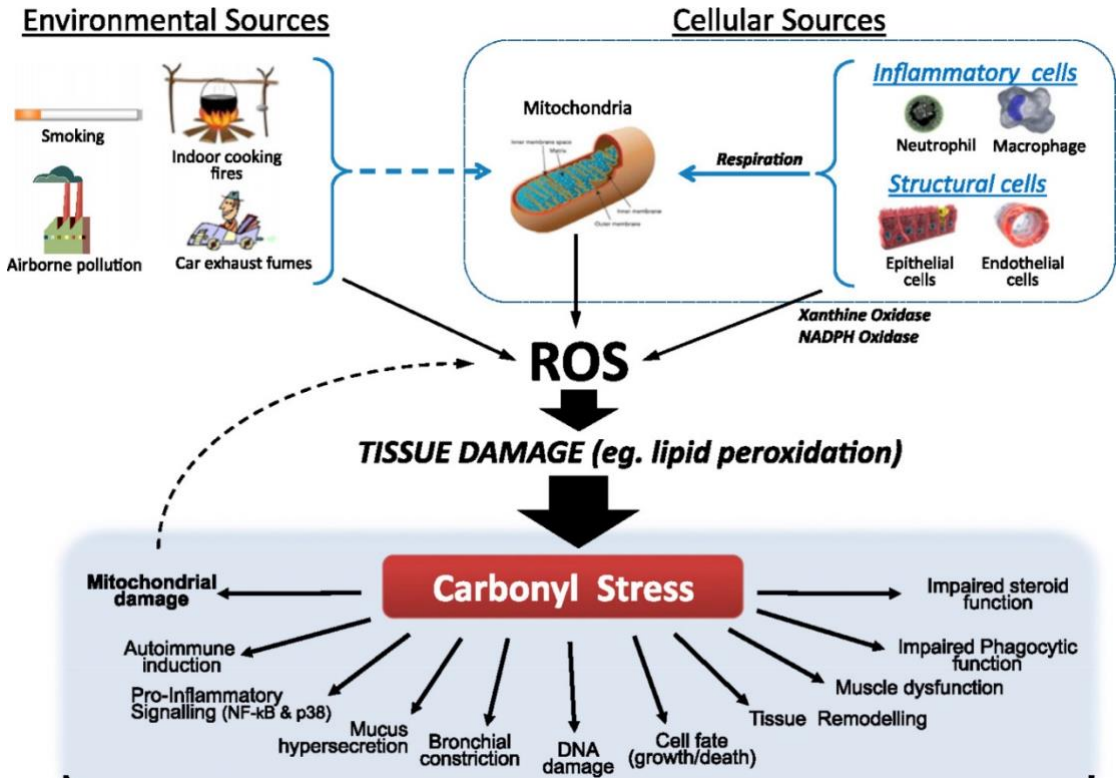


**Figure 2.5: Oxidative stress** (Kirkham and Barnes, 2013)

In addition to mitochondria, ROS are produced by various enzymes such as nicotinamide adenine dinucleotide phosphate (NADPH) oxidases and xanthine oxidase (XO) (Andrés Juan et al., 2021). The sum of ROS produced by metabolic processes can be induced by environmental stimuli in the form of various stresses, including pollution, tobacco smoke, alcohol, transition metals, heavy metals, pesticides, industrial solvents, drugs such as ARVs, paracetamol, halothane, and radiation among others (Gupta, 2010).

ROS does not only include $O_2^-$, $H_2O_2$, and HO• but also a group of nitrogen-containing molecules called reactive nitrogen species (RNS) (Doshi et al., 2012). Nitroxyl anion, nitrosonium cation, higher oxides of nitrogen, S-nitrosothiols, and dinitrosyl iron complexes are all examples of RNS (Martínez and Andriantsitohaina, 2009). Another prominent effect of ROS is lipid peroxidation, which occurs when membrane phospholipids are brought into contact with a ROS oxidising agent (Andrés Juan et al., 2021). Lipid peroxidation is a process in which free radical species remove electrons from lipids, and subsequently, the lipids become reactive free radicals which can propagate lipid peroxidation chain reactions (Su et al., 2019). Lipid peroxidation forms several oxidation products, including lipid hydroperoxides (LOOH) and aldehydes such as malondialdehyde (MDA) and 4-hydroxynonenal (4-HNE) (Mas-Bargues et al., 2021).

Among the aldehydes produced by lipid peroxidation, MDA has gained the most attention, given that MDA is produced at high levels during lipid peroxidation and is commonly used as a measure of oxidative stress (Barrera et al., 2018). MDA is widely used as a biomarker for lipid peroxidation because of its ready reaction with thiobarbituric acid (Ayala et al., 2014). Uncontrolled production of free radicals/ROS occurs when antioxidants (e.g., glutathione, superoxide dismutase, catalase, and vitamins) are saturated due to factors such as ageing, stress, physical damage, or pathological disease (Alkadi, 2018).

### 2.7. Antioxidants

Antioxidants are compounds that scavenge free radicals/ROS and intracellularly retain a more reduced redox state (Henriksen, 2019). The antioxidant defence system comprises endogenous and exogenous antioxidants (Kuciel-Lewandowska et al., 2018). Endogenous antioxidants

produced by the body are divided into enzymatic and non-enzymatic antioxidants (Matough et al., 2012). Enzymatic antioxidants include superoxide dismutases (SODs), catalases (CAT), and glutathione peroxidases (GPx). Non-enzymatic antioxidants include polyamides, linolenic acid, bilirubin, albumin, uric acid, glutathione, transferrin, ceruloplasmin, and coenzyme Q10 (Kuciel-Lewandowska et al., 2018). Exogenous antioxidants are vitamin A, vitamin C, vitamin E, selenium (Se), carotenoids, and polyphenols (Bouayed and Bohn, 2010).

Antioxidants can directly decrease oxidative damage by accepting or donating an electron to eliminate the unpaired condition of the radical (Lü et al., 2010). Antioxidants can also indirectly decrease free radicals by inhibiting the activity or expression of free radical-generating enzymes. Examples of free radical-generating enzymes are NADPH oxidase and XO (Lü et al., 2010). Another function associated with antioxidants is increasing the activity or expression of intracellular enzymatic antioxidants such as SOD, CAT, and GPx (Lü et al., 2010). SOD, CAT, and GPx are the first-line antioxidant enzymes that suppress or prevent the formation of free radicals/ROS. These enzymes are known to neutralise any molecule with the potential of developing into a free radical or any free radical with the potential to induce the production of other radicals (Ighodaro and Akinloye, 2018). The expression of SOD, CAT, and GPx is regulated by the non-coding DNA sequence antioxidant response element (ARE). ARE is activated by the nuclear factor erythroid 2-related factor 2 (Nrf2) (de Vries et al., 2008).

### 2.7.1. Superoxide dismutase

Superoxide dismutases (SODs) are a group of metalloenzymes that decrease $O_2^-$ levels by catalysing the dismutation of the $O_2^-$ free radical into molecular oxygen and $H_2O_2$ (see Figure 2.6) (Younus, 2018). They require a metal cofactor for their antioxidant activity. In this regard, SODs are classified into three forms, including iron SOD (Fe-SOD), manganese-dependent SOD (Mn-SOD) and copper-zinc-SOD (Cu/Zn-SOD) (Ighodaro and Akinloye, 2018). Superoxide dismutase 2 (SOD2) is a Mn-SOD. It is encoded by the SOD2 gene mapping to chromosome 6, which is present in prokaryotes and mitochondria of eukaryotes (Ighodaro and Akinloye, 2018). The SOD2 is a key component of the antioxidant defence system against mitochondrial superoxide radicals (Pourvali et al., 2016).

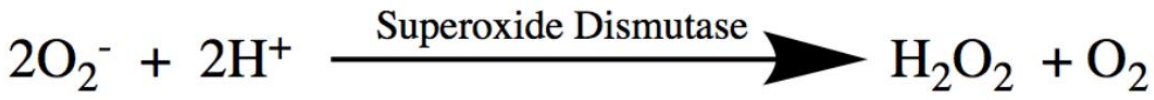


**Figure 2.6: Superoxide Dismutase enzyme reaction** (Saif, 2004)

### 2.7.2. Catalase

Catalase (CAT) is a homotetramer in which each monomer (62.5 kDa) contains a haem B (also known as protoheme IX) group responsible for the enzymatic activity (Glorieux et al., 2015). The CAT participates in the dismutation of $H_2O_2$ to oxygen and water ($H_2O$) in a two-step reaction (Grigoras, 2017). The first step of the reaction involves the formation of compound I, the product of the reaction of $H_2O_2$ with catalase haem (Reaction (1)). Subsequently, compound I is decomposed upon reaction with a second $H_2O_2$ molecule in the catalytic reaction, releasing oxygen and water (Reaction (2)) (Sies, 2017):

Compound I: catalase−$Fe^{3+}$ + $H_2O_2$ → catalase−$FeO^{3+}$ + $H_2O$

(Compound I) (1)

Catalytic reaction: catalase−$FeO^{3+}$ + $H_2O_2$ → catalase−$Fe^{3+}$ + $O_2$ + $H_2O$

In sum: $2H_2O_2 \rightarrow O_2 + 2H_2O$ (2)

2.7.3. Glutathione

Glutathione (GSH) is a thiol tripeptide (γ-glutamylcysteinylglycine) comprised of three amino acids (glutamic acid, cysteine, and glycine) (Noctor et al., 2011). The synthesis of GSH from cysteine, glutamate, and glycine is catalysed sequentially by two cytosolic enzymes, glutamate cysteine ligase (GCL) and GSH synthetase (Wu et al., 2004). GCL catalyses the first of two ATP-dependent steps in GSH synthesis, forming γ-glutamylcysteine (γ-GC) from glutamate and cysteine. The second step is catalysed by GSH synthetase, which joins glycine to γ-GC, thus forming GSH (Franklin et al., 2009).

GCL consists of two separately coded proteins, a catalytic subunit (GCLC) and a modifier subunit (GCLM) (Krejsa et al., 2010). It has been shown that GSH production is paralleled with GCLC gene expression, which is regulated primarily at the transcription level. The GCLC gene has oxidative stress-responsive elements in the promoter/enhancer region. Several *cis*-acting DNA elements contribute to the transcriptional up-regulation of the GCLC gene in response to oxidative stress, providing a protective mechanism against oxidative stress (Koide et al., 2003).

In all mammalian tissues, GSH is the most abundant non-protein thiol that protects against oxidative stress (Lu, 2013). The antioxidant function of GSH is primarily accomplished by GSH peroxidase-1 (GPx-1)-catalysed reactions, reducing $H_2O_2$ to water and lipid peroxides to their corresponding alcohols, mainly in the mitochondria and cytosol (Ighodaro and Akinloye, 2018). The main reaction that GPx-1 (selenocysteine (Sec)-containing enzyme) catalyses is $2GSH + H_2O_2 \rightarrow GSSG + 2H_2O$ (see Figure 2.7) (Behnisch-Cornwell et al., 2020).


**Figure 2.7: Glutathione peroxidase enzymatic reaction** (Mattmiller et al., 2013)

Reducing equivalents come from two equivalents of GSH, which are oxidised to glutathione disulfide (GSSG). For the maintenance of free radical detoxification in a cell, GSSG needs to be converted to GSH by the glutathione reductase (GR) enzyme using NADPH (see Figure 2.8) (Sarıkaya and Doğan, 2020).

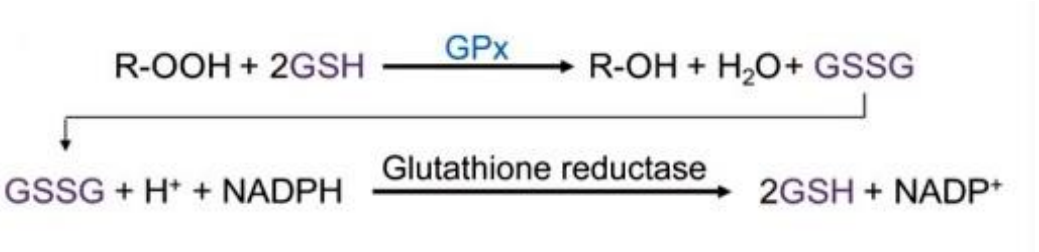


**Figure 2.8: Glutathione peroxidase enzymatic reaction** (Mattmiller et al., 2013)

### 2.7.4. Nuclear factor erythroid 2-related factor 2

The expression of most antioxidant enzymes is tightly regulated by the antioxidant response element (ARE), a non-coding DNA sequence activated by nuclear factor erythroid 2-related

factor 2 (Nrf2) (de Vries et al., 2008). The Nrf2, a nucleus transcription factor bound to its inhibitor, Kelch-like ECH-associated protein (Keap1), is a vital transcription factor regulating cellular redox homeostasis (Guo et al., 2020). Following exposure to oxidants (see Figure 2.9), Nrf2 is dissociated from Keap1 through oxidation of the cysteine residues of the Nrf2–Keap1 complex (Nagiah et al., 2015). The active form of Nrf2, Nrf2 (Phospho S40) (p-Nrf2) translocates to the nucleus and binds to ARE in the upstream regulatory regions of genes, encoding for detoxification and antioxidant enzymes, thereby enhancing transcription (Holmström et al., 2016).

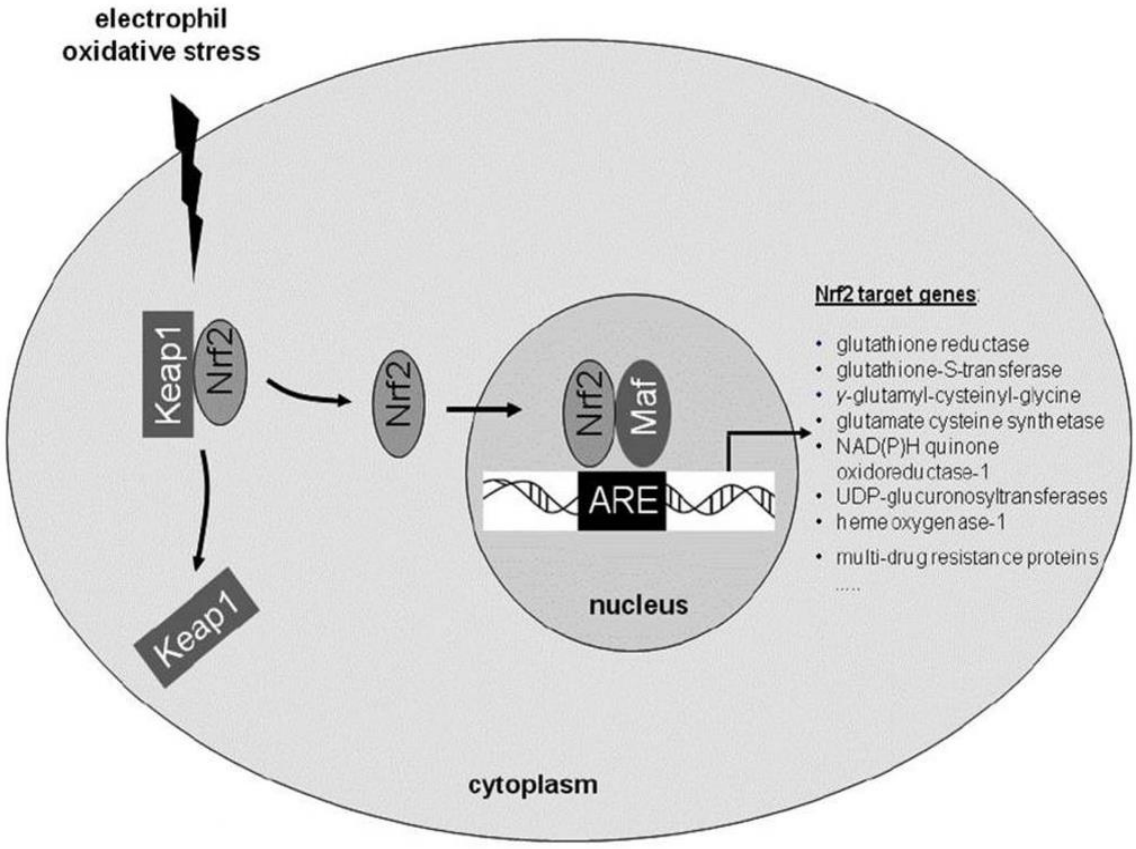


**Figure 2.9: Activation of the antioxidant transcription factor, nuclear factor erythroid 2-related factor 2** (Lee et al., 2012)

Individual ART regimens have varied degrees of toxicity that are tissue-specific and time-dependent, according to research into ART and its related illnesses. Oxidative stress and mitochondrial dysfunction are identified as key metabolic pathways involved in ART-induced toxicity (Ndlovu et al., 2023). The toxicity of ART has led to the use of medicinal plants by PLHIV, to ameliorate the side effect and improve overall health (Biswas et al., 2019).

## 2.8. The use of African traditional medicinal plants

An estimated 72% of Black South Africans use traditional medicines for basic healthcare needs (Sobiecki, 2014). This can be ascribed to several factors, including easy access to medicinal plants, low costs, and extensive knowledge and expertise within the local communities (Street et al., 2008). There are about ten prominently used South African medicinal plants, which include *Aspalathus linearis* (Fabaceae), *Agathosma betulina* (Rutaceae), *Aloe ferox* (Asphodelaceae), and *Hypoxis hemerocallidea* (African potato) (Street and Prinsloo, 2013). Each medicinal plant contains a wide range of diverse bioactive compounds and high levels of phytochemicals, which act as natural antimicrobial, anticancer, antispasmodic, antipyretic, antioxidant, and antiviral agents in the human body (Altemimi et al., 2017; Biswas et al., 2019). South African medicinal plants have also shown efficacy in treating hypertension, heartburn, arthritis, rheumatism, type 2 diabetes mellitus, gastrointestinal disturbances, menstrual difficulties, headache, heartburn, and gout (Street and Prinsloo, 2013). PLHIV frequently use African Traditional Medicines (ATMs) with Western medications, including ARVs (Sibanda et al., 2016). The ATMs may diminish the side effects of ARVs and their cytotoxicity and promote treatment adherence (Sibanda et al., 2016). However, research studies evaluating the potential herb-drug interactions in a clinical setting are still warranted.

Medicinal plants which traditional medicine practitioners in Sub-Saharan Africa most extensively use for adjuvant HIV/AIDS treatment and related disorders are *Hypoxis hemerocallidea* (African potato), *Sutherlandia frutescens* (Cancer bush) (Peltzer et al., 2011), and *Moringa oleifera* (MO) (Biswas et al., 2019). African potato, cancer bush, MO are also known as "inkofe" (Zulu name), "lerumo lamadi" (Sotho name), "peperwortelboom" (Afrikaans name) (Mofokeng et al., 2020; Aboyade et al., 2014; Tshabalala et al., 2020). In SA, the African potato and the cancer bush are considered one of the two most popular medicinal plants used to boost the immune system of HIV patients (Mills et al., 2005; Dukhi and Taylor, 2018). Despite the popularity of their use and the support of Ministries of Health and NGOs in certain African nations, no clinical trials are investigating the efficacy and limited evidence of harm for the potential of drug interactions with antiretroviral drugs (Mills et al., 2005). MO is considered a highly nutritive tree in many parts of Africa and Asian countries (Luhlaza-ISS, 2006). The various health benefits of MO, particularly its leaves, are well-researched, documented and confirmed in several studies. MO's most well-studied and exploited uses are medicinal and nutritional (Luhlaza-ISS, 2006).

A Nigerian study by Gambo and colleagues in 2021 showed that MO leaf powder supplementation increased the CD4+ T cell count of PLHIV on ART (TLE) (Gambo et al., 2021). This can be attributed to MO's nutraceutical benefits (Gambo et al., 2021). A study by Monera-Penduka and colleagues in 2017 showed that MO was well tolerated when taken with nevirapine by HIV patients. MO inhibits the CYP3A4 enzyme, which is responsible for metabolising nevirapine. However, the safety profile of nevirapine was not altered when co-administered with MO (Monera-Penduka et al., 2017). The MO tree extracts have also shown inhibitory activity, specifically against HIV-1, Herpes Simplex Virus (HSV), and Hepatitis B

Virus (HBV), which damages the liver by causing inflammation, cirrhosis and liver cancer (Biswas et al., 2019). However, there is limited information about the use of MO amongst HIV/AIDS patients receiving TLD in SA and its effects on patient compliance and outcomes.

*Moringa oleifera* is a medicinal tree from the family of Moringaceae, commonly found in Asia and Africa (Vergara-Jimenez et al., 2017). In SA, MO is farmed in several provinces, including Gauteng, Limpopo, Mpumalanga, and KwaZulu-Natal (Luhlaza-ISS, 2006). The MO tree is known for its anti-helmintic, antiseptic, detergent, anti-ulcerogenic, anti-inflammatory, anti-microbial, antioxidant, anti-hyperglycaemic, anti-clastogenic, anticancer, and anti-fibrotic effects (Salami et al., 2021). For centuries, many cultures worldwide have used MO to treat skin infections, blackheads, anxiety, anaemia, asthma, bronchitis, catarrh, chest congestion, cholera, and other illnesses (Razis et al., 2014).

Ayurveda, the traditional Indian system of medicine, is an ancient yet living tradition equal to conventional Western medicine and traditional Chinese medicine (Patwardhan et al., 2005). It is based on drug discovery, whereby therapeutically active ingredients are first identified based on ethnic uses and then verified through clinical trials. It is a holistic healing system and is based on over 7000 plants and about 8000 remedies, all of which have been documented (Mukherjee et al., 2014). The Ayurveda traditional system of medicine shows that MO can prevent approximately 300 diseases, and its leaves have been exploited for both preventive and curative purposes (Leone et al., 2015).

## 2.9. *Moringa oleifera*

*Moringa oleifera*, commonly known as the 'Drumstick' or horseradish tree, is a small, soft-wooded deciduous tree with sparse foliage cover (Tomar et al., 2020). MO is a fast-growing, highly drought-tolerant, and multi-purpose tree. It is usually five to 10 metres tall but can grow up to 15 metres (Devkota and Bhusal, 2020).

**Figure 2.10: *Moringa oleifera* tree** (Leone et al., 2015)

Various parts of the tree (see Figure 2.12) consist of numerous bioactive components, including vitamins, flavonoids, phenolic acids, isothiocyanates, tannins, and saponins (Vergara-Jimenez et al., 2017).

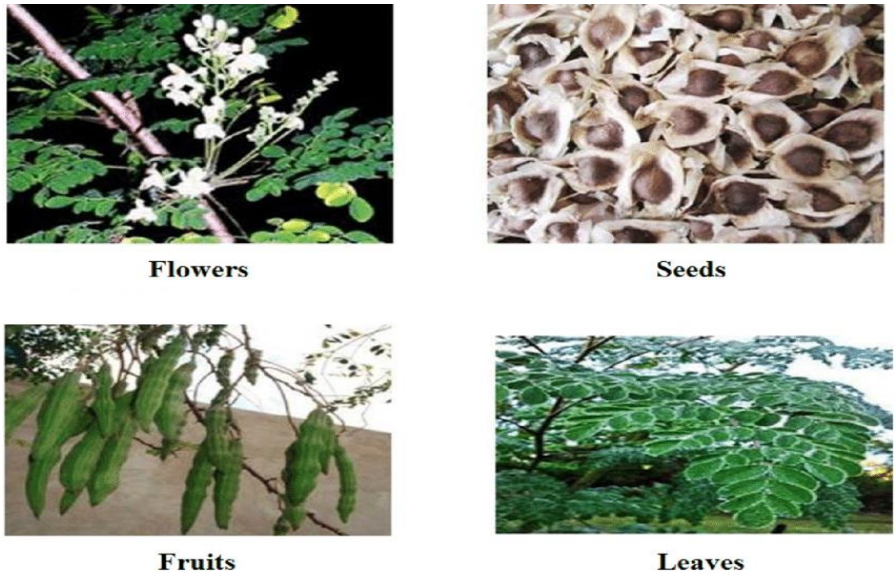


**Figure 2.11: Constituents of the *Moringa oleifera* tree** (Paikra et al., 2017)

The roots, bark, gum, leaf, flowers, fruit (pods), seed and seed oil of the MO tree have various biological activities that protect against gastric ulceration and hypertension, in addition to anti-diabetic and anti-inflammatory effects (Stohs and Hartman, 2015). The leaves contain the largest amounts of vitamin C and A, flavonoids, including myricetin, quercetin, and rutin, as well as phenolic acids and carotenoids, such as lutein, β-carotene, and zeaxanthin (Nizioł-ŁUkaszewska et al., 2020).

The strong antioxidant activity exhibited by flavonoids *in vitro* is primarily due to their ability to trap free radicals via the metal chelation and donation of electrons or hydrogen atoms (Lin et al., 2018). Phenolic acids are distributed ubiquitously in plants and play a significant protective role in oxidative stress conditions (de la Rosa et al., 2018). Phenolic acids possess antioxidant activity due to their chemical nature: hydroxyl groups attached to the pentyl ring. They stabilise free radicals by donating a hydroxyl group, and the degree of antioxidant activity

is determined by the position and number of the phenolic hydroxyl groups (Chen et al., 2020). Carotenoids are well-known for their ability to physically and chemically quench oxygen. They scavenge ROS and play a protective role in several ROS-mediated disorders, such as various forms of cancer, cardiovascular diseases, and neurological and eye-related disorders (Fiedor and Burda, 2014).

The MO aqueous leaf extracts contain large amounts of bioactive compounds or high levels of phytochemicals that synergistically induce their medicinal effects (Zhang et al., 2015). *In vivo,* the aqueous leaf extract, a rich source of antioxidant compounds, protects against oxidative stress-induced diseases (Paikra et al., 2017). *In vitro* studies have reported the renal and hepatoprotective properties of MO against several drugs, such as gentamicin, pyrazinamide, rifampicin, isoziazide and acetaminophen, which are mainly attributable to its leaves (Brilhante et al., 2017). Scientists often use the $HepG_2$ cell line as an *in vitro* model system that mimics the natural *in vivo* environment to assess the effects of aqueous leaf extracts, drug metabolism, and hepatotoxicity studies (Harjumäki et al., 2020; Donato et al., 2015).

### 2.10. The use of human $HepG_2$ liver cells *in vitro*

Currently, drugs used to treat several viral infections, such as HBV, HSV, or HIV, display consistent side effects, including mitochondrial toxicity (Pinti et al., 2003). Several *in vitro* models and techniques have been developed to analyse the effects of such drugs. The $HepG_2$ cells (derived from the human hepatoma) are an excellent model to investigate mitochondrial toxicity due to their high organelle content and mtDNA and are extensively used by several investigators (Pinti et al., 2003). The $HepG_2$ cell line was established from a liver tumour biopsy obtained from a 15-year-old Caucasian male in the 1970s (Ren et al., 2018). It is the

most frequently used hepatoma cell line in the testing and research on drug-induced liver injury (Ren et al., 2018).

Several scientists have researched ART using the $HepG_2$ cell line. In 2017, Paemanne and colleagues used the $HepG_2$ cell line to investigate the effect of the nevirapine (NVP) regimen on mitochondrial dysfunction and the study results showed that NVP induces mitochondrial dysregulation in $HepG_2$ cells (Paemanee et al., 2017). In 2014, Shamsabadi investigated the hepatotoxic effects of the components of Atripla (composed of emtricitabine, tenofovir, and efavirenz) and Eviplera (composed of emtricitabine, tenofovir, and Rilpivirine) on $HepG_2$ cells. (Shamsabadi, 2014). A research study by Nagiah and colleagues in 2015 has also established the appropriate application of this cell line as an *in vitro* model to evaluate drug metabolism or drug toxicity of antiretroviral drugs, including tenofovir. This research study will therefore take on a similar approach to assess tenofovir-induced cytotoxicity and will incorporate MO treatment to assess its hepatoprotective effects.

Various biological activities of several parts of the MO plant have been reported to date. However, *in vitro* studies that have assessed the hepatoprotective effects of MO aqueous leaf extract against ART-induced cytotoxicity in human $HepG_2$ liver cells are limited. Therefore, this study aimed to investigate the effect of MO aqueous leaf extract on oxidative stress and antioxidant responses following acute and chronic exposure to an antiretroviral drug (tenofovir) in human $HepG_2$ liver cells *in vitro*.

# Chapter 3

## 3. Methodology

### 3.1. Description of research design

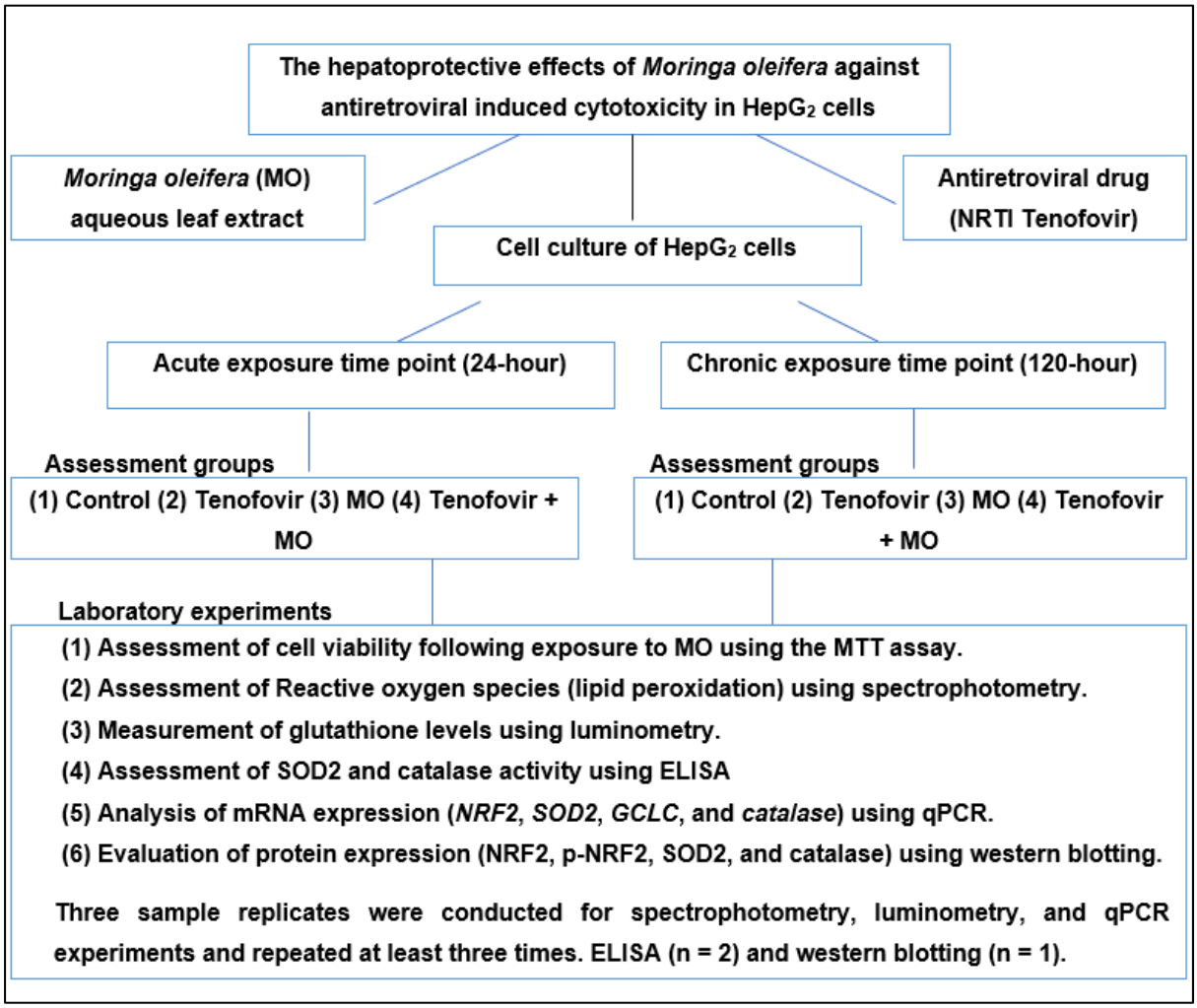


**Figure 3.1: Schematic overview of the methodology**

This research was an intervention-based *in vitro* study (Thiese, 2014; Nagiah et al., 2015). An intervention (experimental) study design evaluates the research study questions. It provides a clear explanation of the methodology and detailed information on the execution and analysis of the results (Thiese, 2014). The MO aqueous leaf extract and antiretroviral drug (tenofovir) were prepared. The human $HepG_2$ cells were cultured and exposed to four groups over two

time periods (24-hour and 120-hour) (cell morphology: Appendix C). The two time periods (acute and chroic) were taken from a study by Nagiah et al. (2015) that evaluated the toxicity of ART. This study then incorporated MO to assess its protective effect against ART-induced toxicity. Spectrophotometry-based techniques were used to assess reactive oxygen species (lipid peroxidation). Luminometry was used to quantify glutathione levels, and the enzyme-linked immunosorbent assay (ELISA) was used to quantify SOD2 and catalase activity. Protein expression levels of NRF2, p-NRF2, SOD2, and catalase were determined using western blot analysis. The mRNA expression of *NRF2, SOD2, GCLC,* and *catalase* was determined using qPCR analysis. Hoechst staining assay was conducted to analyse live cells and assess mycoplasma contamination (Appendix I)

### 3.2. Measurement description

The study was conducted by the researcher, under the supervision of the study supervisors, using the laboratory equipment and resources available in the Department of Basic Medical Sciences, the Department of Human Molecular Biology, the Department of Haematology and Cell Biology, and the Department of Chemical Pathology in the University of the Free State. Following the approval of the study by the Health Sciences Research Ethics Committee [Ethics number: UFS-HSD2021/1571-0002], data was collected. COVID-19 regulations were followed during laboratory procedures, including wearing protective masks, maintaining social distance, and using sanitising stations. Data recording was done in spreadsheets and regularly backed up on iCloud and Google Drive.

## 3.3. Procedures and techniques

### 3.3.1. Materials

The MO leaves were collected from Durban, KwaZulu-Natal (SA), and verified by a herbarium (verification number: 151125) (Appendix B). The University of KwaZulu-Natal donated the human HepG2 cell line (hepatocyte carcinoma, 85011430-1VL). Cell culture reagents were purchased from ThermoFisher Scientific (Johannesburg, SA), and the antiretroviral drug (tenofovir) (SML1795-5MG) was purchased from Sigma-Aldrich (SA).

### 3.3.2. Cell culture of human $HepG_2$ cells

The human $HepG_2$ cells were cultured in a complete culture media (CCM), at 37°C, 5% $CO_2$, in a humidified atmosphere. The CCM consisted of the Eagle's minimum essential medium (EMEM), 10% fetal calf serum, 1% penicillin-streptomycin-fungizone, and 1% L-glutamine. $HepG_2$ cells were then seeded in sterile 25 $cm^3$ cell culture flasks and subjected to treatment once the cells reached 80% confluency.

Cell culturing process:

The CCM was pre-warmed in a bead warmer (37°C) . A vial of $HepG_2$ cells was suspended in a sterile 75 $cm^3$ cell culture flask inside a sterile working environment, the laminar flow hood. CCM (15 ml) was added into the 75 $cm^3$ cell culture flask, and cells were then observed under the Inverted biological microscope (XD-202) to document the cell morphology. The cell culture flask was placed into the incubator (37°C, 5% $CO_2$). After 24 hours, the cell culture flask was taken out of the incubator, and the cells were observed under the microscope to observe the attachment and cell morphology. The culture flask was then placed inside the

laminar flow hood, CCM was aspirated, and the culture flask was rinsed three times with 5 ml of pre-warmed phosphate-buffered saline (PBS). After every rinsing step, PBS was discarded. Then, 10 ml CCM was added into the culture flask and placed into the incubator. This process was repeated every other day until the cells reached 80% confluency. Following this, cells were trypsinized and seeded into sterile 25 $cm^3$ cell culture flasks for treatment exposure.

Trypsinization:

To assess confluency, the cell culture flasks were taken out of the incubator and the cells were observed under the microscope. Following 80% confluency, the cells were then placed inside the laminar flow hood, CCM was aspirated, and the culture flasks were rinsed three times with 5 ml of pre-warmed PBS. Following this, the adherent cells were dissociated from the culture flask by adding 6 ml of trypsin into the culture flask. After adding trypsin, the culture flask was placed into the incubator for 15 minutes (min) to allow the dissociation of the cells. After 15 min, the cells were observed under the microscope to assess if they had detached from the surface of the culture flask. Then 15 ml of CCM was added into the flask to neutralise trypsin. The cells were then transferred to a 50 ml conical tube and centrifuged [720 xg (2000 rpm), 10 min, room temperature (R-T)] using the centrifuge. The supernatant was removed, and the cells were re-suspended in 2 ml of CCM. The cells were then vortexed, and a cell count was performed.

Cell count:

Cells in suspension (20 µl) and trypan blue (20 µl) were added to an Eppendorf. Then 10 µl of the mixture was added into a cell counting chamber, and the number of live cells was calculated

using the TC20™ Automated cell counter. Following this, the cells were equally seeded in sterile 25 $cm^3$ cell culture flasks and subdivided into four groups once the cells reached 80% confluency.

### 3.3.3. Antiretroviral drug (tenofovir) preparation

A stock solution of tenofovir, 2.1762 mM [5 mg in 8 ml of dimethyl sulfoxide, (DMSO)] was prepared and stored at -20ºC until use. The human $HepG_2$ cells were then treated with tenofovir at a maximum plasma level concentration of 1.2 μM (Nagiah et al., 2015; Walker et al., 2002; Venhoff et al., 2007).

### 3.3.4. *Moringa oleifera* aqueous leaf extract preparation

The MO leaf extract was prepared using 10 g of crushed air-dried leaves. Deionised water (100 ml) was added, and the mixture was boiled for 20 min using the Magnetic Stirrer. Subsequently, the mixture was transferred to a 50 ml conical tube and centrifuged [720 xg, 10 min, room temperature (R-T)] using the centrifuge. Thereafter, 2 ml of MO supernatant was aliquoted in 15 ml conical tubes, lyophilised using the Virtis Benchtop Freeze dryer, and stored at 4ºC until use. Upon treatment, the MO stock solution was prepared [10 mg MO in 1 mL CCM] and filter sterilised with a 0.22 μM filter (Millipore) (Tiloke et al., 2019).

### 3.3.5. Assessment of cell viability

The 3-(4, 5-Dimethyl-2-thiazolyl)-2, 5-diphenyl-2H-tetrazolium bromide (MTT) colorimetric assay was used to assess the effect of MO aqueous leaf extract on cell viability to determine the half-maximal inhibitory concentration ($IC_{50}$) to be used for all subsequent assays. The MTT assay is based on forming an insoluble formazan product from a water-soluble MTT compound

(Kamiloglu et al., 2020). Viable cells with active metabolism convert yellow MTT salt into a dark purple-coloured formazan. The principle of the MTT assay is represented in Figure 3.2.

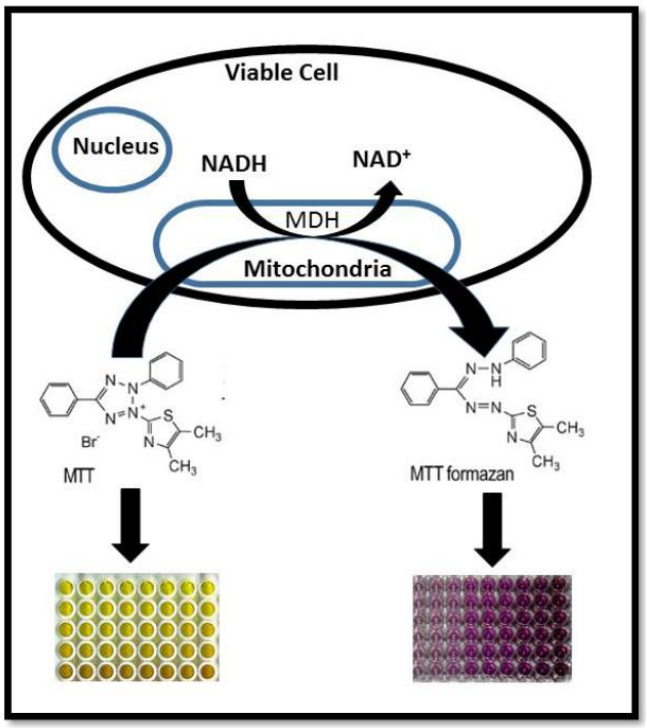


**Figure 3.2: Schematic overview of cell viability assay.** The reduction of MTT yellow salt to insoluble purple formazan by viable cells (Shunmugam, 2016).

HepG2 cells (15 000 cells/well) were seeded in a 96-well plate and allowed to attach overnight (37°C, 5% $CO_2$). Cells were then treated with varying MO aqueous leaf extract concentrations (0, 0.1, 0.5, 1, 1.5, 2, 2.5, 5 mg/ml) in triplicate (300 µl CCM/well) and incubated (37°C, 5% $CO_2$) for 24 hours. After incubating with MO aqueous leaf extract concentrations (0 – 5 mg/ml), 300 µl of treatment media was removed from each well. The cells were then rinsed with 100 µl of pre-warmed PBS once. CCM (100 µl) was then added to each well. Then 20 µl of 5 mg/ml MTT salt dissolved in 1 ml of PBS was then added to each well, and the plate was incubated

at 37°C for 3 hours. Following incubation, the MTT solution with CCM was aspirated. Following this, 100 µl of DMSO was added to each well and incubated (37°C, 30 min) (Tiloke et al., 2019). The absorbance was measured spectrophotometrically at 560 nm using a reference wavelength of 600 nm on a Promega GloMax® Discover microplate reader after the formazan crystals had dissolved. The percentage cell-viability and the $IC_{50}$ were determined as described by Mosmann, 1983. $HepG_2$ cells were treated at an 80% confluency using the pre-determined $IC_{50}$ for all subsequent assays.

### 3.3.6. Acute and chronic drug exposure

Cells were cultured in two sterile 25 $cm^3$ cell culture flasks. After reaching an 80% confluency, the cells were trypsinized and equally seeded into eight sterile 25 $cm^3$ cell culture flasks for treatment exposure. Once the cells had reached an 80% confluency, media was discarded, and the cells were rinsed with 5 ml of pre-warmed PBS three times. The $HepG_2$ cells were then exposed to three treatment groups over two time periods (24-hour and 120-hour). The groups included an untreated control, tenofovir, MO, and a tenofovir and MO combination treatment group. For the chronic 120-hour period, treatment media was replenished every 48 hours (Nagiah et al., 2015). The 24- and 120-hour group supernatants were stored at -20˚C.

### 3.3.7. Assessment of reactive oxygen species

The ROS levels were quantified as per the method described by Nagiah and colleagues in 2015, using lipid peroxidation as a marker of oxidative stress. Extracellular malondialdehyde (MDA), a product of lipid peroxidation, was measured using the thiobarbituric acid reactive substances (TBARS) assay. The TBARS assay was conducted per the method described by Phulukdaree and colleagues in 2010, using thiobarbituric acid to detect MDA levels. The TBARS assay is represented in Figure 3.3.

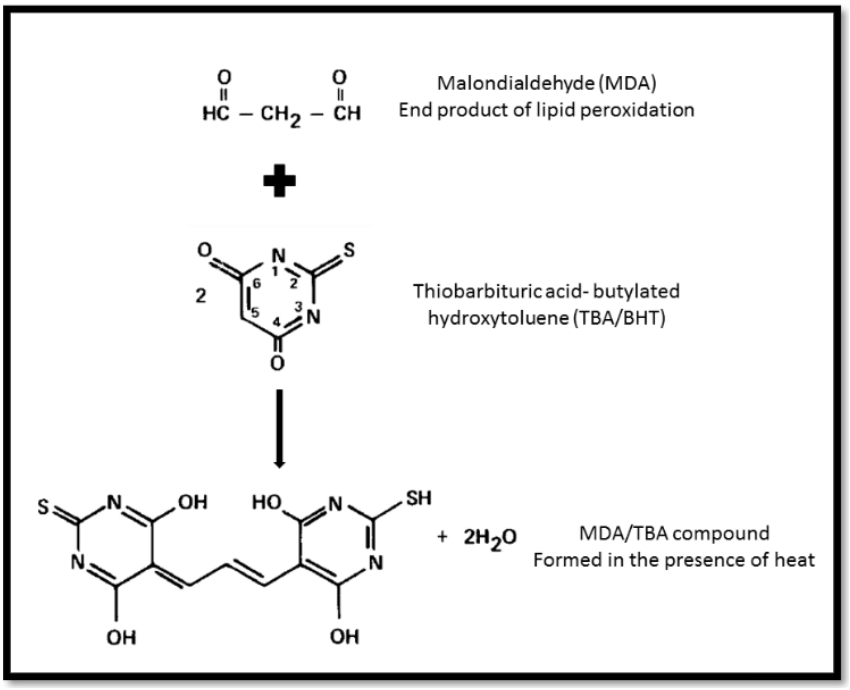


**Figure 3.3: Schematic overview of TBARS assay.** MDA reacts with TBA/BHT forming a red fluorescence compound (Shunmugam, 2016).

The following material was required for the assay: Phosphoric acid ($H_3PO_4$), hydrochloric acid (HCl), Sodium hydroxide (NaOH), Thiobarbituric acid (TBA), butylated hydroxyl toluene (BHT), butanol, and glass tubes. After preparing working solutions, the glass tubes were

labelled from 1-10 and placed in a test tube rack. Test tubes 1-4 had the 24-hour groups, 5-8 had the 120-hour groups, and 9-10 had the positive and negative control, respectively. In each test tube, the following solutions were added:

| Test tube 1-8 | Test tube 9 (Positive control) | Test tube 10 (Negative control) |
|---|---|---|
| 100 µl of samples | 200 µl of 2% of $H_3PO_4$ | 100 µl of CCM |
| 200 µl of 2% of $H_3PO_4$ | 400 µl of 7% of $H_3PO_4$ | 200 µl of 2% of $H_3PO_4$ |
| 400 µl of 7% of $H_3PO_4$ | 400 µl of TBA/BHT | 400 µl of 7% of $H_3PO_4$ |
| 400 µl of TBA/BHT | 1 µl of MDA | |

Thereafter, 200 µl of 1M HCl was added to all test tubes. All test tubes were boiled at 100˚C for 15 min using the Benchmark 2 Block Digital Heat Block. The test tubes were then allowed to cool to R-T for a further 10 min. After cooling, 1.5 ml of butanol was added to each test tube. Each test tube was then vortexed for 10 seconds. The test tubes were allowed to stand until the butanol phase ($1^{st}$ layer) was visible. Then, 1 200 µl of butanol phase was aliquoted into Eppendorf tubes. From each Eppendorf, 200 µl was added to a 96-well plate in triplicates. The samples' optical density was measured spectrophotometrically at 560 nm using a reference wavelength of 600 nm on a Promega GloMax® Discover microplate. MDA concentrations (mM) were calculated by dividing the mean absorbance of the samples by the absorption coefficient (156 $mM^{-1}$).

### 3.3.8. Assessment of antioxidant markers

(i) Luminometry – Quantification of glutathione levels

Glutathione levels in the samples were measured using the Glutathione-Glo™ Assay (Promega, Madison) per the manufacturer's guidelines (V6911). The assay is a luminescence-based system that detects and quantifies the total amount of GSH in cultured cells. It uses a multi-well plate format in which stable luminescent signals correlate with GSH concentration. Light emitted by luciferase depends on the amount of luciferin produced, which depends on the GSH present. As a result, the luminescent signal is proportional to GSH levels. In the presence of GSH, glutathione S-transferase (GST) was used to catalyse the conversion of a luciferin derivative into luciferin. Luciferin formed was detected in a coupled reaction using the Ultra-Glo™ Recombinant Luciferase to generate a glow-type luminescence. The Glutathione-Glo™ Assay is represented in Figure 3.4.

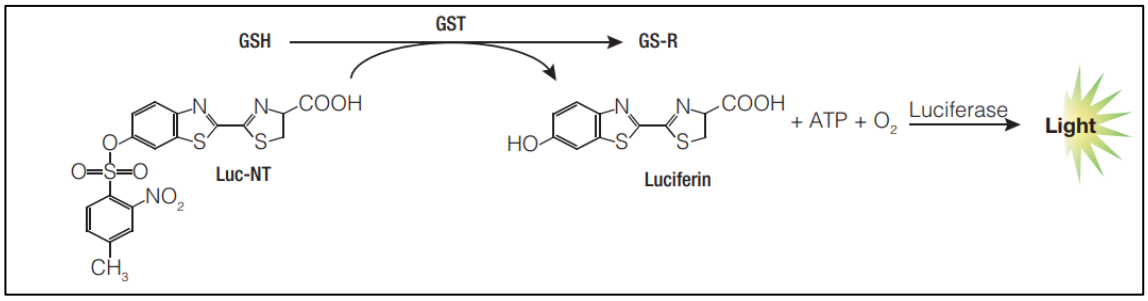


**Figure 3.4: Schematic overview of Glutathione-Glo™ Assay.** Adapted from the Glutathione-Glo™ Assay protocol (V6911)

The standards and working solution were prepared as per the manufacturer's guidelines. For the experiment 6 standards (0, 3.125, 6.25, 12.5, 25, 50 µM) were prepared. To prepare the working solution per well, 48 µl of reaction buffer, 1 µl of luciferin NT, and 1 µl of GST were

required. The cells were washed with 5 ml of pre-warmed PBS three times after treatment. The adherent cells were then trypsinized and seeded into a white 96-well plate in triplicate (20,000 cells/well), followed by adding 50 µl/well of standards (duplicate). Then 50 µl of the working solution was added to each well. Subsequently, the 96-well plate was incubated in the dark at R-T for 30 min. Then 100 µl of reconstituted luciferin detection reagent was added to each well, and the plate was incubated further for 15 min in the dark at R-T. A Promega GloMax® Discover microplate measured the luminescence. A standard reference curve was determined (Appendix F and G). The data were expressed as relative light units (RLU).

(ii) ELISA – Quantification of SOD2 and catalase activity

The SOD2 and catalase activity were quantified using the Human SOD2 SimpleStep ELISA® Kit (ab178012) and Human Catalase Activity Kit (ab83464). Cell supernatant samples from various treatment groups and standards were added to the wells to perform these assays, accompanied by an antibody mix. The wells were washed after incubation to remove unbound material. The 3,3′,5,5′-Tetramethylbenzidine (TMB) Development Solution was added and catalysed by the horseradish peroxide (HRP) during incubation, resulting in a blue colouration. The stop solution was added to stop the reaction and change the colour from blue to yellow. Luminescence signals generated were proportional to the amount of analyte and activity. The optical density (OD) was measured at 450 nm for SOD2 activity and at 560 nm for catalase activity using the Promega GloMax® Discover microplate. The data were expressed as OD and fold-change. ELISA is represented in Figure 3.5.

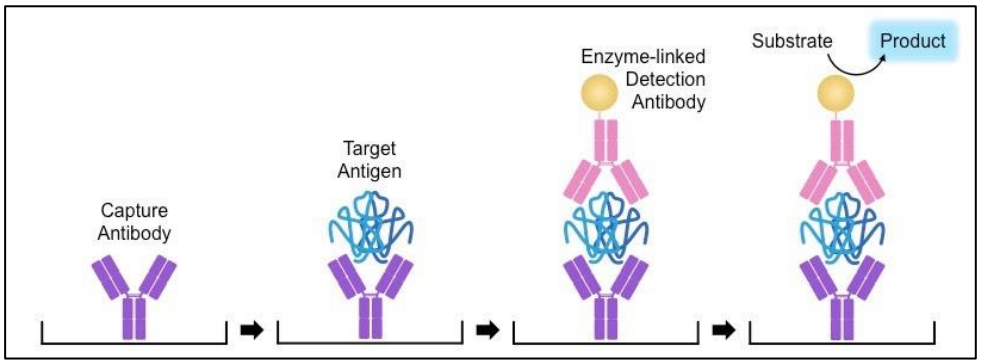


**Figure 3.5: Schematic overview of ELISA** (Ibrahim, 2020)

*SOD2 ELISA*

The standards and reagents were prepared according to the manufacturer's instructions. For the experiment 8 standards (0, 0.78, 1.56, 3.12, 6.25, 12.5, 25, 5 ng/ml) were prepared. Samples (50 µl) and standards (50 µl) were added to appropriate wells in duplicates and triplicates, respectively. Then 50 µl of the Antibody Cocktail was added to each well. The plate coated with capture antibody which targets an antigen was then sealed with foil and incubated for 1 hour at R-T on a plate shaker set to 400 rpm. Each well was then washed with 3 x 350 µl 1X Wash Buffer PT. TMB Substrate (100 µl) was added to each well and incubated for 10 min in the dark on a plate shaker set to 400 rpm. Thereafter, 100 µl of Stop Solution was added to each well, and the plate was placed on a plate shaker for 1 min to mix. The OD was recorded at 450 nm on a Promega GloMax® Discover microplate. A standard reference curve was determined (Appendix D).

*Catalase ELISA*

The standards, reagents, and developer mix were prepared according to the manufacturer's instructions. The experiment had 6 standards (0, 2, 4, 6, 8, 10 nmol). Following this, 100 µl standard dilutions [90 µl Standard + 10 µl Stop Solution], 5 µl positive control and 73 µl of catalase assay buffer, 78 µl samples, and 78 µl samples High Control (HC) were all added to appropriate wells. Standards were plated in duplicate and samples in triplicates. Then 10 µl Stop Solution was added into each Sample HC wells and incubated at 25ºC for 5 min to completely inhibit the catalase activity in the sample HC wells. Thereafter, 12 µl of fresh 1 mM $H_2O_2$ solution was added into each sample, positive control and sample HC wells and incubated at 25ºC for 30 min. Stop Solution (10 µl) was then added to each sample and positive control wells. Developer Mix (50 µl) was added into each standard, sample, sample HC and positive control wells and incubated at 25ºC for 10 min protected from light. Then the ELISA plate was measured immediately at OD 560 nm on a Promega GloMax® Discover microplate. A standard reference curve was determined (Appendix E).

(iii) qPCR – Determination of mRNA expression (*NRF2, GCLC, SOD2, catalase*)

Quantitative PCR (qPCR) was used to determine mRNA expression levels using mRNA primers. The reverse transcription qPCR (RT-qPCR) method starts with sample RNA isolation. The total RNA was isolated using the Tri Reagent™ as per the manufacturer's guidelines (T9424). Once the RNA was isolated and standardised, it was reverse transcribed (RT) into a cDNA template (High-Capacity RNA-to-cDNA™ Kit 4387406) before mRNA primers were used for amplification.

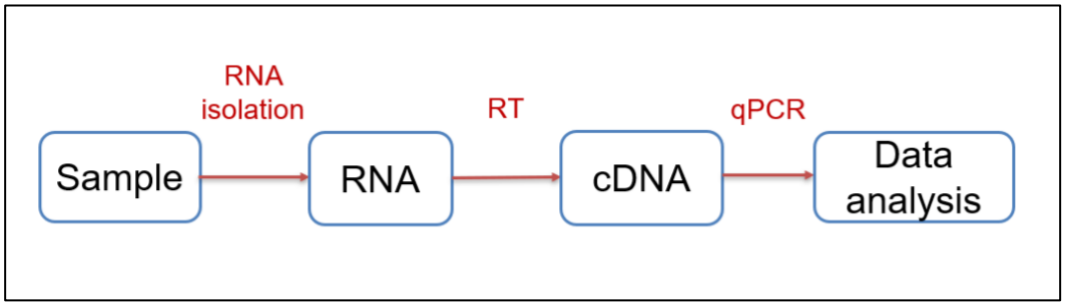


**Figure 3.6: Schematic overview of qPCR**

Following treatment, the cells were rinsed three times with PBS. Tri Reagent™ (500 µl) and PBS (500 µl) were added and incubated in the dark for 5 minutes at R-T to isolate RNA . The isolated RNA was then purified per the manufacturer's instructions using the Direct-zol™ RNA Miniprep (R2053). Then the sensitivity and integrity of RNA were assessed using the Qubit™ RNA HS Assay (Q32852) and Qubit™ RNA IQ Assay (Q33221) kits, respectively (Appendix K). The RNA was then standardised to 2000 ng and reverse transcribed into a cDNA template (High-Capacity RNA-to-cDNA™ Kit 4387406). The qPCR reaction consisted of the iQ™ SYBR® Green Supermix (5 µl) (BioRad, 1708880), cDNA (1 µl), sense (1 µl; 25 µM), and antisense (1 µl; 25 µM) primers and nuclease-free water (2 µl) to quantify mRNA levels of the genes of interest:

1) *Nrf2* (sense: 5′-AGTGGATCTGCCAACTACTC-3′; antisense: 5′-CATCTACAAACGGGAATGTCTG-3′),
2) *SOD2* (sense: 5′-GAGATGTTACACGCCCAGATAGC-3′; antisense:5′-AATCCCCAGCAGTGGAATAAGG-3′),
3) *Catalase* (sense: 5′-TAAGACTGACCAGGGCATC-3′; antisense: 5′-CAACCTTGGTAGATCGAA-3′) (Anderson et al., 2018),

4) *GCLC* (sense: 5'-TTTGGTCAGGGAGTTTCCAG-3'; antisense: 5'-TGAACAGGCCATGTCAACTG-3') (Dose et al., 2016).

The reaction mix (10 µl) was exposed to an initial denaturation (95°C, 10 min) that was accompanied by 40 cycles of denaturation (95°C, 15s), annealing [*Nrf2* (58°C, 40s), *SOD2* (57°C, 40s), *GCLC* (59°C, 40s), *CAT* (58°C, 40s)] and extension (72°C, 30s). A housekeeping gene, glyceraldehyde 3-phosphate dehydrogenase (*GAPDH*): (sense: 5'-TCCACCACCCTGTTGCTGTA-3', antisense: 5'-ACCACAGTCCATGCCATCAC-3') (Nagiah et al., 2015), were amplified simultaneously under the same reaction conditions. All qPCR experiments were conducted using the QuantStudio™ 5 Real-Time PCR System (Applied Biosystems) and analysed using the QuantStudio analysis software. Changes to gene expression were calculated according to the $2^{-\Delta\Delta Ct}$ method described by Livak and colleagues in 2001 and expressed as fold-change relative to the control.

(iv) Western Blot – Determination of protein expression (NRF2, p-NRF2, SOD2, catalase)

Western Blot was conducted per the method Nagiah and colleagues described in 2015 to determine the protein expression of NRF2, p-NRF2, SOD2, and catalase (Nagiah et al., 2015). Briefly, the protein was isolated, quantified, and standardised. Protein concentration was determined using the bovine serum albumin assay and a standard reference curve was determined (Appendix H). Western blotting is represented in Figure 3.7.

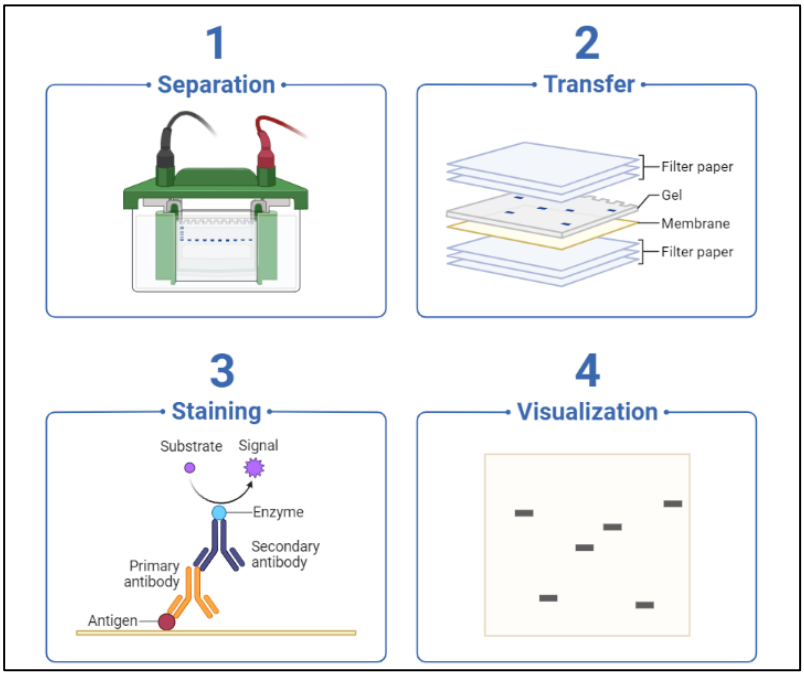


**Figure 3.7: Schematic overview of Western blot** (adapted from Biorender.com software)

Once the proteins were standardised to 1 mg/ml, Laemmli's sample buffer was added to the standardised protein (1:1). The samples were heated at 100ºC for 5 min on a heating block. Following sample preparation, a western blot was performed using the sodium dodecyl sulphate polyacrylamide gel electrophoresis (SDS-PAGE; Mini- PROTEAN® Tetra cell). The 10% TGX Stain-Free Fast Cast SDS–PAGE gels were placed in a Mini-PROTEAN Tetra System and filled the inner chamber with cold 1x SDS-PAGE running buffer. Samples were

loaded onto the gels (28 µl/well). The first lane position on each gel was loaded with 10 µl of Pre-stained Protein Ladder (Precision Plus Protein™ WesternC™ Blotting Standards, #1610376) to aid with molecular weight determination for specific protein bands. The second lane was loaded with a control sample, and subsequent lanes contained samples from treated groups. Thereafter, proteins were separated by electrophoresis (150 V). Following protein separation, the SDS–PAGE gel was removed from the electrophoresis chamber and placed on the ChemiDoc™ Imaging System (Model: 120031531) for stain-free gel activation. Subsequently, resolved proteins were electro-transferred onto NC membranes using the Trans-Blot Turbo Transfer System (2.5A – 5V – 5 min). Following the electro-transfer of proteins, the EveryBlot Blocking Buffer (12010020) (5 ml) was added onto the NC membranes to prevent non-specific binding of proteins and incubated on a shaker (2 hours, R-T). The membrane was washed thrice with 5 ml of Tris-tween buffered saline (TTBS) for 15 min.

The membrane was subsequently incubated (overnight, 4°C) with the primary antibody [rabbit anti-Nrf2 (12721); rabbit anti-Nrf2 (phospho S40) [EP1809Y] (ab76026); rabbit anti-SOD2/MnSOD [EPR2560Y] (ab68155); or rabbit anti-Catalase [EPR20198] (ab209211)], diluted to 1:1000 in 5% bovine serum albumin (BSA). Following incubation with the primary antibody, the membrane was washed with TTBS three times for 15 min. The membrane was then incubated (2 hours, R-T) with an HRP-conjugated labelled secondary antibody (goat anti-rabbit (7074S)) (1:5000 in 5% BSA) followed by a wash step in 1x TTBS, then with deionised water (3 times, 5 min). The HRP-conjugated labelled secondary antibody binds to the primary antibody to form an antibody complex. Protein bands were detected using the Enhanced chemiluminescence Clarity™ Western ECL Substrate Chemiluminescence Reagents utilising the ChemiDoc™ imaging system to activate the protein signal. A volume of 200 µl of each of

the ECL viewing substrates (Clarity Western Peroxide and Clarity Western Luminol/Enhancer Reagent) was prepared away from light and thoroughly mixed. Thereafter, a volume of 400 µl of the ECL mixture was evenly added onto the membrane. Once ECL has been added, an enzyme-substrate reaction occurs. HRP catalyses the oxidation of luminol by peroxide, producing an excited state product called 3-aminophthalate. This product decays to a lower energy state by releasing photons of light. The proteins of interest were then visualised using the ChemiDoc™ imaging software. Relative band density was measured by Bio-Rad's Image Lab™ Software (version 6.1). In order to control for protein loading, protein expression was normalised against HRP Anti-beta Actin antibody [BA3R] (ab173838) (1:2000 in 5% BSA). The relative band intensity was calculated by was calculated as the ratio between arbitrary units of the band of the antigen and the arbitrary units of the band of the internal control, β-actin.

### 3.4. Statistical analysis

Statistical analyses were performed using the GraphPad Prism V9 software package (GraphPad Software, Inc., San Diego, CA). Data were expressed as means with standard deviation. The dose-response equation was used to determine $IC_{50}$ for MTT assay. One-way ANOVA was used to compare the means of multiple groups relative to the control and followed by a post-hoc analysis using the Bonferroni correction test. The data were considered statistically significant with a $p < 0.05$.

# Chapter 4

## 4. Results

The result chapter reports on the research study findings generated from the methodology of the study. The experimental setup involved exposing $HepG_2$ cells to three treatment groups alongside an untreated control group. Seven experiments were conducted in line with the research study objectives, and each experiment was repeated at least three times. Results are presented in the form of graphs and tables.

### 4.1. $HepG_2$ Cell Viability Assay

The half-maximal inhibitory concentration ($IC_{50}$) was determined to assess the effect of MO on the cell viability of $HepG_2$ cells. The $IC_{50}$ was subsequently used for all downstream assays. The effect of MO aqueous leaf extract on $HepG_2$ cell viability was assessed for 24 hours (see Figure 4.1).

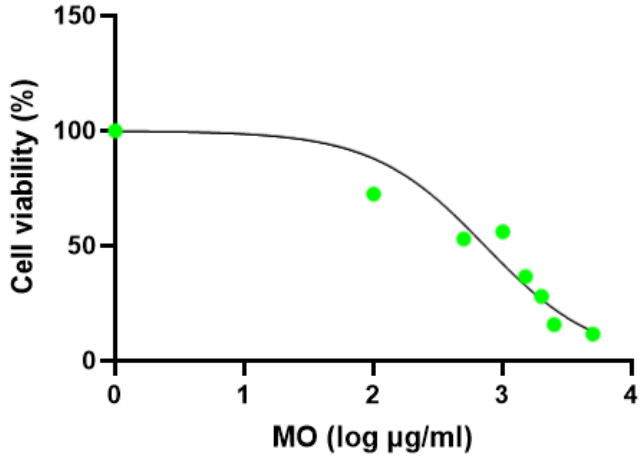


**Figure 4.1: $HepG_2$ cell viability following 24-hour treatment exposure to MO was determined using an MTT assay**

The $HepG_2$ cells were treated with varying MO concentrations (0-5000 µg/ml), and following 24 hours of treatment exposure, an $IC_{50}$ of 732.9 µg/ml was determined. The results revealed a dose-dependent decline in $HepG_2$ cell viability following a 24-hour treatment exposure to MO aqueous leaf extract. An $IC_{50}$ of 732.9 µg/ml was determined by the dose-response equation [Y=100/(1+(IC50/X)^HillSlope)] using GraphPad Prism software version 9. The $IC_{50}$ of 732.9 µg/ml was used in all subsequent assays.

## 4.2. Assessment of Reactive Oxygen Species (Lipid Peroxidation)

Oxidative stress is induced by reactive oxygen species (ROS). Lipid peroxidation, which occurs due to ROS, was used as a marker of oxidative stress. Extracellular malondialdehyde (MDA), a product of lipid peroxidation, was measured using the thiobarbituric acid reactive substances (TBARS) assay, as presented in Figures 4.2 A and B.

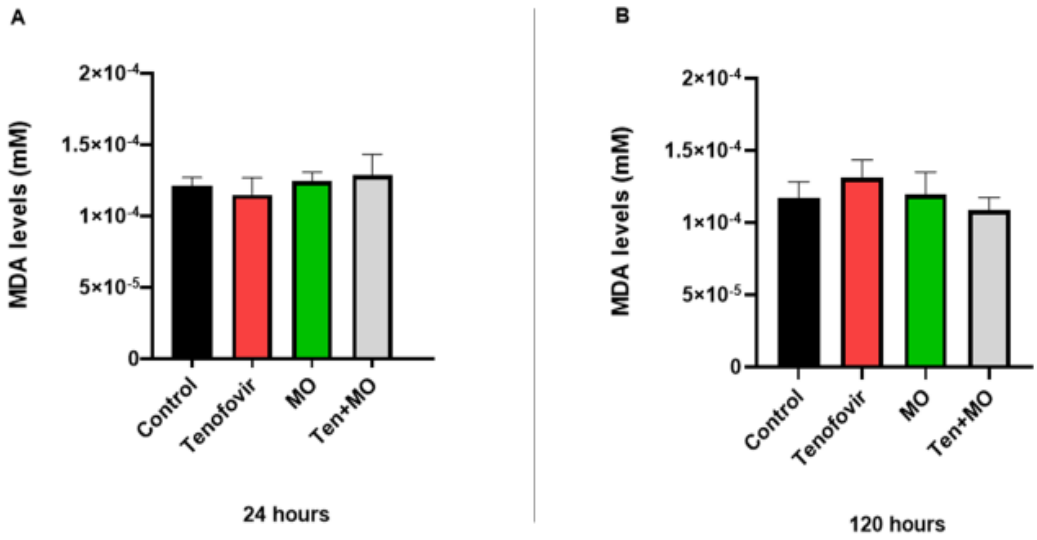


**Figure 4.2: Lipid peroxidation in $HepG_2$ cells following (A) acute (24-hour) and (B) chronic (120-hour) exposure to treatment groups.** No statistically significant difference was observed relative to the control ($p > 0.05$).

The results reported no significant difference however, a trend was observed. MDA levels were decreased in tenofovir-treated cells after a 24-hour exposure. However, following 120 hours, tenofovir increased MDA levels. MO and the combination group increased MDA levels at 24-hour treatment exposure. However, following a 120-hour exposre, MDA levels were decreased by MO and the combination treatment group.

### 4.3. Quantification of Superoxide Dismutase 2 Activity

Superoxide dismutase 2 (SOD2) is a critical component of the antioxidant defence system. The SOD2 enzyme reduces ROS levels by catalysing the dismutation of the superoxide free radical into oxygen and hydrogen peroxide ($H_2O_2$). The ELISA was conducted to quantify SOD2 levels, as presented in Figures 4.3 A and B.

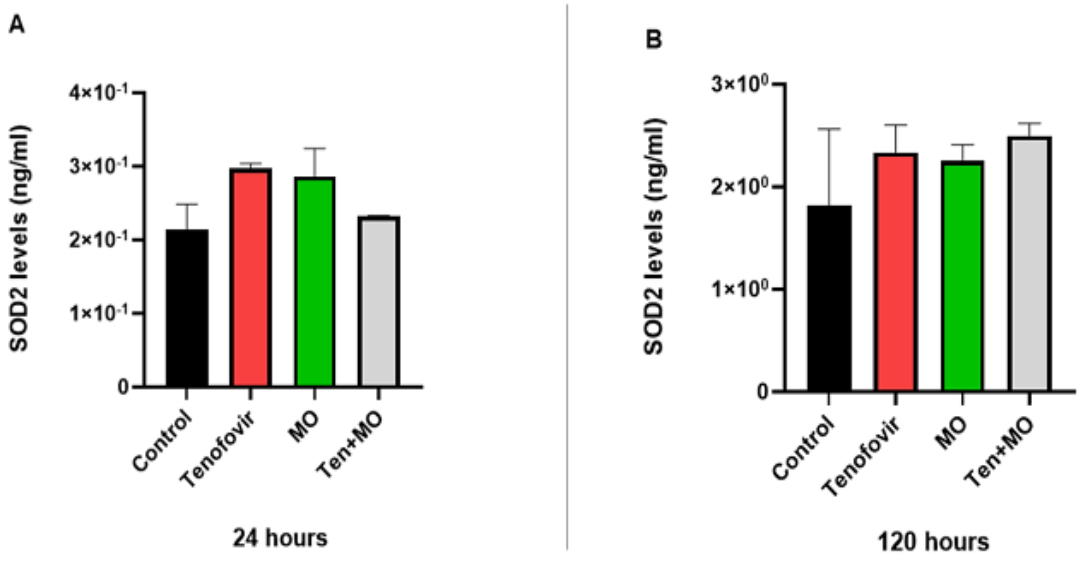


**Figure 4.3: Quantitative ELISA analysis of SOD2 levels in HepG2 cells following (A) acute (24-hour) and (B) chronic (120-hour) exposure to treatment groups.** No statistically significant difference was observed relative to the control ($p > 0.05$).

No statistically significant difference was observed compared to the control but a trend was seen. SOD2 was increased by all treatment groups, following acute and chronic treatment exposure compared to the control group.

### 4.4. Quantification of Catalase Activity

Catalase is an antioxidant enzyme that participates in the dismutation of $H_2O_2$ to oxygen and water. The ELISA was conducted to quantify catalase levels, as presented in Figures 4.4 A and B.

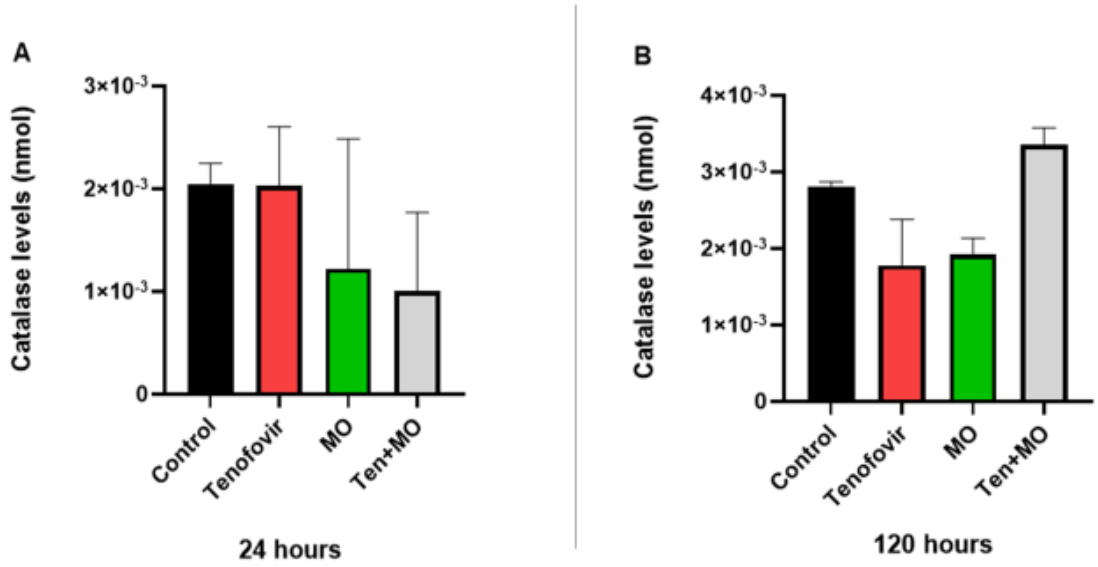


**Figure 4.4: Quantitative ELISA analysis of catalase levels in HepG2 cells following (A) acute (24-hour) and (B) chronic (120-hour) exposure to treatment groups.** No statistically significant difference was observed relative to the control ($p > 0.05$).

The results reported no significant difference but a trend was seen. Following a 24-hour treatment exposure, all the treatment groups decreased calatale levels. At 120-hour exposure,

tenofovir and MO decreased catalase levels. However, the combination treatment group increased catalase levels compared to the control.

## 4.5. Quantification of Glutathione

The antioxidant function of glutathione (GSH) is to reduce $H_2O_2$ to water and lipid peroxides to their corresponding alcohols. The Glutathione-Glo™ Assay was used to quantify the total amount of GSH levels, as presented in Figures 4.5 A and B.

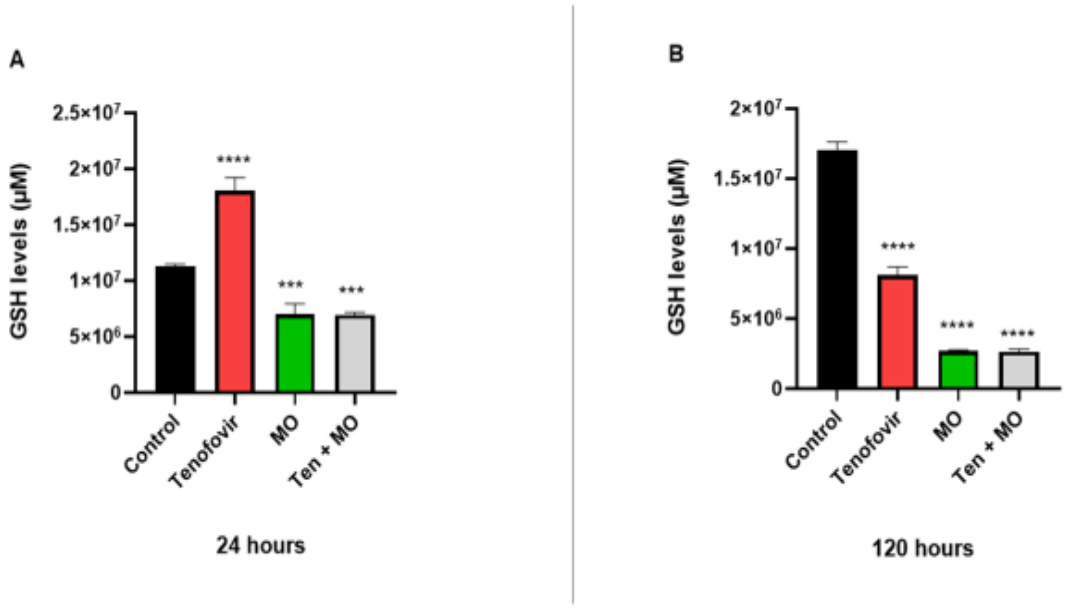


**Figure 4.5: GSH levels in HepG$_2$ cells following (A) acute (24-hour) and (B) chronic (120-hour) exposure to treatment.** Statistically significant differences were observed between the treatment and control groups (***, $p = 0.0006$, ***, $p = 0.0007$ and ****, $p < 0.0001$).

**Table 4.1:** GSH levels in $HepG_2$ liver cells after acute and chronic treatment exposure

| Acute (24-hour) treatment exposure Mean ± SEM (µM) | | | P value |
|---|---|---|---|
| Ctrl vs TDF | $1{,}13 \times 10^7 \pm 1{,}69 \times 10^5$ | $1{,}81 \times 10^7 \pm 1{,}14 \times 10^6$ | ****p < 0.0001 |
| Ctrl vs MO | $1{,}13 \times 10^7 \pm 1{,}69 \times 10^5$ | $6{,}99 \times 10^6 \pm 9{,}57 \times 10^5$ | ***p = 0.0007 |
| Ctrl vs TDF + MO | $1{,}13 \times 10^7 \pm 1{,}69 \times 10^5$ | $6{,}97 \times 10^6 \pm 1{,}82 \times 10^5$ | ***p = 0.0006 |
| Chronic (120-hour) treatment exposure Mean ± SEM | | | P value |
| Ctrl vs TDF | $1{,}70 \times 10^7 \pm 6{,}09 \times 10^5$ | $8{,}13 \times 10^6 \pm 5{,}67 \times 10^5$ | ****p < 0.0001 |
| Ctrl vs MO | $1{,}70 \times 10^7 \pm 6{,}09 \times 10^5$ | $2{,}71 \times 10^6 \pm 7{,}81 \times 10^4$ | ****p < 0.0001 |
| Ctrl vs TDF + MO | $1{,}70 \times 10^7 \pm 6{,}09 \times 10^5$ | $2{,}65 \times 10^6 \pm 1{,}66 \times 10^5$ | ****p < 0.0001 |

***** Significantly different compared to control; **SEM**: standard error of the mean; **Ctrl**: control; **TDF**: tenofovir; **MO**: *Moringa oleifera*

Following a 24-hour treatment exposure, the data revealed a significant increase in GSH levels in the tenofovir-treated group (****p < 0.0001). MO (***p = 0.0007) and the combination treatment group (***p = 0.0006) revealed decreased GSH levels relative to the control. Following a 120-hour treatment exposure, all treatment groups showed decreased GSH levels relative to the control (****p < 0.0001).

## 4.6. qPCR – Determination of mRNA expression (*NRF2, SOD2, GCLC, catalase*)

The quantitation polymerase chain reaction (qPCR) was conducted to determine the gene expression of *NRF2, SOD2, CCLC,* and *catalase*, as presented below.

### (i) mRNA expression of *NRF2*

The transcription factor NRF2 is a key player in antioxidant defence. It induces the transcription of antioxidants and cytoprotective genes, including GSH, by interacting with the antioxidant response elements (Kavain et al., 2021). The mRNA expression of *NRF2* was determined following treatment, as presented in Figures 4.6 A and B.

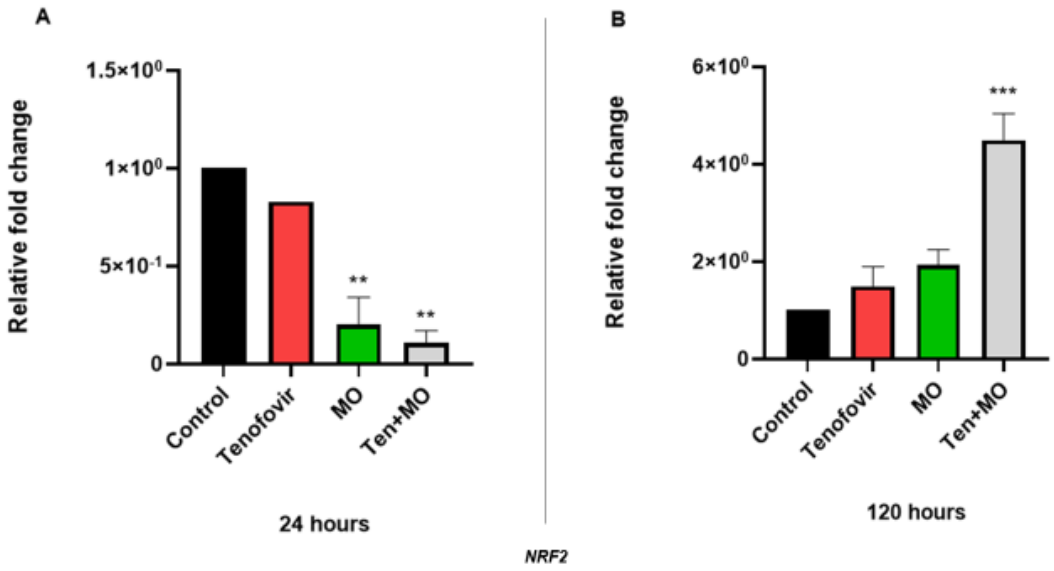


**Figure 4.6: mRNA expression of *NRF2* in HepG$_2$ cells following (A) acute (24-hour) and (B) chronic (120-hour) exposure to treatment.** Statistically significant differences were observed between the treatment and control groups (**, $p < 0.001$, and ***, $p < 0.0003$).

Following a 24-hour treatment exposure, the data revealed that tenofovir ($p > 0.05$), ( MO (**$p = 0.0019$) and the combination treatment group (**$p = 0.0011$) decreased *NRF2* expression relative to the control. However, following a 120-hour treatment exposure, tenofovir ($p > 0.05$), MO ($p > 0.05$), and the combination group (***$p < 0.0003$) increased *NRF2* expression relative to the control.

### (ii) mRNA expression of *GCLC*

The antioxidant function of the *GCLC* is to encode the production of proteins involved in GSH synthesis. Figures 4.7 A and B present the results for the gene expression of *GCLC*.

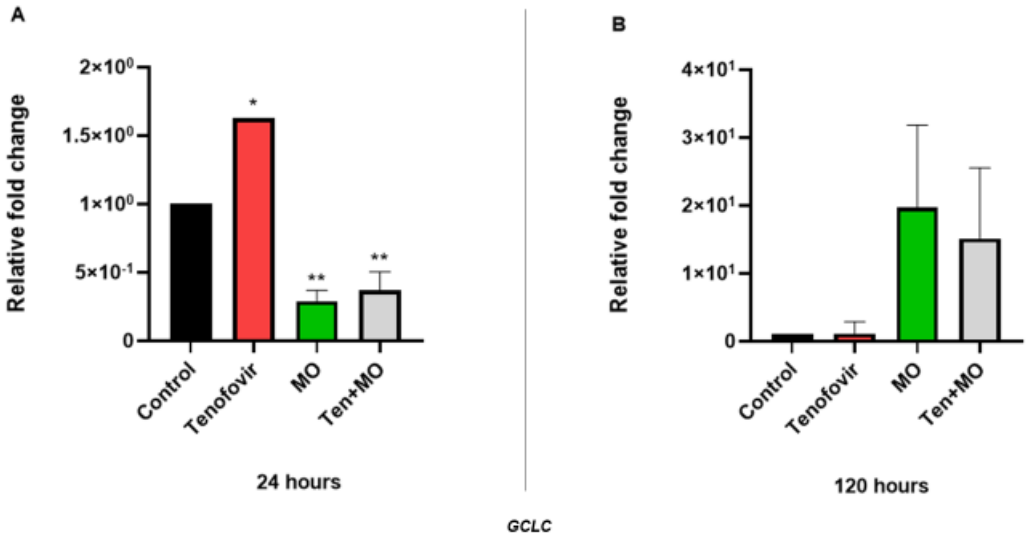


**Figure 4.7: mRNA expression of *GCLC* in HepG2 cells following (A) acute (24-hour) and (B) chronic (120-hour) exposure to treatment.** Statistically significant differences were observed between the treatment and control groups (*, $p < 0.05$ and**, $p < 0.001$).

Following a 24-hour treatment exposure, the data revealed a significant increase in *GCLC* expression in tenofovir-treated cells (*p < 0.0398). MO (**p = 0.0044) and the combination treatment group (**p = 0.0078) significantly decreased *GCLC* expression relative to the control. Although no significant difference was observed following a 120-hour exposure, a treand was seen. There was no change in *GCLC* expression in tenofovir-treated cells, MO and combination group increased *GCLC* expression.

### (iii) mRNA expression of *SOD2*

Gene expression of *SOD2* is presented below in Figures 4.8 A and B.

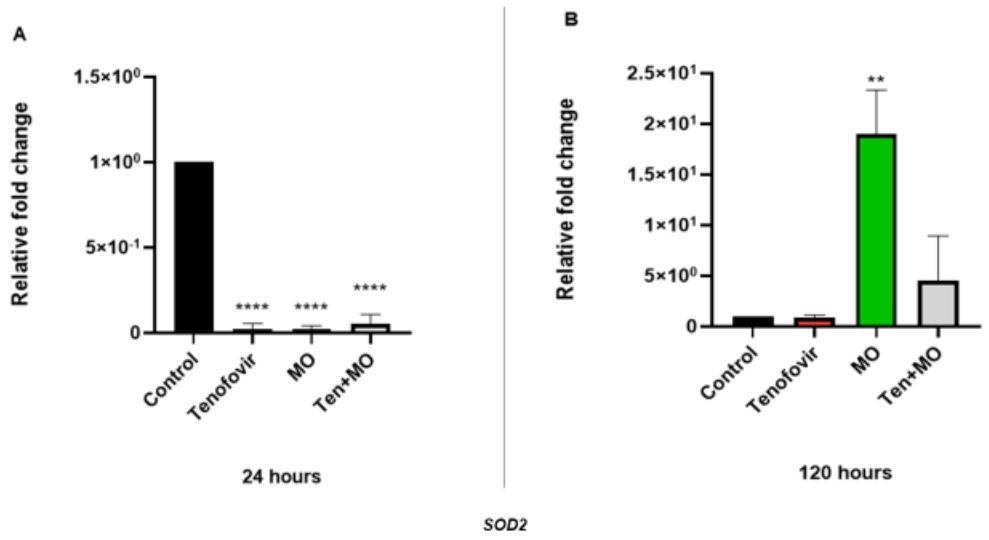


**Figure 4.8: mRNA expression of *SOD2* in HepG$_2$ cells following (A) acute (24-hour) and (B) chronic (120-hour) exposure to treatment.** Statistically significant differences were observed between the treatment and control groups (**, p < 0.001, and ****, p < 0.0001).

Following a 24-hour treatment exposure, the data revealed that tenofovir (****p < 0.0001), MO (****p < 0.0001), and the combination treatment group (****p < 0.0001) significantly

decreased *SOD2* expression relative to the control. However, following a 120-hour treatment exposure, there was so significant change in of *SOD2* expression in tenofovir-treated cells ($p > 0.05$). MO significantly increased *SOD2* expression relative to the control (**$p = 0.0047$). The combination group increased the expression of *SOD2* ($p > 0.05$) compared to the control group.

### (iv) mRNA expression of *catalase*

Figures 4.9 A and B present gene expression of *catalase*.

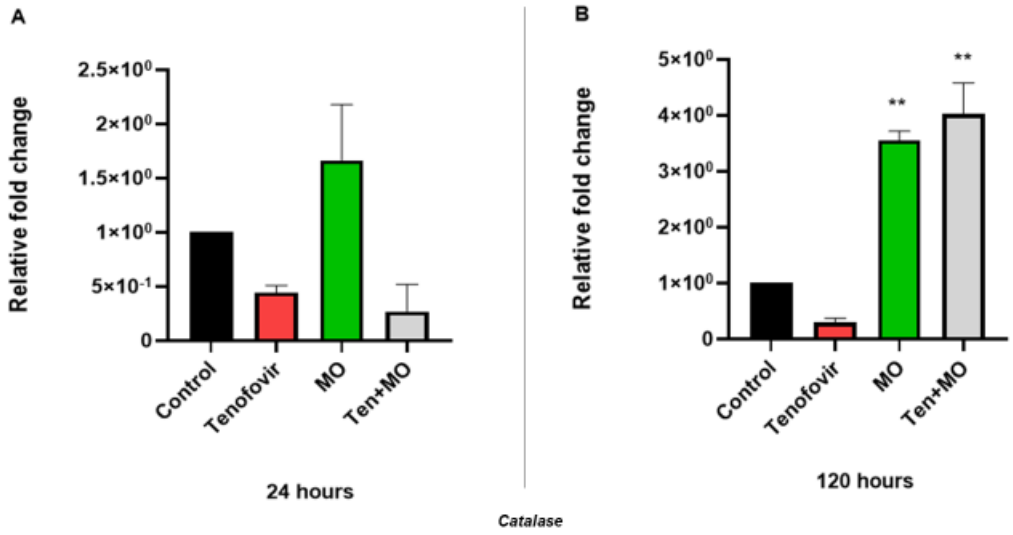


**Figure 4.9: mRNA expression of *catalase* in HepG2 cells following (A) acute (24-hour) and (B) chronic (120-hour) exposure to treatment.** Statistically significant differences were observed between the treatment and control groups (**, $p < 0.001$). MO (**$p = 0.0027$) and the combination group (**$p = 0.0014$) significantly increased *catalase* expression following a 120-hour treatment exposure.

The results reported no significant difference following a 24-hour treatment exposure but a trend was observed. Tenofovir and the combination group decreased *catalase* expression.

However, MO increased *catalase* expression compared to control ($p > 0.05$). Following a 120-hour exposure tenofovir decreased *catalase* expression. However, MO (**p = 0.0027) and the combination group (**p = 0.0014) significantly increased *catalase* expression compared to the control.

## 4.7. Western Blot – Preliminary Determination of Protein Expression (NRF2, p-NRF2, SOD2, catalase)

### (i) Protein expression of NRF2

During oxidative stress, NRF2 is activated and is a key player in regulating antioxidants. Protein expression of NRF2 following acute and chronic treatment exposure is presented in Figures 4.10 A and B.

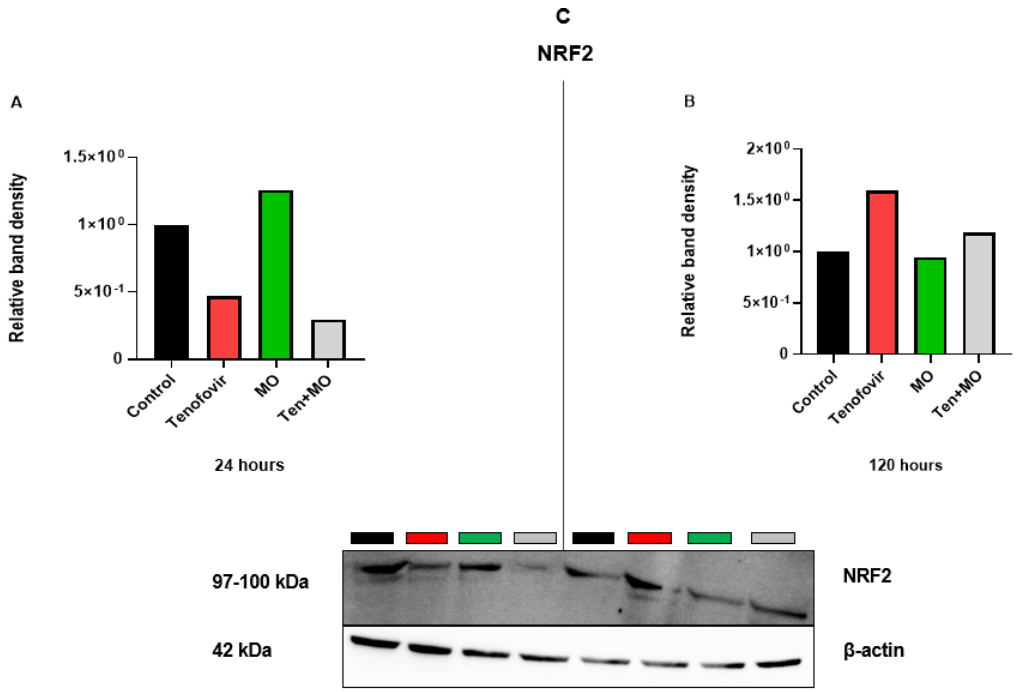

**Figure 4.10: Protein expression of NRF2 in HepG$_2$ cells following (A) acute (24-hour) and (B) chronic (120-hour) exposure to treatment. (C)** representative western blot and densitometric analysis for NRF2 (n = 1)

Following a 24-hour treatment exposure, the data revealed that tenofovir and the combination treatment group decreased NRF2 expression relative to the control. MO increased NRF2 expression. However, following a 120-hour treatment exposure, MO decreased NRF2 expression relative to the control. Tenofovir, as well as the combination group, increased NRF2 expression compared to the control.

### (ii) Protein expression of p-NRF2

During oxidative stress, NRF2 is stimulated and phosphorylated to its active form (p-NRF2). p-NRF2 translocates to the nucleus, binds to the antioxidant response element, and allows the transcription of antioxidants. Protein expression of p-NRF2 following acute and chronic treatment exposure is presented in Figures 4.11 A and B.

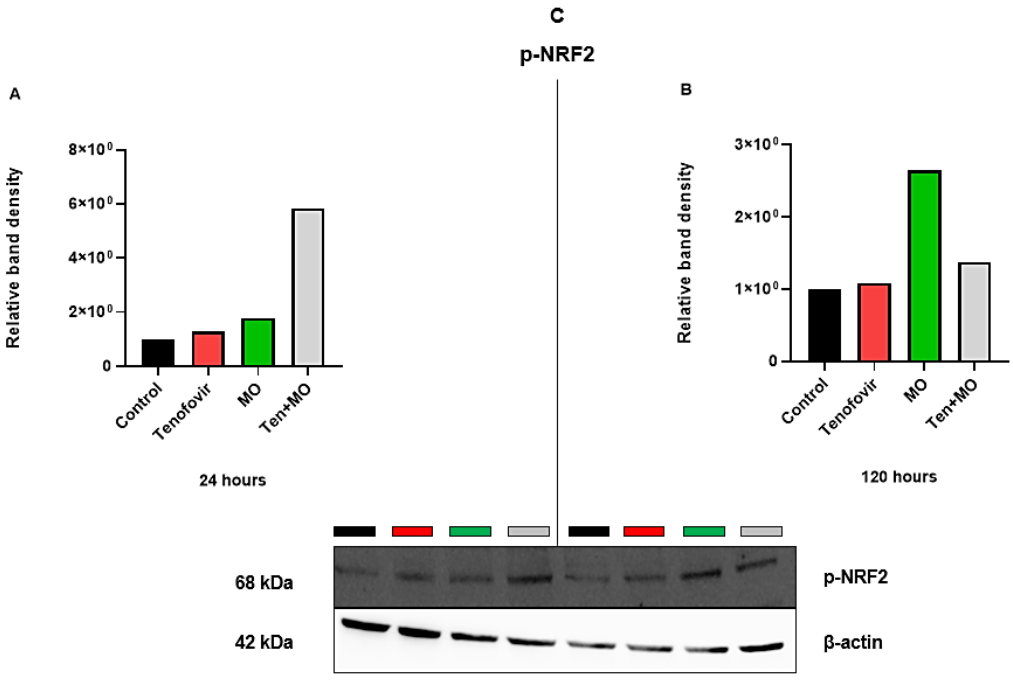

**Figure 4.11: Protein expression of p-NRF2 in HepG$_2$ cells following (A) acute (24-hour) and (B) chronic (120-hour) exposure to treatment. (C)** representative western blot and densitometric analysis for p-NRF2 (n = 1)

The data revealed that tenofovir, MO, and the combination treatment group increased p-NRF2 expression relative to the control at acute and chronic treatment exposure.

### (iii) Protein expression of SOD2

Protein expression of SOD2 following acute and chronic treatment exposure is presented in Figures 4.12 A and B.

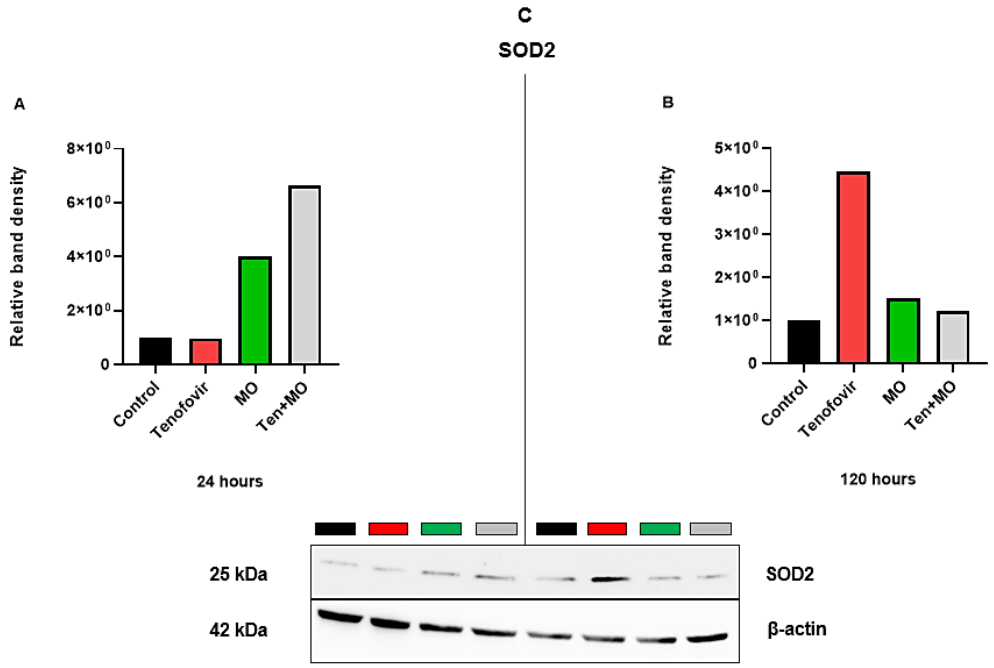


**Figure 4.12: Protein expression of SOD2 in HepG$_2$ cells following (A) acute (24-hour) and (B) chronic (120-hour) exposure to treatment. (C)** representative western blot and densitometric analysis for SOD2 (n = 1)

Following a 24-hour treatment, the tenofovir-treated group decreased SOD2 expression. However, at 120 hours, tenofovir increased SOD2 compared to the control. MO and the combination treatment group increased SOD2 expression relative to the control at acute and chronic treatment exposure.

### (iv) Protein expression of catalase

Protein expression of catalase following acute and chronic treatment exposure is presented in Figures 4.13 A and B.

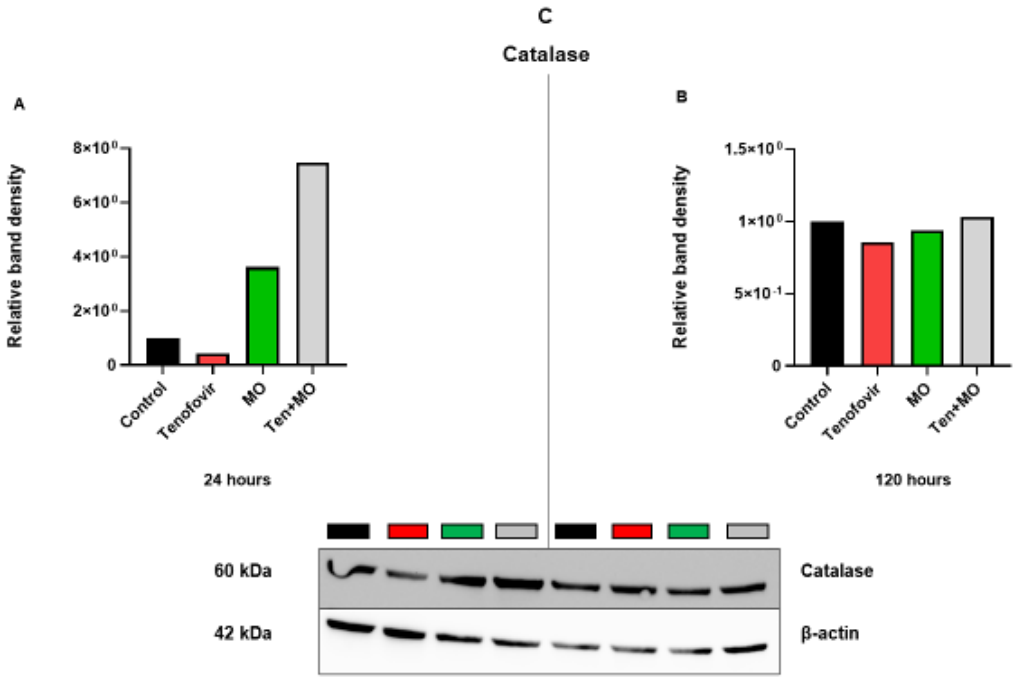


**Figure 4.13: Protein expression of catalase in HepG2 cells following (A) acute (24-hour) and (B) chronic (120-hour) exposure to treatment. (C)** representative western blot and densitometric analysis for catalase (n = 1)

Data revealed that the tenofovir-treated group decreased catalase expression compared to the control group at acute and chronic treatment exposure. Following 24-hour treatment, MO

increased catalase expression. However, at 120 hours, MO decreased catalase relative to the control. Compared to the control, the combination group increased catalase expression at acute and chronic treatment exposure.

# Chapter 5

## 5. Discussion

Lipid peroxidation was used as a marker of oxidative stress. The thiobarbituric reactive substances (TBARS) assay was used to quantify extracellular malondialdehyde (MDA), a by-product of lipid peroxidation. The findings (Figures 4.2 A and B) showed decreased MDA levels in tenofovir-treated cells after 24-hour exposure. However, at 120 hours, tenofovir increased MDA levels ($p > 0.05$). Similar to these findings, a study by Ndlovu et al. (2023) reported that following a 96-hour treatment exposure, tenofovir increased MDA levels in $HepG_2$ cells (Ndlovu et al., 2023). A study by Nagiah et al. (2015) showed an increase in extracellular MDA levels following the exposure of $HepG_2$ cells to tenofovir at 24 or 120 hours (Nagiah et al., 2015). In a study by Mohan et al. (2023), $HepG_2$ cells were treated with Tenofovir, Lamivudine, and Dolutegravir in singular and combinational doses for a period of 120 hours to assess the effect of ART on metabolic syndrome. The results revealed a significant increase in MDA levels in tenofovir-treated cells compared to the control (Mohan et al., 2023). These findings suggest that tenofovir induces oxidative stress in $HepG_2$ cells by upregulating lipid peroxidation.

Following a 24-hour treatment exposure, tenofovir significantly increased GSH levels (Figure 4.5 A), as MDA levels decreased at that point (Figure 4.2 A). However, over time, the cytotoxic effect of tenofovir was observed when GSH levels significantly decreased (Figure 4.5 B) due to increased MDA levels (Figure 4.2 B). In line with these findings, an *in vivo* study by Adikwu et al. (2016) showed that treatment with tenofovir/nevirapine for 30 days significantly decreased GSH levels in the liver and kidney of male albino rats compared to the untreated control (Adikwu and Williams, 2016). Further supporting these findings, an *in vitro* study by

Ndlovu et al. (2023) also showed a significant decrease in GSH levels following a 96-hour treatment exposure to tenofovir (Ndlovu et al., 2023). The findings suggest that increased levels of reactive oxygen species (ROS) exceeded the antioxidant capacity of GSH to neutralise toxicity and maintain cellular redox homeostasis. The findings (Figure 4.3 A and B) showed that tenofovir-treated cells increased SOD2 activity ($p > 0.05$) following 24 and 120-hour exposure. However, even though tenofovir-treated cells induced SOD2, other antioxidants, catalase (Figure 4.4 A and B) ($p > 0.05$) and GSH were downregulated following a 24 and 120-hour treatment exposure.

The effect of MO on oxidative stress and antioxidant responses was evaluated. The findings (Figures 4.2 A and B) showed no significant change in MDA levels of MO-treated cells compared to the control following acute and chronic treatment exposure ($p > 0.05$). These findings align with a recent study by Duranti et al. (2021), which showed that following a 24-hour exposure of skeletal muscles to MO, there was no significant change in MDA levels relative to the control (Duranti et al., 2021). In a study by Mansour et al. (2014), the ameliorative role of MO aqueous leaf extract against γ-radiation (IRR)-induced oxidative stress in hepatic and renal tissues in rats was evaluated. The findings revealed that the administration of MO for 15 days before irradiation induced a complete restoration of MDA levels to the control level (Mansour et al., 2014). Contrary to these findings, a study by Tiloke et al. (2019) showed a significant increase in MDA levels in $HepG_2$ cells exposed to MO for 24 hours (Tiloke et al., 2019). A study by Shunmugam (2016) also showed that following a 72-hour exposure, the MDA levels were significantly elevated in the MO-treated $HepG_2$ cells compared to the control (Shunmugam, 2016). Findings by Tiloke et al. (2019) and Shunmugam (2016) suggest that MO can enhance oxidative metabolism, leading to increased production of ROS in $HepG_2$ cells. However, it is noteworthy that MO-treated cells can counteract ROS production

over time due to the upregulation of endogenous enzymatic activities (Figure 4.2 A and B; Duranti et al., 2021; Mansour et al., 2014).

The antioxidant effect of MO was also observed when the combination group (tenofovir + MO) decreased MDA levels (Figure 4.2 B) ($p > 0.05$). In line with these findings, a study by Ndlovu et al. (2023) exposed $HepG_2$ cells to tenofovir for 96 hours, followed by MO leaf extract for 24 hours. The results showed a decrease in MDA levels in cells treated with tenofovir and MO compared to the control (Ndlovu et al., 2023). The decrease in ROS can be attributed to the MO leaf extract, which contains the most significant amounts of flavonoids, including quercetin, phenolic acids, and carotenoids. Flavonoids act as antioxidants, eliminating free radicals (Nizioł-ŁUkaszewska et al., 2020). The findings (Figure 4.3 and 4.4) revealed that MO-treated cells increased SOD2 and decreased catalase following 24 and 120-hour exposure ($p > 0.05$). The combination group however, increased SOD2 and catalase activity after 24 and 120 hours relative to the control ($p > 0.05$). MO leaf extract treatment exposure significantly decreased GSH levels at acute and chronic treatment exposure relative to the control (Figures 4.5 A and B). This resulted in a significant decrease in GSH levels in the combination group. The substantial reduction in GSH levels might be because $H_2O_2$ oxidizes cysteine in GSH to produce glutathione disulphide (GSSG), thereby decreasing the antioxidant capacity of GSH (Tiloke et al., 2013).

The effect of tenofovir and MO on GSH was further evaluated by assessing the expression of the glutamate-cysteine ligase catalytic subunit (*GCLC*) gene. *GCLC* encodes glutamate cysteine ligase (GCL), an enzyme catalysing the first of two ATP-dependent steps in GSH synthesis. NRF2 is a transcription factor activated during oxidative stress. It regulates the expression of over 1000 genes in the cell, including the *SOD2*, *CAT*, and *GCLC* genes (Zang

et al., 2020; Duranti et al., 2021; Franklin et al., 2009). Following a 24-hour treatment exposure, the data (Figure 4.7 A) revealed a significant increase in *GCLC* expression in tenofovir-treated cells. MO and the combination treatment group significantly decreased *GCLC* compared to the control. However, over time, *GCLC* was downregulated comparable to control in tenofovir-treated cells and upregulated by the MO and combination treatment group (Figure 4.7 B) ($p > 0.05$). Initially, following a 24-hour exposure, the findings (Figures 4.6 A, 4.8 A) showed that MO and combination group significantly decreased *NRF2* and *SOD2* expression. Then overtime, the antioxidant effect of MO was observed when MO and the combination treatment group increased the mRNA expression of *NRF2*, *SOD2*, and *CAT* following a 120-hour treatment exposure (Figures 4.6 B, 4.8 B, and 4.9). In line with these findings, a study by Cheng et al. (2019) showed that $HepG_2$-C8 cells exposed to MO isothiocyanate for 24 hours increased mRNA expression of *NRF2* and *NRF2*-regulated gene, *GCLC* compared to the control (Cheng et al., 2019). In 2020, Soliman and colleagues explored the protective effects of MO leaf extract against oxidative stress and hepatic and renal injuries caused by methotrexate (MTX) therapy. The results revealed that mRNA expression of *NRF2* was upregulated in mice treated with 300 mg/kg of MO for 12 days prior to administration with MTX (Soliman et., 2020). Upregulation of *NRF2* by MO resulted in the activation of several genes (*SOD2, CAT*, and *GCLC*) that encode antioxidant proteins.

Protein expression was evaluated, and the preliminary results (Figures 4.10, 4.11, and 4.12) showed a gradual increase in NRF2, p-NRF2, and SOD2 expression following acute and chronic exposure in tenofovir-treated cells. CAT was, however, decreased following acute and chronic treatment exposure. In 2023, Mohan and colleagues reported an increased protein expression of p-NRF2 and CAT and no significant change in SOD2 in tenofovir-treated $HepG_2$ cells relative to the control following a 120-hour exposure (Mohan et al., 2023). The

upregulation of NRF2, p-NRF2, and SOD2 in tenofovir-treated cells might suggest that high levels of ROS were present in the mitochondria following exposure, activating the NRF2-antioxidant pathway. MO leaf extract upregulated NRF2 (Figure 4.10 A) and CAT (Figure 4.13 A). Then following a 120-hour exposure, NRF2 (Figure 4.10 B) and CAT (Figure 4.13 B) were downregulated, comparable to the control. The initial upregulation of NRF2 following MO treatment might have been due to a rise in ROS levels, leading to increased production of CAT to counteract ROS. Then the decrease in ROS levels led to the downregulation of NRF2 and CAT, as seen following 120-hour exposure. The upregulation of p-NRF2 and SOD2 (Figure 4.11 and 4.12) by MO-treated cells suggests that p-NRF2 activated antioxidant response element (ARE) and allowed the transcription of antioxidants, including SOD2. The antioxidant effect of MO was further observed (Figures 4.10, 4.11, 4.12, and 4.13) when the combination group upregulated the protein expression of NRF2, p-NRF2, SOD2, and CAT to protect against oxidative stress. Supporting these findings, a study by Ndlovu et al. (2023) reported a significant increase in protein expression of NRF2, p-NRF2, SOD2, and CAT in $HepG_2$ cells treated with tenofovir and MO (Ndlovu et al., 2023). MO leaf extract contains many bioactive compounds, predominantly isothiocyanate origin, and polyphenols that are reported to activate the NRF2-ARE pathway, inducing antioxidant production (Manjunath et al., 2023). Therefore, this study showed that MO has a hepatoprotective effect against antiretroviral-induced cytotoxicity. It has thus provided evidence to support the notion that MO can help mitigate the harmful impact of antiretroviral medications on liver cells, potentially offering a protective mechanism against drug-induced liver damage.

# Chapter 6

## 6. Conclusion

Nucleoside reverse transcriptase inhibitors (NRTIs) form the backbone of combination antiretroviral therapy (ART) in HIV treatment (Nagiah et al., 2015). NRTI-based ART has successfully been used to manage HIV and improve the overall health of HIV/AIDS patients (Ikekpeazu et al., 2019; Balogun and Serghides, 2022). However, the prolonged use of NRTIs has been associated with adverse metabolic effects, such as dyslipidaemia, lipodystrophy, hepatic steatosis, and lactic acidosis (Balogun and Serghides, 2022). Mitochondrial toxicity and oxidative stress are recognised as significant side effects of NRTI-based ART (Bañó et al., 2020). Due to the side effects associated with ART, people living with HIV (PLHIV), especially in the rural areas of South Africa (SA), tend to use traditional remedies such as medicinal trees/plants to ameliorate the side effects associated with the use of ART (Biswas et al., 2019).

*Moringa oleifera* (MO) is one of the medicinal trees used in traditional medicine by PLHIV as adjuvant therapy to improve their health (Monera-Penduka et al., 2017). MO is an ancient remedy tree known as the “miraculous plant” or the “Tree of Life” due to its many prominent uses and significant health benefits. It is nutrient-rich, with exceptional bioactive compounds, such as polyphenols, possessing several medicinal properties (Azlan et al., 2022). Due to the high concentrations of polyphenols in its leaves and flowers, MO is important in protecting the liver from damage, oxidation, and toxicity (García Milla et al., 2021). However, there is a scarcity of studies evaluating the hepatoprotective effects of MO in NRTI-induced oxidative stress in developing countries. Therefore, this study aimed to evaluate the effect of MO on oxidative stress and antioxidant response in $HepG_2$ cells in vitro following acute (24-hour) and chronic (120-hour) exposure to tenofovir, an NRTI.

The study showed that prolonged exposure to tenofovir may, to some extent, cause toxicity, mainly through oxidative stress. Tenofovir upregulated lipid peroxidation, downregulated glutathione, and expression of some antioxidants. Furthermore, although GSH (which is the 1st line defence for antioxidant pathway) was downregulated, other oxidant pathways were upregulated, which eventually counteracted the hepatotoxicity induced by tenofovir – therefore, time-dependent, for chronic exposure is required to ensure sufficient activation of that antioxidant pathways. MO attenuated ART's toxicity, as observed in the combination treatment group, by downregulating lipid peroxidation and upregulating the NRF2-antioxidant pathway, thus reducing oxidative stress. In conclusion, MO aqueous leaf extract can potentially ameliorate toxicity induced by tenofovir. It has great therapeutic potential and may be considered a potential adjuvant therapy for people living with HIV/AIDS.

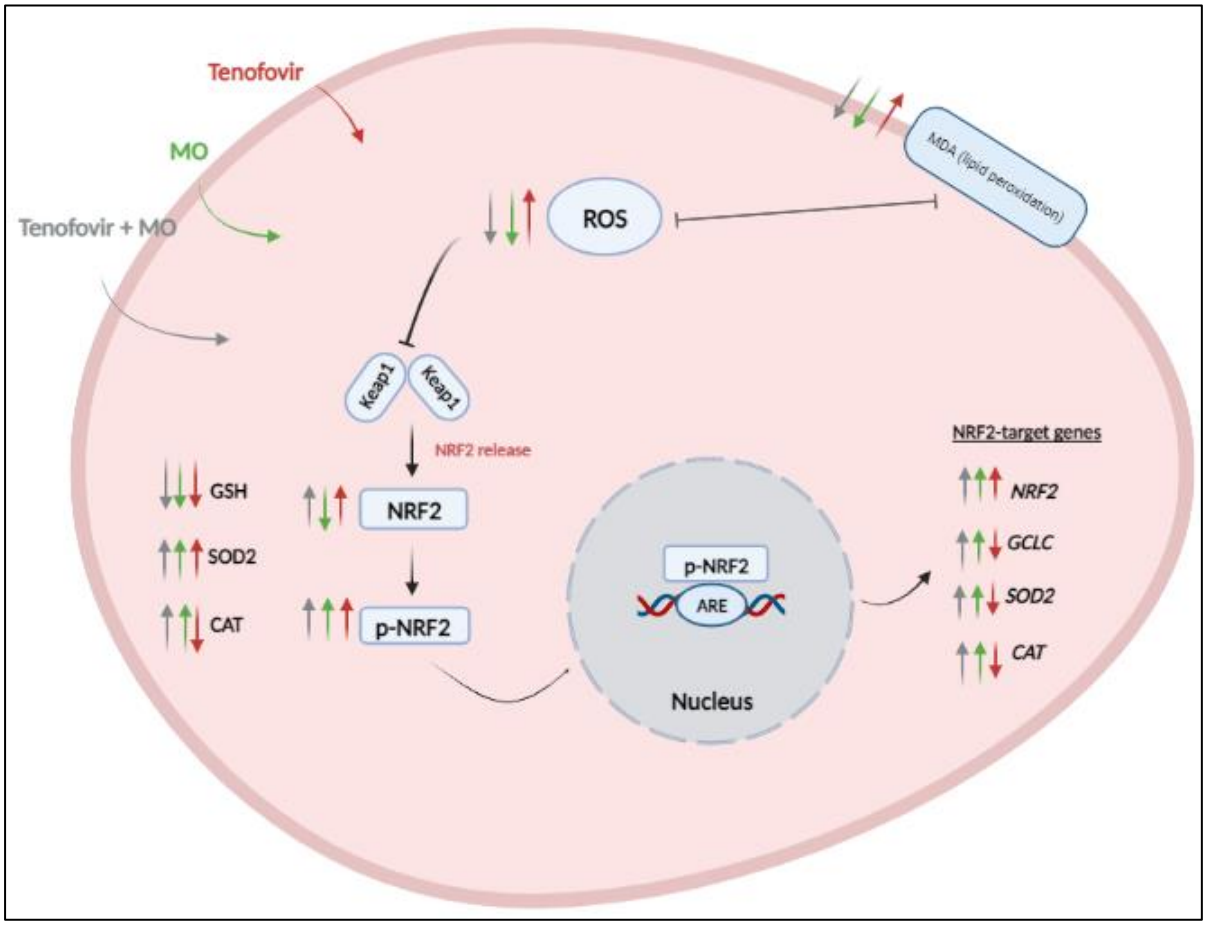


**Figure 6.1: A brief overview of the effect of treatment groups on oxidative stress and antioxidant response in HepG$_2$ cells *in vitro* following acute (24-hour) and chronic (120-hour) exposure to tenofovir** (created by the researcher, M. Saki, in 2023 using Biorender.com software).

## 6.1. Recommendation for future studies

Future study can have a baseline ($t_0$) and additional time points ($t_{48}$, $t_{72}$, and $t_{96}$) to observe the effect of MO at different time points and add more validity to the results. ELISA results reported no significant difference, therefore, an increase in time points might produce statistically significant difference. Additionally, studies can further assess intracellular ROS using flow cytometry to investigate the cytotoxicity of tenofovir. Studies can also assess which

bioactive compounds are responsible for inducing the NRF2-antioxidant pathway following chronic exposure of $HepG_2$ cells to ART. Bioactive compounds from leaves can be extracted using the ultrasound-assisted extraction method. High-performance liquid chromatography with tandem mass spectrometry can be used to separate and identify active components. Further studies are also required to determine the antioxidant effect of MO leaf extract in a multicellular system (*in vivo* model) following treatment with prescribed ART. Using *in vivo* models, researchers can observe the holistic responses and systemic effects of interventions or treatments, providing a more comprehensive understanding of the biological processes under investigation. This may bridge the gap between laboratory findings and their translation into effective therapies or interventions in living organisms by assessing MO's biodistribution, safety, and efficacy in a model system that closely mimics the complex interactions and conditions present in a living organism. For translational research, it is recommended that a patient on ART be on long-term use of MO, for it is unlikely to benefit from short-term use. However, further research is warranted.

## 6.2. Limitations of the study

The present study provided valuable insights into the extent to which MO can reduce oxidative stress by regulating antioxidants. However, there were limitations. Tenofovir is not administered on its own but rather as a combination therapy. The current study only reported on the effect of tenofovir and combination treatment group, and did not look at the effect of the other two drugs in the TLD treatment regimen. The findings for TBARS and ELISA (Catalase activity) were consistent with the literature but were not statistically significant. ELISA (n = 2) and western blotting (n = 1) could not be conducted in triplicate and repeated thrice. However, although these experimental techniques could not report statistically significant differences, a

trend was seen. This may be attributed, at least in part, to the limited optimisation of purification steps, antibodies' incubation time, and primary antibody dilutions.

## References


Aavani, P., and Allen, L. J. S. (2019). The role of CD4 T cells in immune system activation and viral reproduction in a simple model for HIV infection. *Applied Mathematical Modelling*, *75*, 210–222. https://doi.org/10.1016/j.apm.2019.05.028.

Aboyade, O.M., Styger, G., Gibson, D., and Hughes, G. (2014). Sutherlandia frutescens: The meeting of science and traditional knowledge. *The Journal of Alternative and Complementary Medicine*, *20*(2), pp.71-76.

Adikwu, E., and Williams, A. (2016). "Ameliorative effects of vitamins C and E on tenofovir/nevirapine-induced hepatorenal oxidative stress in albino rats", *Indonesian Journal of Pharmacy*, Universitas Gadjah Mada - Faculty of Pharmacy, Vol. 27 No. 4, pp. 211–219, doi: 10.14499/indonesianjpharm27iss4pp211.

Akay, C., Cooper, M., Odeleye, A., Jensen, B. K., White, M. G., et al. (2014). Antiretroviral drugs induce oxidative stress and neuronal damage in the central nervous system. *Journal of NeuroVirology*, *20*(1), 39–53. https://doi.org/10.1007/s13365-013-0227-1.

Alessandro Leone, Alberto Spada, Alberto Battezzati, Alberto Schiraldi, J. A., and S. B. (2015). Cultivation, genetic, ethnopharmacology, phytochemistry and pharmacology of Moringa oleifera leaves: An overview. *International Journal of Molecular Sciences*, *16*(6), 12791–12835. https://doi.org/10.3390/ijms160612791.

Alkadi, H. (2018). A Review on Free Radicals and Antioxidants. *Infectious Disorders - Drug Targets*, *20*(1), 16–26. https://doi.org/10.2174/1871526518666180628124323.

Altemimi, A., Lakhssassi, N., Baharlouei, A., Watson, D.G., and Lightfoot, D.A. (2017).

Phytochemicals: Extraction, isolation, and identification of bioactive compounds from plant extracts. *Plants*, *6*(4), 42.

Anderson, P. L., Kiser, J. J., Gardner, E. M., Rower, J. E., Meditz, A., and Grant, R. M. (2011). Pharmacological considerations for tenofovir and emtricitabine to prevent HIV infection. *Journal of Antimicrobial Chemotherapy*, *66*(2), 240–250. https://doi.org/10.1093/jac/dkq447.

Anderson, S. M., Naidoo, R. N., Pillay, Y., Tiloke, C., Muttoo, S., et al. (2018). HIV induced nitric oxide and lipid peroxidation, influences neonatal birthweight in a South African population. *Environment International*, *121*, 1–12. https://doi.org/10.1016/j.envint.2018.08.042.

Andrade, J., Ramos, D., Ramos Andrade Júnior, D. DE, Becco Souza, R. DE, Alves Dos Santos, S., et al. (2005). Oxygen free radicals and pulmonary disease. *Jornal Brasileiro de Pneumologia*, *31*(311), 608.

Andrés Juan, C., Manuel Pérez de la Lastra, J., Plou, F. J., Pérez-Lebeña, E., and Reinbothe, S. (2021). Molecular Sciences The Chemistry of Reactive Oxygen Species (ROS) Revisited: Outlining Their Role in Biological Macromolecules (DNA, Lipids and Proteins) and Induced Pathologies. *Int. J. Mol. Sci*, *22*, 4642. https://doi.org/10.3390/ijms.

AVERT. (2020). *South Africa 90-90-90 Progress*. *August*, 2020. https://www.avert.org/infographics/south-africa-90-90-90-progress.

Ayala, A., Mario, F,M., and Sandro, A. (2014). Lipid peroxidation: production, metabolism, and signalling mechanisms of malondialdehyde and 4-hydroxy-2-nenonal. *Oxidative medicine and cellular longevity* 2014.

Azlan, U.K., Mediani, A., Rohani, E.R., Tong, X., Han, R., Misnan, N.M., Jam, F.A., *et al.* (2022). "A Comprehensive Review with Updated Future Perspectives on the Ethnomedicinal and Pharmacological Aspects of Moringa oleifera", *Molecules*, MDPI, 1 September, doi: 10.3390/molecules27185765.

Balogun, K., and Serghides, L. (2022). "Comparison of the Effects of Three Dual-Nucleos(t)ide Reverse Transcriptase Inhibitor Backbones on Placenta Mitochondria Toxicity and Oxidative Stress Using a Mouse Pregnancy Model", *Pharmaceutics*, MDPI, Vol. 14 No. 5, doi: 10.3390/pharmaceutics14051063.

Bañó, M., Morén, C., Barroso, S., Juárez, D.L., Guitart-Mampel, M., González-Casacuberta, I., Canto-Santos, J., *et al.* (2020). "Mitochondrial Toxicogenomics for Antiretroviral Management: HIV Post-exposure Prophylaxis in Uninfected Patients", *Frontiers in Genetics*, Frontiers Media S.A., Vol. 11, doi: 10.3389/fgene.2020.00497.

Barrera, G., Pizzimenti, S., Daga, M., Dianzani, C., Arcaro, A., et al. (2018). Lipid peroxidation-derived aldehydes, 4-hydroxynonenal and malondialdehyde in aging-related disorders. *Antioxidants*, *7*(8). https://doi.org/10.3390/antiox7080102.

Behnisch-Cornwell, S., Wolff, L., and Bednarski, P. J. (2020). The effect of glutathione peroxidase-1 knockout on anticancer drug sensitivities and reactive oxygen species in haploid HAP-1 cells. *Antioxidants*, *9*(12), 1–16. https://doi.org/10.3390/antiox9121300.

Bessong, P. O., Matume, N. D., and Tebit, D. M. (2021). Potential challenges to sustained viral load suppression in the HIV treatment programme in South Africa: a narrative overview. *AIDS Research and Therapy*, *18*(1), 1–17. https://doi.org/10.1186/s12981-020-00324-w.

Biswas, D., Nandy, S., Mukherjee, A., Pandey, D. K., and Dey, A. (2019). *Moringa oleifera*

*Lam.* and derived phytochemicals as promising antiviral agents: A review. *South African Journal of Botany*, *129*, 272-282. https://doi.org/10.1016/j.sajb.2019.07.049.

Bouayed, J., and Bohn, T. (2010). Exogenous antioxidants - Double-edged swords in cellular redox state: Health beneficial effects at physiologic doses versus deleterious effects at high doses. *Oxidative Medicine and Cellular Longevity*, *3*(4), 228–237. https://doi.org/10.4161/oxim.3.4.12858.

Brilhante, R. S. N., Sales, J. A., Pereira, V. S., Castelo-Branco, D. de S. C. M., Cordeiro, R. de A., et al. (2017). Research advances on the multiple uses of *Moringa oleifera*: A sustainable alternative for socially neglected population. *Asian Pacific Journal of Tropical Medicine*, *10*(7), 621–630. https://doi.org/10.1016/j.apjtm.2017.07.002.

Castellino, S., Moss, L., Wagner, D., Borland, J., Song, I., et al. (2013). Metabolism, excretion, and mass balance of the HIV-1 integrase inhibitor dolutegravir in humans. *Antimicrobial Agents and Chemotherapy*, *57*(8), 3536–3546. https://doi.org/10.1128/AAC.00292-13.

Chen, J., Yang, J., Ma, L., Li, J., Shahzad, N., and Kim, C. K. (2020). Structure-antioxidant activity relationship of methoxy, phenolic hydroxyl, and carboxylic acid groups of phenolic acids. *Scientific Reports*, *10*(1), 1–9. https://doi.org/10.1038/s41598-020-59451-z.

Cheng, D., Gao, L., Su, S., Sargsyan, D., Wu, R., Raskin, I., and Kong, A.N. (2019). Moringa isothiocyanate activates Nrf2: potential role in diabetic nephropathy. *The AAPS journal*, *21*, pp.1-14.

Chhatwani, C., Purohit, J., Vakil, A., and Khunt, S. (2016). Tenofovir Induced Severe Lactic Acidosis and Hepatitis. *National Journal of Medical Research*, *6*(3), 288–289.

De Cock, K. M., Jaffe, H. W., and Curran, J. W. (2012). The evolving epidemiology of HIV/AIDS. *Aids*, *26*(10), 1205–1213. https://doi.org/10.1097/QAD.0b013e328354622a.

de la Rosa, L. A., Moreno-Escamilla, J. O., Rodrigo-García, J., and Alvarez-Parrilla, E. (2018). Phenolic compounds. In *Postharvest Physiology and Biochemistry of Fruits and Vegetables* (pp. 253–271). Elsevier. https://doi.org/10.1016/B978-0-12-813278-4.00012-9.

de Vries, H. E., Witte, M., Hondius, D., Rozemuller, A. J. M., Drukarch, B., et al. (2008). Nrf2-induced antioxidant protection: A promising target to counteract ROS-mediated damage in neurodegenerative disease? In *Free Radical Biology and Medicine* (Vol. 45, Issue 10, pp. 1375–1383). Pergamon. https://doi.org/10.1016/j.freeradbiomed.2008.09.001.

Delpech, V., and Gahagan, J. (2009). The global epidemiology of HIV. *Medicine*, *37*(7), 317–320. https://doi.org/10.1016/j.mpmed.2009.04.002.

Desta, A., Biru, T. T., and Kefale, A. T. (2020). Health related quality of life of people receiving highly active antiretroviral therapy in Southwest Ethiopia. *PLoS ONE*, *15*(8 August). https://doi.org/10.1371/journal.pone.0237013.

Devkota, S., and Bhusal, K. K. (2020). Moringa oleifera: A miracle multipurpose tree for agroforestry and climate change mitigation from the Himalayas–A review. *Cogent Food and Agriculture*. Informa Healthcare. https://doi.org/10.1080/23311932.2020.1805951.

Donato, M.T., Tolosa, L., and Gómez-Lechón, M.J. (2015). Culture and functional characterization of human hepatoma HepG2 cells. In *Protocols in In Vitro Hepatocyte Research* (pp. 77-93). Humana Press, New York, NY.

Dose, J., Matsugo, S., Yokokawa, H., Koshida, Y., Okazaki, S., et al. (2016). Free radical

scavenging and cellular antioxidant properties of astaxanthin. *International Journal of Molecular Sciences*, *17*(1), 1–14. https://doi.org/10.3390/ijms17010103.

Doshi, S. B., Khullar, K., Sharma, R. K., and Agarwal, A. (2012). Role of reactive nitrogen species in male infertility. *Reproductive Biology and Endocrinology*, *10*, 1–11. https://doi.org/10.1186/1477-7827-10-109.

Dukhi, N., and Taylor, M. (2018). A focus on four popular "functional foods" as part of a strategy to combat metabolic disease through the increased consumption of fruits and vegetables. *Current Research in Nutrition and Food Science*, *6*(2), 294–306. https://doi.org/10.12944/CRNFSJ.6.2.05.

Dumitrescu, T. P., Peddiraju, K., Fu, C., Bakshi, K., Yu, S., et al. (2020). Bioequivalence and Food Effect Assessment of 2 Fixed-Dose Combination Formulations of Dolutegravir and Lamivudine. *Clinical Pharmacology in Drug Development*, *9*(2), 189–202. https://doi.org/10.1002/cpdd.740.

Ďuračková, Z. (2010). Some current insights into oxidative stress. *Physiological research*, *59*(4).

Duranti, G., Maldini, M., Crognale, D., Horner, K., Dimauro, I., Sabatini, S., and Ceci, R. (2021). "Moringa oleifera leaf extract upregulates nrf2/ho-1 expression and ameliorates redox status in c2c12 skeletal muscle cells", *Molecules*, MDPI AG, Vol. 26 No. 16, doi: 10.3390/molecules26165041.

Eggleton, J.S., and Nagalli, S. (2020). Highly Active Antiretroviral Therapy (HAART). *StatPearls*.

Eilami, O., Nazari, A., Dousti, M., Sayehmiri, F., and Ghasemi, M. (2019). Investigation of

HIV/AIDS prevalence and associated risk factors among female sex workers from 2010 to 2017: A meta-analysis study. *HIV/AIDS - Research and Palliative Care*, *11*, 105–117. https://doi.org/10.2147/HIV.S196085.

Elias, A., Nelson, B., Oputiri, D., and Geoffrey, O.B.P. (2013). Antiretroviral toxicity and oxidative stress. *American Journal of Pharmacology and Toxicology*, *8*(4), 187.

Else, L.J., Jackson, A., Puls, R., Hill, A., Fahey, P., et al. (2012). Pharmacokinetics of lamivudine and lamivudine-triphosphate after administration of 300 milligrams and 150 milligrams once daily to healthy volunteers: results of the ENCORE 2 study. *Antimicrobial agents and chemotherapy*, *56*(3), 1427-1433.

Fernandez-Fernandez, B., Montoya-Ferrer, A., Sanz, A. B., Sanchez-Niño, M. D., Izquierdo, M. C., et al. (2011). Tenofovir nephrotoxicity: 2011 update. *AIDS Research and Treatment*, *2011*. https://doi.org/10.1155/2011/354908.

Fiedor, J., and Burda, K. (2014). Potential role of carotenoids as antioxidants in human health and disease. *Nutrients*, *6*(2), 466–488. https://doi.org/10.3390/nu6020466.

Franklin, C. C., Backos, D. S., Mohar, I., White, C. C., Forman, H. J., and Kavanagh, T. J. (2009). Structure, function, and post-translational regulation of the catalytic and modifier subunits of glutamate cysteine ligase. *Molecular Aspects of Medicine*, *30*(1–2), 86–98. https://doi.org/10.1016/j.mam.2008.08.009.

Gabazana, Z., and Sitole, L. (2021). Raman-based metabonomics unravels metabolic changes related to a first-line tenofovir-based treatment in a small cohort of South African HIV-infected patients. *Spectrochimica Acta - Part A: Molecular and Biomolecular Spectroscopy*, *248*, 119256. https://doi.org/10.1016/j.saa.2020.119256.

Gambo, A., Moodley, I., Babashani, M., Babalola, T.K., and Gqaleni, N. (2021). A double-blind, randomized controlled trial to examine the effect of Moringa oleifera leaf powder supplementation on the immune status and anthropometric parameters of adult HIV patients on antiretroviral therapy in a resource-limited setting. *PloS one*, *16*(12), p.e0261935.

Geboers, S., Haenen, S., Mols, R., Brouwers, J., Tack, J., Annaert, P., and Augustijns, P. (2015). Intestinal behavior of the ester prodrug tenofovir DF in humans. *International Journal of Pharmaceutics*, *485*(1–2), 131–137. https://doi.org/10.1016/j.ijpharm.2015.03.002.

Glorieux, C., Zamocky, M., Sandoval, J. M., Verrax, J., and Calderon, P. B. (2015). Regulation of catalase expression in healthy and cancerous cells. In *Free Radical Biology and Medicine* (Vol. 87, pp. 84–97). https://doi.org/10.1016/j.freeradbiomed.2015.06.017.

Grigoras, A. G. (2017). Catalase immobilization—A review. In *Biochemical Engineering Journal* (Vol. 117, pp. 1–20). https://doi.org/10.1016/j.bej.2016.10.021.

Guo, K., Ge, J., Zhang, C., Lv, M. W., Zhang, Q., Talukder, M., and Li, J. L. (2020). Cadmium induced cardiac inflammation in chicken (Gallus gallus) via modulating cytochrome P450 systems and Nrf2 mediated antioxidant defense. *Chemosphere*, *249*. https://doi.org/10.1016/j.chemosphere.2020.125858.

Gupta, S.D. (2010). Role of free radicals and antioxidants in *in vitro* morphogenesis. *Reactive oxygen species and antioxidants in higher plants, edited by Science Publishers*, 229-247.

Ha, B., Larsen, K. P., Zhang, J., Fu, Z., Montabana, E., Jackson, L. N., Chen, D. H., and Puglisi, E. V. (2021). High-resolution view of HIV-1 reverse transcriptase initiation complexes

and inhibition by NNRTI drugs. *Nature Communications*, *12*(1), 1–11. https://doi.org/10.1038/s41467-021-22628-9.

Hall, A. M., Bass, P., and Unwin, R. J. (2014). Drug-induced renal fanconi syndrome. *Qjm*, *107*(4), 261–269. https://doi.org/10.1093/qjmed/hct258.

Harjumäki, R., Nugroho, R.W.N., Zhang, X., Lou, Y.R., Yliperttula, M., et al. (2019). Quantified forces between HepG2 hepatocarcinoma and WA07 pluripotent stem cells with natural biomaterials correlate with in vitro cell behavior. *Scientific reports*, *9*(1), pp.1-14.

Heeney, J. L., Dalgleish, A. G., and Weiss, R. A. (2006). Origins of HIV and the evolution of resistance to AIDS. *Science*, *313*(5786), 462–466. https://doi.org/10.1126/science.1123016.

Henriksen, E. J. (2019). Role of Oxidative Stress in the Pathogenesis of Insulin Resistance and Type 2 Diabetes. In *Bioactive Food as Dietary Interventions for Diabetes* (pp. 3–17). Elsevier. https://doi.org/10.1016/b978-0-12-813822-9.00001-1.

Heyer, A., and Ogunbanjo, G. A. (2006). Adherence to HIV antiretroviral therapy. Part I: A review of factors that influence adherence. *South African Family Practice*, *48*(8), 5–9. https://doi.org/10.1080/20786204.2006.10873433.

Holmström, K. M., Kostov, R. V., and Dinkova-Kostova, A. T. (2016). The multifaceted role of Nrf2 in mitochondrial function. In *Current Opinion in Toxicology* (Vol. 2, pp. 80–91). Elsevier B.V. https://doi.org/10.1016/j.cotox.2016.10.002.

Ibrahim, O.O. (2020). Coronavirus SARS-CoV-2 is the newly emerged zoonotic virus causing pandemic death and economic loss. *EC Pulmonol. Respir. Med*, *9*, pp.65-75.

Ighodaro, O. M., and Akinloye, O. A. (2018). First line defence antioxidants-superoxide dismutase (SOD), catalase (CAT) and glutathione peroxidase (GPX): Their fundamental role in the entire antioxidant defence grid. *Alexandria Journal of Medicine, 54*(4), 287–293. https://doi.org/10.1016/j.ajme.2017.09.001.

Ikekpeazu, J. E., Orji, O. C., Uchendu, I. K., and Ezeanyika, L. U. S. (2019). Mitochondrial and Oxidative Impacts of Short and Long-term Administration of HAART on HIV Patients. *Current Clinical Pharmacology*, *15*(2), 110–124. https://doi.org/10.2174/1574884714666190905162237.

James, A. M., Ofotokun, I., Sheth, A., Acosta, E. P., and King, J. R. (2012). Tenofovir: Once-daily dosage in the management of HIV infection. *Clinical Medicine Insights: Therapeutics*, *4*, 201–216. https://doi.org/10.4137/CMT.S8316.

Kaeni, M. C. (2020). Safety, tolerability and adherence of DTG-based regimen among adult HIV patients attending Kenyatta national hospital. *Doctoral dissertation, University of Nairobi.*

Kamiloglu, S., Sari, G., Ozdal, T., and Capanoglu, E. (2020). Guidelines for cell viability assays. Food Frontiers, 1(3), 332-349.

Kandel, C. E., and Walmsley, S. L. (2015). Dolutegravir – A review of the pharmacology, efficacy, and safety in the treatment of HIV. *Drug Design, Development and Therapy*, *9*, 3547–3555. https://doi.org/10.2147/DDDT.S84850.

Kavian, N., Mehlal, S., Jeljeli, M., Saidu, N.E.B., Nicco, C., et al. (2018). The Nrf2-antioxidant response element signaling pathway controls fibrosis and autoimmunity in scleroderma. *Frontiers in immunology, 9*, p.1896.

Kearney, B. P., Flaherty, J. F., and Shah, J. (2004). Tenofovir disoproxil fumarate: Clinical pharmacology and pharmacokinetics. *Clinical Pharmacokinetics*, *43*(9), 595–612. https://doi.org/10.2165/00003088-200443090-00003.

Kirchhoff, F. (2016). Encyclopedia of AIDS. *Encyclopedia of AIDS*, *January 2013*. https://doi.org/10.1007/978-1-4614-9610-6.

Kirkham, P.A., and Barnes, P.J. (2013). Oxidative stress in COPD. *Chest*, *144*(1), pp.266-273.

Kis, O., Robillard, K., Chan, G. N. Y., and Bendayan, R. (2010). The complexities of antiretroviral drug-drug interactions: role of ABC and SLC transporters. *Trends in Pharmacological Sciences*, *31*(1), 22–35. https://doi.org/10.1016/j.tips.2009.10.001.

Kline, E. R., Bassit, L., Hernandez-Santiago, B. I., Detorio, M. A., Liang, B., et al. (2009). Long-term exposure to AZT, but not d4T, increases endothelial cell oxidative stress and mitochondrial dysfunction. *Cardiovascular Toxicology*, *9*(1), 1–12. https://doi.org/10.1007/s12012-008-9029-8.

Kohler, J. J., Hosseini, S. H., Hoying-Brandt, A., Green, E., Johnson, D. M., et al. (2009). Tenofovir renal toxicity targets mitochondria of renal proximal tubules. *Laboratory Investigation*, *89*(5), 513–519. https://doi.org/10.1038/labinvest.2009.14.

Koide, S. I., Kugiyama, K., Sugiyama, S., Nakamura, S. I., Fukushima, H.,et al. (2003). Association of polymorphism in glutamate-cysteine ligase catalytic subunit gene with coronary vasomotor dysfunction and myocardial infarction. *Journal of the American College of Cardiology*, *41*(4), 539–545. https://doi.org/10.1016/S0735-1097(02)02866-8.

Kouanfack, C., Mpoudi-Etame, M., Eymard-Duvernay, S., Leroy, S., Boyer, S., et al. (2019). Dolutegravir-Based or Low-Dose Efavirenz-Based Regimen for the Treatment of HIV-

1. *The New England Journal of Medicine*, *381*(9), 816-826.

Krejsa, C. M., Franklin, C. C., White, C. C., Ledbetter, J. A., Schieven, G. L., and Kavanagh, T. J. (2010). Rapid activation of glutamate cysteine ligase following oxidative stress. *Journal of Biological Chemistry*, *285*(21), 16116–16124. https://doi.org/10.1074/jbc.M110.116210.

Kuciel-Lewandowska, J. M., Pawlik-Sobecka, L., Płaczkowska, S., Kokot, I., and Paprocka-Borowicz, M. (2018). The assessment of the integrated antioxidant system of the body and the phenomenon of spa reaction in the course of radon therapy: A pilot study. *Advances in Clinical and Experimental Medicine*, *27*(10), 1341–1346. https://doi.org/10.17219/acem/69450.

Lambert, A. J., and Brand, M. D. (2009). Reactive oxygen species production by mitochondria. *Methods in Molecular Biology (Clifton, N.J.)*, *554*(December), 165–181. https://doi.org/10.1007/978-1-59745-521-3_11.

Lee, D. H., Gold, R., and Linker, R. A. (2012). Mechanisms of oxidative damage in multiple sclerosis and neurodegenerative diseases: Therapeutic modulation via fumaric acid esters. *International Journal of Molecular Sciences*, *13*(9), 11783–11803. https://doi.org/10.3390/ijms130911783.

Leone, A., Spada, A., Battezzati, A., Schiraldi, A., Aristil, J., and Bertoli, S. (2015). Cultivation, genetic, ethnopharmacology, phytochemistry and pharmacology of *Moringa oleifera* leaves: An overview. *International journal of molecular sciences*, *16*(6), pp.12791-12835.

Levi, J., Raymond, A., Pozniak, A., Vernazza, P., Kohler, P., and Hill, A. (2016). Can the

UNAIDS 90-90-90 target be achieved? A systematic analysis of national HIV treatment cascades. *BMJ Global Health*, *1*(2), 1–10. https://doi.org/10.1136/bmjgh-2015-000010.

Lin, M., Zhang, J., and Chen, X. (2018). Bioactive flavonoids in *Moringa oleifera* and their health-promoting properties. In *Journal of Functional Foods* (Vol. 47). https://doi.org/10.1016/j.jff.2018.06.011.

Livak, K.J., and Schmittgen, T.D. (2001). Analysis of relative gene expression data using real-time quantitative PCR and the 2− ΔΔCT method. *methods*, *25*(4), pp.402-408.

Loeliger, K. B., Niccolai, L. M., Mtungwa, L. N., Moll, A., and Shenoi, S. V. (2016). "I have to push him with a wheelbarrow to the clinic": Community health workers' roles, needs, and strategies to improve HIV care in rural South Africa. *AIDS Patient Care and STDs*, *30*(8), 385–394. https://doi.org/10.1089/apc.2016.0096.

Lü, J. M., Lin, P. H., Yao, Q., and Chen, C. (2010). Chemical and molecular mechanisms of antioxidants: Experimental approaches and model systems. *Journal of Cellular and Molecular Medicine*, *14*(4), 840–860. https://doi.org/10.1111/j.1582-4934.2009.00897.x.

Lu, S. C. (2013). Glutathione synthesis. In *Biochimica et Biophysica Acta - General Subjects* (Vol. 1830, Issue 5, pp. 3143–3153). https://doi.org/10.1016/j.bbagen.2012.09.008.

Luhlaza-ISS. (2006). *Growing and Agro-Processing of Moringa Oleifera With Commercial Potential in South Africa*. *43*, 1–108. https://drive.google.com/file/d/1iZfoUMXG_2FZIucWnWxos0FdPnak_b1S/view.

Mabaso, M., Makola, L., Naidoo, I., Mlangeni, L.L., Jooste, S., and Simbayi, L. (2019). HIV prevalence in South Africa through gender and racial lenses: results from the 2012 population-based national household survey. *International journal for equity in*

*health*, *18*(1), 1-11.

Mallon, P. W. G., Unemori, P., Sedwell, R., Morey, A., Rafferty, M., et al. (2005). In vivo, nucleoside reverse-transcriptase inhibitors alter expression of both mitochondrial and lipid metabolism genes in the absence of depletion of mitochondrial DNA. *Journal of Infectious Diseases*, *191*(10), 1686–1696. https://doi.org/10.1086/429697.

Manjunath, S.H., Nataraj, P., Swamy, V.H., Sugur, K., Dey, S.K., Ranganathan, V., et al. (2023). Development of Moringa oleifera as functional food targeting NRF2 signaling: antioxidant and anti-inflammatory activity in experimental model systems. *Food & Function*, *14*(10), pp.4734-4751.

Mansour, H.H., Abd El Azeem, M.G., and Ismael, N.E. (2014). Protective effect of Moringa oleifera on γ-radiation-induced hepatotoxicity and nephrotoxicity in rats. *AJPCT*, *2*(4), pp.495-508.

Mas-Bargues, C., Escrivá, C., Dromant, M., Borrás, C., and Viña, J. (2021). Lipid peroxidation as measured by chromatographic determination of malondialdehyde. Human plasma reference values in health and disease. *Archives of Biochemistry and Biophysics*, *709*. https://doi.org/10.1016/j.abb.2021.108941.

Mattmiller, S. A., Carlson, B. A., and Sordillo, L. M. (2013). Regulation of inflammation by selenium and selenoproteins: Impact on eicosanoid biosynthesis. *Journal of Nutritional Science*, *2*, 1–13. https://doi.org/10.1017/jns.2013.17.

Matough, F. A., Budin, S. B., Hamid, Z. A., Alwahaibi, N., and Mohamed, J. (2012). The role of oxidative stress and antioxidants in diabetic complications. *Sultan Qaboos University Medical Journal*, *12*(1), 556–569. https://doi.org/10.12816/0003082.

Max, B., and Sherer, R. (2000). Management of the adverse effects of antiretroviral therapy and medication adherence. *Clinical Infectious Diseases, 30,* S96–S116. https://doi.org/10.1086/313859.

Mendelsohn, A. S., and Ritchwood, T. (2020). COVID-19 and Antiretroviral Therapies: South Africa's Charge Towards 90–90–90 in the Midst of a Second Pandemic. *AIDS and Behavior*, *24*(10), 2754–2756. https://doi.org/10.1007/s10461-020-02898-y.

Milla, P.G., Peñalver, R., and Nieto, G. (2021). Health benefits of uses and applications of Moringa oleifera in bakery products. *Plants*, *10*(2), p.318.

Mills, E., Cooper, C., Seely, D., and Kanfer, I. (2005). African herbal medicines in the treatment of HIV: Hypoxis and Sutherlandia. An overview of evidence and pharmacology. *Nutrition Journal, 4*, 1–6. https://doi.org/10.1186/1475-2891-4-19.

Mofokeng, M.M., Araya, H.T., Amoo, S.O., Sehlola, D., du Plooy, C.P., Bairu, M.W., Venter, S., and Mashela, P.W. (2020). Diversity and Conservation through Cultivation of Hypoxis in Africa—A Case Study of Hypoxis hemerocallidea. *Diversity*, *12*(4), p.122.

Mohan, H., Lenis, M. G., Laurette, E. Y., Tejada, O., Sanghvi, T., et al. (2021). Dolutegravir in pregnant mice is associated with increased rates of fetal defects at therapeutic but not at supratherapeutic levels. *EBioMedicine, 63,* 103167. https://doi.org/10.1016/j.ebiom.2020.103167.

Mohan, J., Ghazi, T., Sibiya, T., and Chuturgoon, A.A. (2023). Antiretrovirals Promote Metabolic Syndrome through Mitochondrial Stress and Dysfunction: An In Vitro Study. *Biology*, *12*(4), p.580.

Monera-Penduka, T. G., Maponga, C. C., Wolfe, A. R., Wiesner, L., Morse, G. D., and Nhachi,

C. F. B. (2017). Effect of Moringa oleifera Lam. leaf powder on the pharmacokinetics of nevirapine in HIV-infected adults: A one sequence cross-over study. *AIDS Research and Therapy*, *14*(1), 1–7. https://doi.org/10.1186/s12981-017-0140-4.

Moses, K., Adefisayo O, A., Maryam, B., Adeoye, A., Oluwatosin, A., et al. (2020). Virologic Response among Key Populations Living With HIV following a Switch to Dolutegravir-Based Regimen in Southern Nigeria. *International Journal of Virology and AIDS*, *7*(2). https://doi.org/10.23937/2469-567x/1510069.

Mosmann, T. (1983). Rapid colorimetric assay for cellular growth and survival: application to proliferation and cytotoxicity assays. Journal of immunological methods, 65(1-2), 55-63.

Mukherjee, A., Banerjee, M., Mandal, V., Shukla, A. C., and Mandal, S. C. (2014). Modernization of Ayurveda: A brief overview of Indian initiatives. *Natural Product Communications*, *9*(2), 287–290. https://doi.org/10.1177/1934578x1400900239.

Nagiah, S., Phulukdaree, A., and Chuturgoon, A. (2015). Mitochondrial and Oxidative Stress Response in HepG2 Cells Following Acute and Prolonged Exposure to Antiretroviral Drugs. *Journal of Cellular Biochemistry*, *116*(9), 1939–1946. https://doi.org/10.1002/jcb.25149.

Nair, S., Bayer, W., Ploquin, M. J. Y., Kassiotis, G., Hasenkrug, K. J., and Dittmer, U. (2011). Distinct roles of CD4+ T cell subpopulations in retroviral immunity: lessons from the Friend virus mouse model. *Retrovirology*, *8*, 76. https://doi.org/10.1186/1742-4690-8-76.

Nair, V. D. P., Dairam, A., Agbonon, A., Arnason, J. T., Foster, B. C., and Kanfer, I. (2007). Investigation of the antioxidant activity of African potato (Hypoxis hemerocallidea). *Journal of Agricultural and Food Chemistry*, *55*(5), 1707–1711.

https://doi.org/10.1021/jf0619838.

Ncube, S., Madikizela, L. M., Chimuka, L., and Nindi, M. M. (2018). Environmental fate and ecotoxicological effects of antiretrovirals: A current global status and future perspectives. *Water Research*, *145*(August), 231–247. https://doi.org/10.1016/j.watres.2018.08.017.

Ndlovu, S.S., Chuturgoon, A.A., and Ghazi, T. (2023). Moringa oleifera Lam Leaf Extract Stimulates NRF2 and Attenuates ARV-Induced Toxicity in Human Liver Cells (HepG2). *Plants*, *12*(7), p.1541.

Nizioł-ŁUkaszewska, Z., Furman-Toczek, D., Bujak, T., Wasilewski, T., and Hordyjewicz-Baran, Z. (2020). Moringa oleifera L. Extracts as Bioactive Ingredients That Increase Safety of Body Wash Cosmetics. *Dermatology Research and Practice*, *2020*. https://doi.org/10.1155/2020/8197902.

Noctor, G., Queval, G., Mhamdi, A., Chaouch, S., and Foyer, C. H. (2011). *Glutathione*. 1–32. https://doi.org/10.1199/tab.0142.

Orton, P. M., Sokhela, D. G., Nokes, K. M., Perazzo, J. D., and Webel, A. R. (2021). Factors related to functional exercise capacity amongst people with hiv in durban, south africa. *Health SA Gesondheid*, *26*(Who 2020), 1–7. https://doi.org/10.4102/hsag.v26i0.1532.

P Sharma, O. (2014). Clinical Biochemistry of Hepatotoxicity. *Journal of Clinical Toxicology*, *04*(01). https://doi.org/10.4172/2161-0495.s4-001.

Paemanee, A., Sornjai, W., and Kittisenachai, S. (2017). *Nevirapine induced mitochondrial dysfunction in HepG2 cells*. 1–11. https://doi.org/10.1038/s41598-017-09321-y.

Paikra, B. K., Dhongade, H. K. J., and Gidwani, B. (2017). Phytochemistry and pharmacology

of *Moringa oleifera* Lam. *Journal of Pharmacopuncture*, *20*(3), 194–200. https://doi.org/10.3831/KPI.2017.20.022.

Paniagua, A. C., and Amariles, P. (2018). Hepatotoxicity by Drugs. *Pharmacokinetics and Adverse Effects of Drugs - Mechanisms and Risks Factors*, *May*. https://doi.org/10.5772/intechopen.72005.

Patwardhan, B., Warude, D., Pushpangadan, P., and Bhatt, N. (2005). Ayurveda and traditional Chinese medicine: A comparative overview. *Evidence-Based Complementary and Alternative Medicine*, *2*(4), 465–473. https://doi.org/10.1093/ecam/neh140.

Peltzer, K., Friend-du Preez, N., Ramlagan, S., Fomundam, H., Anderson, J., and Chanetsa, L. (2011). Antiretrovirals and the use of traditional, complementary and alternative medicine by HIV patients in KwaZulu-Natal, South Africa: a longitudinal study. *African Journal of Traditional, Complementary and Alternative Medicines*, *8*(4).

Pham-Huy, L. A., He, H., and Pham-Huy, C. (2008). Free radicals, antioxidants in disease and health. In *International Journal of Biomedical Science* (Vol. 4, Issue 2).

Phaniendra, A., Jestadi, D. B., and Periyasamy, L. (2015). Free Radicals: Properties, Sources, Targets, and Their Implication in Various Diseases. *Indian Journal of Clinical Biochemistry*, *30*(1), 11–26. https://doi.org/10.1007/s12291-014-0446-0.

Phulukdaree, A., Moodley, D., and Chuturgoon, A.A. (2010). The effects of Sutherlandia frutescens extracts in cultured renal proximal and distal tubule epithelial cells. South African Journal of Science, 106(1-2), pp.54-58.

Pillay, Y., and Johnson, L. (2021). World AIDS day 2020: Reflections on global and South African progress and continuing challenges. *Southern African Journal of HIV Medicine*,

*22*(1), 1–5. https://doi.org/10.4102/SAJHIVMED.V22I1.1205.

Pillaye, J. N., Marakalala, M. J., Khumalo, N., Spearman, W., and Ndlovu, H. (2020). Mechanistic insights into antiretroviral drug-induced liver injury. *Pharmacology Research and Perspectives*, *8*(4), 1–9. https://doi.org/10.1002/prp2.598.

Pinti, M., Troiano, L., Nasi, M., Ferraresi, R., Dobrucki, J., and Cossarizza, A. (2003). Hepatoma HepG2 cells as a model for in vitro studies on mitochondrial toxicity of antiviral drugs: which correlation with the patient?. *Journal of biological regulators and homeostatic agents*, *17*(2), pp.166-171.

Pourvali, K., Abbasi, M., and Mottaghi, A. (2016). Role of superoxide dismutase 2 gene Ala16Val polymorphism and total antioxidant capacity in diabetes and its complications. *Avicenna Journal of Medical Biotechnology*, *8*(2), 48–56.

Raffi, F., Pozniak, A. L., and Wainberg, M. A. (2014). Has the time come to abandon efavirenz for first-line antiretroviral therapy? *Journal of Antimicrobial Chemotherapy*, *69*(7), 1742–1747. https://doi.org/10.1093/jac/dku058.

Ramlagan, S., Matseke, G., Rodriguez, V. J., Jones, D. L., Peltzer, K.,et al. (2018). Determinants of disclosure and non-disclosure of hiv-positive status, by pregnant women in rural South Africa. *Sahara-J*, *15*(1), 155–163. https://doi.org/10.1080/17290376.2018.1529613.

Razis, A. F. A., Ibrahim, M. D., and Kntayya, S. B. (2014). Health benefits of *Moringa oleifera*. *Asian Pacific Journal of Cancer Prevention*, *15*(20), 8571–8576. https://doi.org/10.7314/APJCP.2014.15.20.8571.

Ren, Z., Food, U. S., Chen, S., Guo, L., and Food, U. S. (2018). *Chapter 8 Use of Liver-Derived*

*Cell Lines for the Study*. *June*. https://doi.org/10.1007/978-1-4939-7677-5.

Saif, S. (2004). *Ap-1 Is Required for Cmx-8933-Induced Sod Upregulation and Is Translocated in Response To a Human Epn Mimetic* (Doctoral dissertation, Worcester Polytechnic Institute).

Salami, A.T., Okonkwo, C.E., Attah, F.A., and Olagoke, O.C. (2021). Bioactive *Moringa oliefera* seed extracts attenuates cholesterol gall stones in hyperglycaemic Swiss mice. *Comparative Clinical Pathology*, 1-10.

Sarıkaya, E., and Doğan, S. (2020). Glutathione Peroxidase in Health and Diseases. *Glutathione Peroxidase in Health and Disease*, 49. https://www.researchgate.net/publication/339093247_Glutathione_Peroxidase_in_Health_and_Diseases.

Sellers, Z.P., Williams, R.A., Overbay, J.W., Cho, J., Henderson, M., and Reed, T.T. (2014). Current Therapeutic Modalities, Enzyme Kinetics, and Redox Proteomics in Traumatic Brain Injury. *Traumatic Brain Injury*, p.39.

Shamsabadi, A. A. (2014). *Investigation into the hepatotoxic effects of Highly Active Anti-Retroviral Therapy ( HAART ) medications*.

Sharp, P. M., and Hahn, B. H. (2010). The evolution of HIV-1 and the origin of AIDS. *Philosophical Transactions of the Royal Society B: Biological Sciences*, *365*(1552), 2487–2494. https://doi.org/10.1098/rstb.2010.0031 .

Shunmugam, L. (2016), *Moringa Oleifera Crude Aqueous Leaf Extract Induces Apoptosis in Human Hepatocellular Carcinoma Cells via the Upregulation of NF-KB and IL-6/STAT3 Pathway*.

Sibanda, M., Manimbulu, N.M., and Naidoo, P. (2016). Concurrent use of Antiretroviral and African traditional medicines amongst people living with HIV/AIDS (PLWA) in the eThekwini Metropolitan area of KwaZulu-Natal. *African health sciences*, *16*(4), 1118-1130.

Sies, H. (2017). Hydrogen peroxide as a central redox signaling molecule in physiological oxidative stress: Oxidative eustress. *Redox Biology*, *11*(December 2016), 613–619. https://doi.org/10.1016/j.redox.2016.12.035.

Smith, R.L., Boer, R.D., Brul, S., Budovskaya, Y., and Spek, H.V.D. (2013). Premature and accelerated aging: HIV or HAART?. *Frontiers in genetics*, *3*, p.328.

Sobiecki, J.F. (2014). The Intersection of Culture and Science in South African Traditional Medicine. *Indo-Pacific Journal of Phenomenology*, *14*(1), 1–10. https://doi.org/10.2989/IPJP.2014.14.1.6.1238.

Soliman, M.M., Aldhahrani, A., Alkhedaide, A., Nassan, M.A., Althobaiti, F., and Mohamed, W.A., (2020). The ameliorative impacts of Moringa oleifera leaf extract against oxidative stress and methotrexate-induced hepato-renal dysfunction. *Biomedicine & Pharmacotherapy*, *128*, p.110259.

Spach, D. H. (2020). Antiretroviral Medications and Initial Therapy HIV Life Cycle and Antiretroviral Drug Targets. *National HIV Curriculum*.

Stohs, S.J., and Hartman, M.J. (2015). Review of the safety and efficacy of *Moringa oleifera*. *Phytotherapy Research*, *29*(6), 796-804.

Street, R. A., and Prinsloo, G. (2013). Commercially important medicinal plants of South Africa: A review. In *Journal of Chemistry*. https://doi.org/10.1155/2013/205048.

Street, R. A., Stirk, W. A., and Van Staden, J. (2008). South African traditional medicinal plant trade-Challenges in regulating quality, safety, and efficacy. *Journal of Ethnopharmacology*, *119*(3), 705–710. https://doi.org/10.1016/j.jep.2008.06.019.

Su, L., Zhang, J., Gomez, H., Murugan, R., Hong, X., et al. (2019). *Review Article Reactive Oxygen Species-Induced Lipid Peroxidation in Apoptosis, Autophagy, and Ferroptosis*. *2019*.

Swain, S. L., McKinstry, K. K., and Strutt, T. M. (2012). Expanding roles for CD4 + T cells in immunity to viruses. *Nature Reviews Immunology*, *12*(2), 136–148. https://doi.org/10.1038/nri3152.

Tai, J., Cheung, S., Chan, E., and Hasman, D. (2004). In vitro culture studies of Sutherlandia frutescens on human tumor cell lines. *Journal of Ethnopharmacology*, *93*(1), 9–19. https://doi.org/10.1016/j.jep.2004.02.028.

Taylor, K., Fritz, K., and Parmar, M. (2020). Lamivudine. In: StatPearls. Treasure Island (FL): StatPearls Publishing.

Temesgen, Z., Warnke, D., and Kasten, M. J. (2006). Current status of antiretroviral therapy. *Expert Opinion on Pharmacotherapy*, *7*(12), 1541–1554. https://doi.org/10.1517/14656566.7.12.1541.

Thiese, M.S. (2014). Observational and interventional study design types; an overview. *Biochemia medica*, *24*(2), pp.199-210.

Tiloke, C., Phulukdaree, A., and Chuturgoon, A.A. (2013). "The antiproliferative effect of Moringa oleifera crude aqueous leaf extract on cancerous human alveolar epithelial cells", *BMC Complementary and Alternative Medicine*, BioMed Central Ltd., Vol. 13, doi:

10.1186/1472-6882-13-226.

Tiloke, C., Phulukdaree, A., Gengan, R.M., and Chuturgoon, A.A. (2019). Moringa oleifera aqueous leaf extract induces cell-cycle arrest and apoptosis in human liver hepatocellular carcinoma cells. *Nutrition and cancer*, *71*(7), pp.1165-1174.

Tomar, M., Subha, K., Dr Reetu., and Bhargavi, H.A. (2020). Moringa oleifera : a health food for animal and human consumption. *Food and Scientific Reports*, *1*(January), 11–14.

Torti, C., Prosperi, M., Motta, D., Digiambenedetto, S., Maggiolo, F., et al. (2012). Factors influencing the normalization of CD4+ T-cell count, percentage, and CD4+/CD8+ T-cell ratio in HIV-infected patients on long-term suppressive antiretroviral therapy. *Clinical Microbiology and Infection*, *18*(5), 449–458. https://doi.org/10.1111/j.1469-0691.2011.03650.x.

Tradit, A. J., Altern, C., Hughes, G. D., Puoane, T. R., Clark, B. L., et al. (2012). Prevalence and predictors of traditional medicine utilization among persons living with AIDS (PLWA) on antiretroviral (ARV) and prophylaxis treatment in both rural and urban areas in South Africa. *Clarks & Associates Statistical Consulting , Nashville . 9.*

Tshabalala, T., Ncube, B., Moyo, H.P., Abdel-Rahman, E.M., Mutanga, O., and Ndhlala, A.R., (2020). Predicting the spatial suitability distribution of Moringa oleifera cultivation using analytical hierarchical process modelling. *South African Journal of Botany*, *129*, pp.161-168.

Umar, D., Waziri, B., Ndagi, U., Mohammed, S., Usman, N., and Abubakar-Muhammad, H. (2020). Impact of Tenofovir/Lamivudine/Dolutegravir (Tld) on the Health-Related Quality of Life and Clinical Outcomes of HIV/AIDS Patients at a Tertiary Health Facility

in Niger State.

Vaillant, A.A.J., and Naik, R., 2020. HIV-1 associated opportunistic infections. *StatPearls*

Van Heuverswyn, F., and Peeters, M. (2007). The origins of HIV and implications for the global epidemic. *Current Infectious Disease Reports*, *9*(4), 338–346. https://doi.org/10.1007/s11908-007-0052-x.

Venhoff, N., Setzer, B., Melkaoui, K., and Walker, U.A. (2007). Mitochondrial toxicity of tenofovir, emtricitabine and abacavir alone and in combination with additional nucleoside reverse transcriptase inhibitors. Antiviral therapy, 12(7), 1075.

Vergara-Jimenez, M., Almatrafi, M. M., and Fernandez, M. L. (2017). Bioactive components in *Moringa oleifera* leaves protect against chronic disease. *Antioxidants*, *6*(4), 1–13. https://doi.org/10.3390/antiox6040091.

Walker, U.A., Setzer, B., and Venhoff, N. (2002). Increased long-term mitochondrial toxicity in 36 combinations of nucleoside analogue reverse-transcriptase inhibitors. AIDS, 16(16), 2165-2173.

Warnke, D., Barreto, J., and Temesgen, Z. (2007). Therapeutic review: Antiretroviral drugs. *Journal of Clinical Pharmacology*, *47*(12), 1570–1579. https://doi.org/10.1177/0091270007308034.

Wassner, C., Bradley, N., and Lee, Y. (2020). A Review and Clinical Understanding of Tenofovir: Tenofovir Disoproxil Fumarate versus Tenofovir Alafenamide. *Journal of the International Association of Providers of AIDS Care*, *19*, 1–10. https://doi.org/10.1177/2325958220919231.

Waters, L., Mehta, V., Gogtay, J., and Boffito, M. (2021). the Evidence for Using Tenofovir Disoproxil Fumarate Plus Lamivudine As a Nucleoside Analogue Backbone for the Treatment of Hiv. *Journal of Virus Eradication*, *7*(January), 100028. https://doi.org/10.1016/j.jve.2021.100028.

Wearne, N., Davidson, B., Blockman, M., Swart, A., and Jones, E. S. W. (2020). HIV, drugs and the kidney. *Drugs in Context*, *9*, 1–17. https://doi.org/10.7573/DIC.2019-11-1.

Weber, I. T., Wang, Y. F., and Harrison, R. W. (2021). Hiv protease: Historical perspective and current research. *Viruses*, *13*(5), 1–12. https://doi.org/10.3390/v13050839.

Wu, G., Fang, Y. Z., Yang, S., Lupton, J. R., and Turner, N. D. (2004). Glutathione Metabolism and Its Implications for Health. In *Journal of Nutrition* (Vol. 134, Issue 3, pp. 489–492). https://doi.org/10.1093/jn/134.3.489.

Younus, H. (2018). Therapeutic potentials of superoxide dismutase. *International Journal of Health Sciences*, *12*(3), 88–93. http://www.ncbi.nlm.nih.gov/pubmed/29896077%0Ahttp://www.pubmedcentral.nih.gov/articlerender.fcgi?artid=PMC5969776.

Zang, H., Mathew, R.O., and Cui, T. (2020). “The Dark Side of Nrf2 in the Heart”, *Frontiers in Physiology*, Frontiers Media S.A., 9 July, doi: 10.3389/fphys.2020.00722.

Zhang, Y. J., Gan, R. Y., Li, S., Zhou, Y., Li, A. N., et al. (2015). Antioxidant phytochemicals for the prevention and treatment of chronic diseases. In *Molecules* (Vol. 20, Issue 12, pp. 21138–21156). https://doi.org/10.3390/molecules201219753.

# APPENDICES

## **APPENDIX A:** ETHICS APPROVAL LETTER

UNIVERSITY OF THE FREE STATE
UNIVERSITEIT VAN DIE VRYSTAAT
YUNIVESITHI YA FREISTATA

UFS·UV
HEALTH SCIENCES
GESONDHEIDSWETENSKAPPE

**Health Sciences Research Ethics Committee**

15-Dec-2021

Dear **Ms Mbasakazi Saki**

Ethics Clearance: **The hepatoprotective effects of Moringa oleifera against antiretroviral induced cytotoxicity in HepG2 cells**

Principal Investigator: **Ms Mbasakazi Saki**

Department: **Basic Medical Sciences Department (Bloemfontein Campus)**

Submission Page

**APPLICATION APPROVED**

Please ensure that you read the whole document

With reference to your application for ethical clearance with the Faculty of Health Sciences, I am pleased to inform you on behalf of the Health Sciences Research Ethics Committee that you have been granted ethical clearance for your project.

Your ethical clearance number, to be used in all correspondence is:**UFS-HSD2021/1571/2501**

The ethical clearance number is valid for research conducted for one year from issuance. Should you require more time to complete this research, please apply for an extension.

We request that any changes that may take place during the course of your research project be submitted to the HSREC for approval to ensure we are kept up to date with your progress and any ethical implications that may arise. This includes any serious adverse events and/or termination of the study.

A progress report should be submitted within one year of approval, and annually for long term studies. A final report should be submitted at the completion of the study.

**Research conducted in any Department of Health facility:** Researchers are required to sign and return the HSREC approval letters to the provincial Department of Health where they applied. It is also a requirement for researchers to submit electronic copies of their final research findings, and/or make a presentation of their findings and recommendations at departmental research days when and where indicated.

The HSREC functions in compliance with, but not limited to, the following documents and guidelines: The SA National Health Act. No. 61 of 2003; Ethics in Health Research: Principles, Structures and Processes (2015); SA GCP(2006); Declaration of Helsinki; The Belmont Report; The US Office of Human Research Protections 45 CFR 461 (for non-exempt research with human participants conducted or supported by the US Department of Health and Human Services- (HHS), 21 CFR 50, 21 CFR 56; CIOMS; ICH-GCP-E6 Sections 1-4; International Council for Harmonisation (ICH) Harmonised Guideline, Integrated Addendum to ICH E6(R1), Guideline for Good Clinical Practice (GCP) E6(R2), 2016, SAHPRA Guidelines as well as Laws and Regulations with regard to the Control of Medicines, Constitution of the HSREC of the Faculty of Health Sciences.

For any questions or concerns, please feel free to contact HSREC Administration: 051-4017794/5 or email EthicsFHS@ufs.ac.za.

Thank you for submitting this proposal for ethical clearance and we wish you every success with your research.

Yours Sincerely

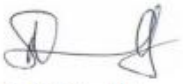

Prof. A. Sherriff
Chairperson: Health Sciences Research Ethics Committee

**Health Sciences Research Ethics Committee**
**Office of the Dean: Health Sciences**
T: +27 (0)51 401 7795/7794 | E: ethicsfhs@ufs.ac.za
IRB 00011992; REC 230408-011; IORG 0010096; FWA 00027947
Block D, Dean's Division, Room D104 | P.O. Box/Posbus 339 (Internal Post Box G40) | Bloemfontein 9300 | South Africa
www.ufs.ac.za

UNIVERSITY OF THE FREE STATE
UNIVERSITEIT VAN DIE VRYSTAAT
YUNIVESITHI YA FREISTATA

UFS·UV
HEALTH SCIENCES
GESONDHEIDSWETENSKAPPE

**Health Sciences Research Ethics Committee**

04-Mar-2022

Dear **Ms Mbasakazi Saki**

Ethics Number: UFS-HSD2021/1571-0002

Ethics Clearance: **The hepatoprotective effects of Moringa oleifera against antiretroviral induced cytotoxicity in HepG2 cells**

Principal Investigator: **Ms Mbasakazi Saki**

Department: **Basic Medical Sciences Department (Bloemfontein Campus)**

Submission Page

**SUBSEQUENT SUBMISSION APPROVED**

With reference to your recent submission for ethical clearance from the Health Sciences Research Ethics Committee. I am pleased to inform you on behalf of the HSREC that you have been granted ethical clearance for your request as stipulated below:

- Approval was granted for the M.Med.Sc. Research project to proceed in the Department of Basic Medical Sciences. The approval document from HSREC has been uploaded.
- The department has acquired the HepG2 cell line via Merck/Sigma. Unfortunately, there is a delay in permit approval from the Department of Health as well as a delay in availability and stock of the cell line. Please refer to the uploaded documents for details on permit application and order delay.
- To prevent a delay of the M.Med.Sc. Research project commencement, the Department of Medical Biochemistry and Chemical Pathology at the University of KwaZulu-Natal has kindly agreed to assist with providing the HepG2 cell line. The document confirming the approval and transfer of the HepG2 cell line from the University of KwaZulu-Natal has been uploaded.
- The research protocols' methodology of the M.Med.Sc. Project remains the same as originally approved by the HSREC.
- An updated Research Study Protocol has been uploaded.

The HSREC functions in compliance with, but not limited to, the following documents and guidelines: The SA National Health Act. No. 61 of 2003; Ethics in Health Research: Principles, Structures and Processes (2015); SA GCP(2020); Declaration of Helsinki; The Belmont Report; The US Office of Human Research Protections 45 CFR 461 (for non-exempt research with human participants conducted or supported by the US Department of Health and Human Services- (HHS), 21 CFR 50, 21 CFR 56; CIOMS; ICH-GCP-E6 Sections 1-4; International Council for Harmonisation (ICH) Harmonised Guideline, Integrated Addendum to ICH E6(R1), Guideline for Good Clinical Practice (GCP) E6(R2), 2016, SAHPRA Guidelines as well as Laws and Regulations with regard to the Control of Medicines, Constitution of the HSREC of the Faculty of Health Sciences.

For any questions or concerns, please feel free to contact HSREC Administration: 051-4017794/5 or email EthicsFHS@ufs.ac.za.

Thank you for submitting this request for ethical clearance and we wish you continued success with your research.

Yours Sincerely

Prof. A. Sherriff
Chairperson : Health Sciences Research Ethics Committee

**Health Sciences Research Ethics Committee**
**Office of the Dean: Health Sciences**
T: +27 (0)51 401 7795/7794 | E: ethicsfhs@ufs.ac.za
IRB 00011992; REC 230408-011; IORG 0010096; FWA 00027947
Block D, Dean's Division, Room D104 | P.O. Box/Posbus 339 (Internal Post Box G40) | Bloemfontein 9300 | South Africa
www.ufs.ac.za

**APPENDIX B:** HERBARIUM LETTER

SANBI
Biodiversity for Life

**KwaZulu-Natal Herbarium (NH)**
South African National Biodiversity Institute

P.O. Box 52099, Berea Road, 4007
South Africa
Tel: +27 31 2024095, Fax: +27 31 2023430
Email: KwaZulu-NatalHerbarium@sanbi.org.za

**Ref:** Plant Identification Dispatch List 19 January 2022

**Client:** Dr Charlette Tiloke
**Address:** Staff No. 0890138
University of the Free State
Department of Basic Medical Science

**Tel:**
**Cell:** 0845251340
**Email:** Tilokec@ufs.ac.za

**ID CODES:**
0 = No challenges
1 = Specimen too poor to ID
2 = Label information inadequate
3 = Cannot match specimen in herbarium
4 = Specialist not available to do ID
5 = Genus requiring/under revision
6 = Specimen closest to name listed (cf)
7 = Please send more material
8 = Please refer to attached note/letter
9 = New record

**FATE:**
K = specimen kept for herbarium
R = specimen returned
S = specimen scrapped

| | Collector | No. | Plant Name | Det. By | Det. Notes | ID Code | Fate |
|---|---|---|---|---|---|---|---|
| 1 | C. Tiloke | 2 | *Moringa oleifera Lam.* | Ngwenya, A.M. 19/1/2022 | | | |

**Curator**
**KwaZulu-Natal Herbarium (NH)**

Please note a handling fee is charged for each specimen received for identification. 1

## **APPENDIX C:** $HEPG_2$ CELL MORPHOLOGY

$HepG_2$ cells were exposed to three treatment groups and a control group. Figure 1 represents the morphology of the cells in response to acute (24-hour) and chronic (120-hour) treatment exposure.

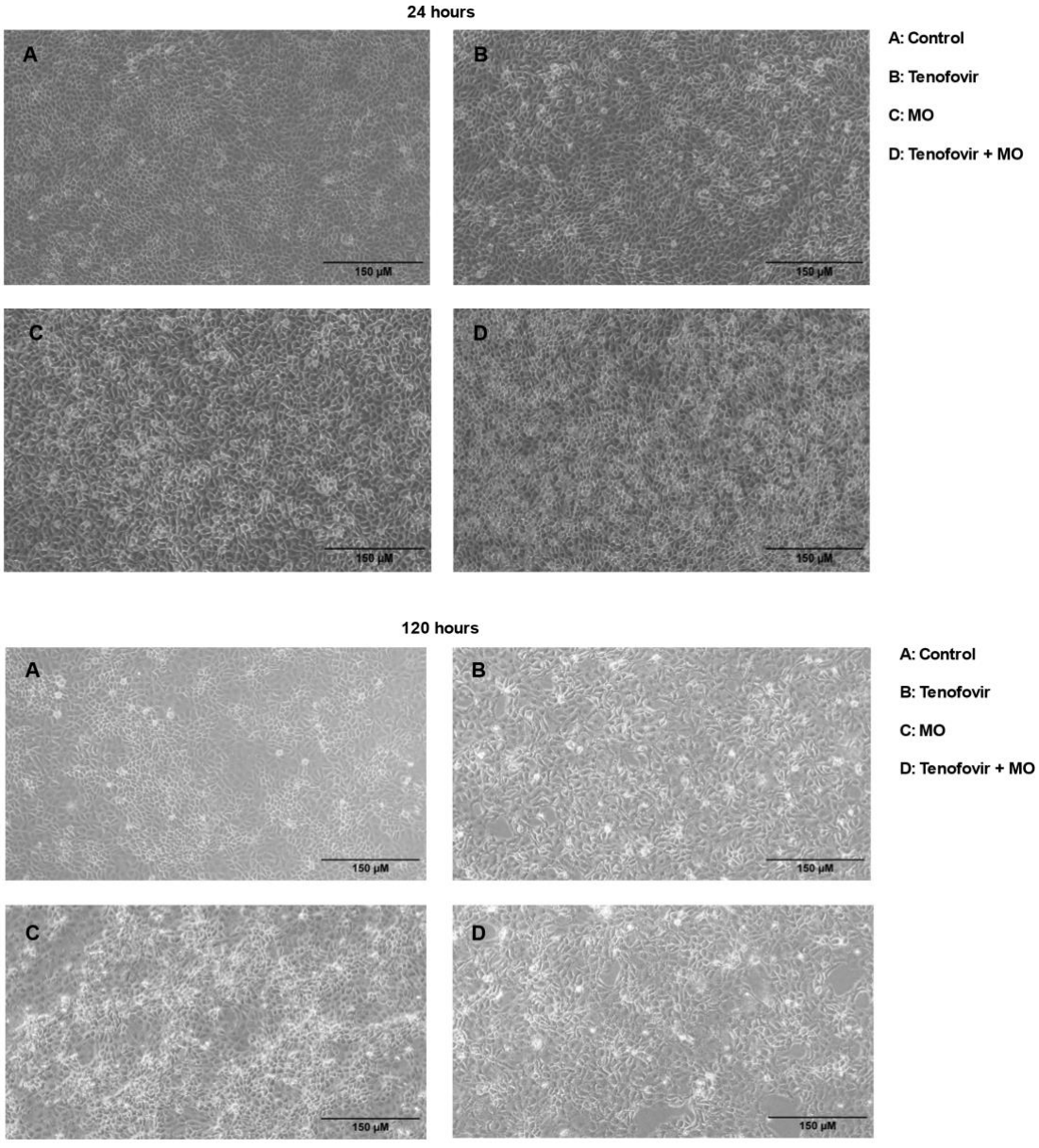


**Figure 1: $HepG_2$ cell morphology following acute (24-hour) and chronic (120-hour) exposure.** Scale bar of 150 µM, 100x magnification.

## **APPENDIX D:** SOD2 STANDARD REFERENCE CURVE

Figure 2 represents the quantification of the SOD2 activity standard reference curve.

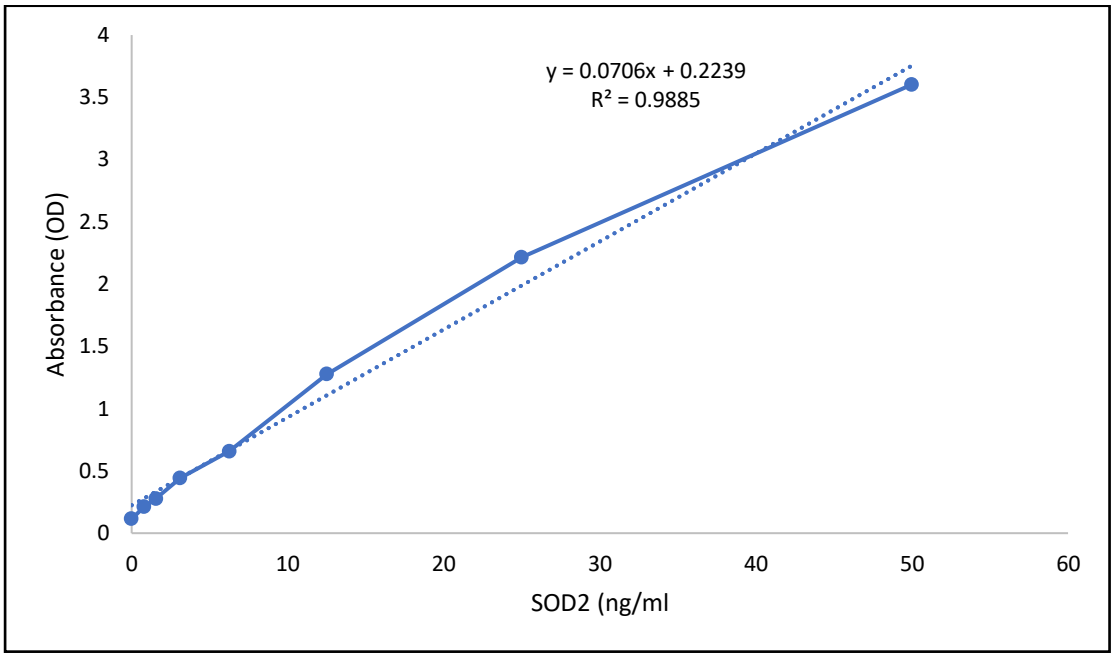


**Figure 2**: **Standard reference curve using a range of known SOD2 concentrations to quantify the concentration of SOD2 in the samples using ELISA.**

## **APPENDIX E:** CATALASE STANDARD REFERENCE CURVE

Figure 3 represents the quantification of the CAT activity standard reference curve.

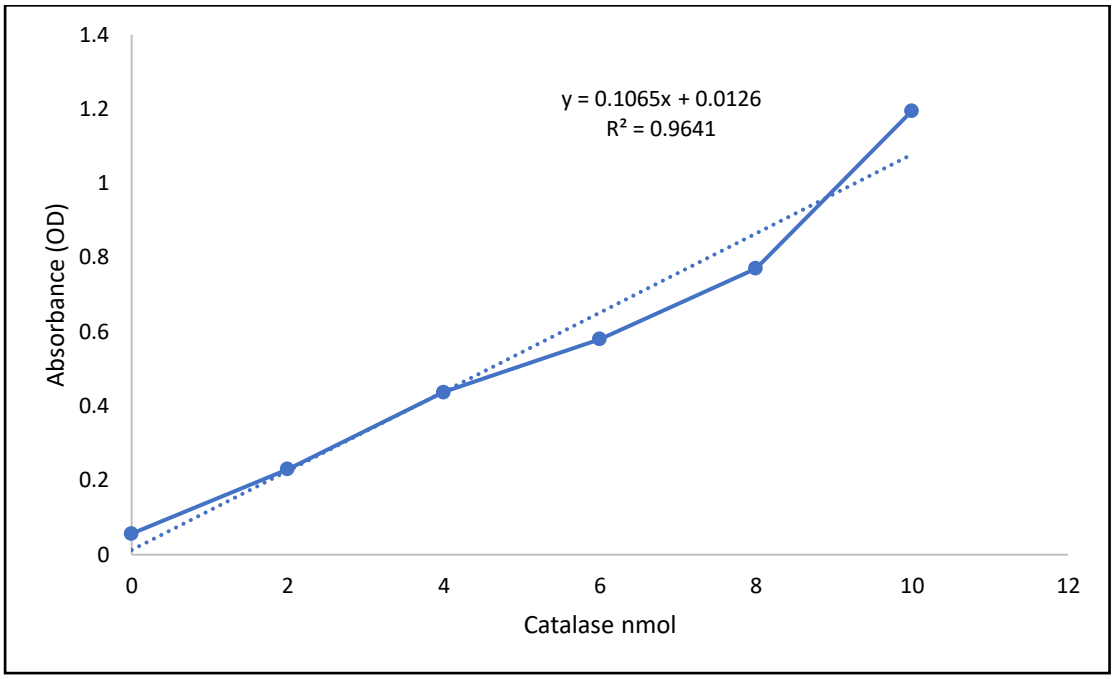


**Figure 3: Standard reference curve using a range of known CAT concentrations to quantify the concentration of CAT in the samples using ELISA.**

**APPENDIX F:** GSH STANDARD REFERENCE CURVE (24-HOUR)

Figure 4 represents the quantification of the GSH activity standard reference curve for the 24-hour treatment exposure time point.

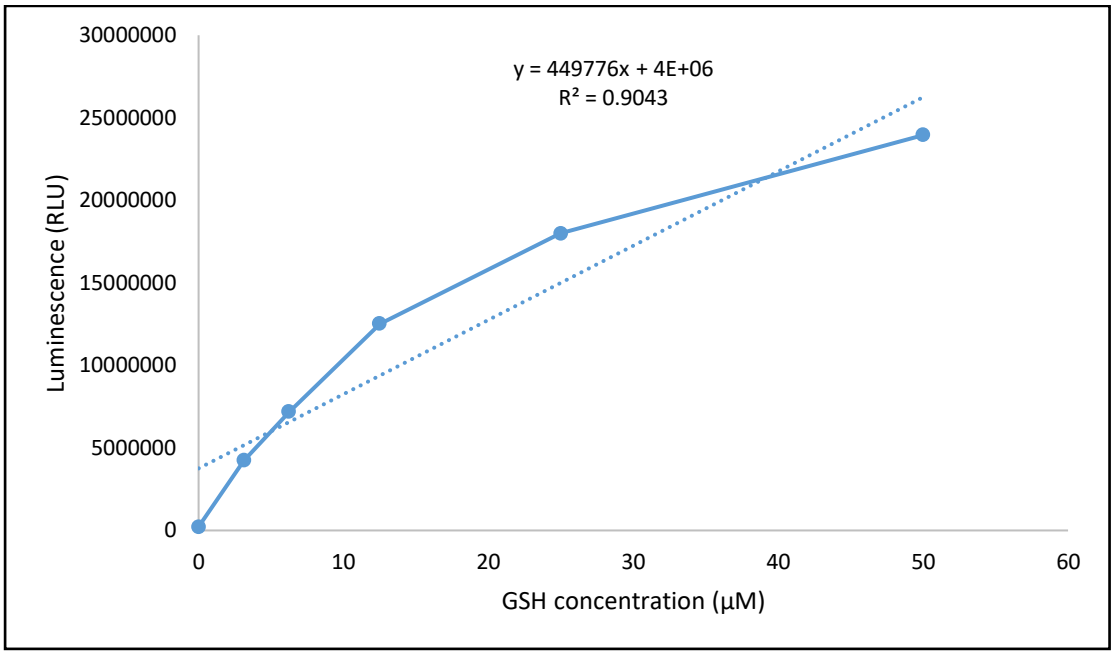


**Figure 4: Standard reference curve using a range of known GSH concentrations to quantify the concentration of GSH in the samples using luminometry.**

**APPENDIX G:** GSH STANDARD REFERENCE CURVE (120-HOUR)

Figure 5 represents the quantification of the GSH activity standard reference curve for the 120-hour treatment exposure time point.

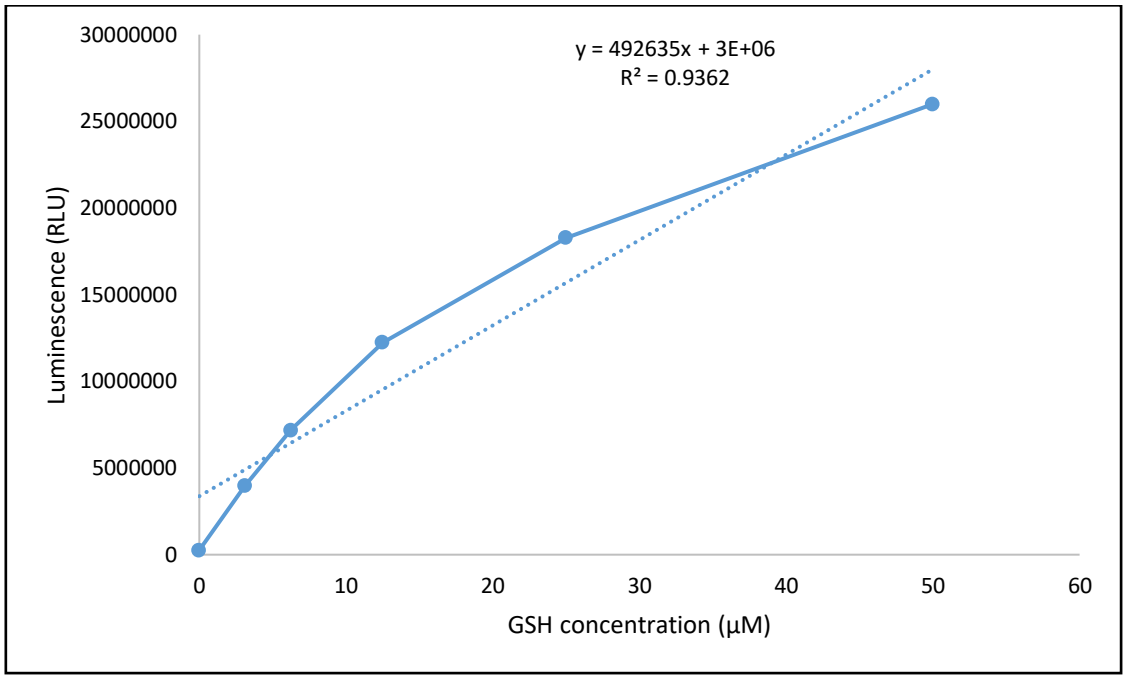


**Figure 5**: **Standard reference curve using a range of known GSH concentrations to quantify the concentration of GSH in the samples using luminometry.**

**APPENDIX H:** PROTEIN QUANTIFICATION

Figure 6 represents the protein quantification using bovine serum albumin (BSA).

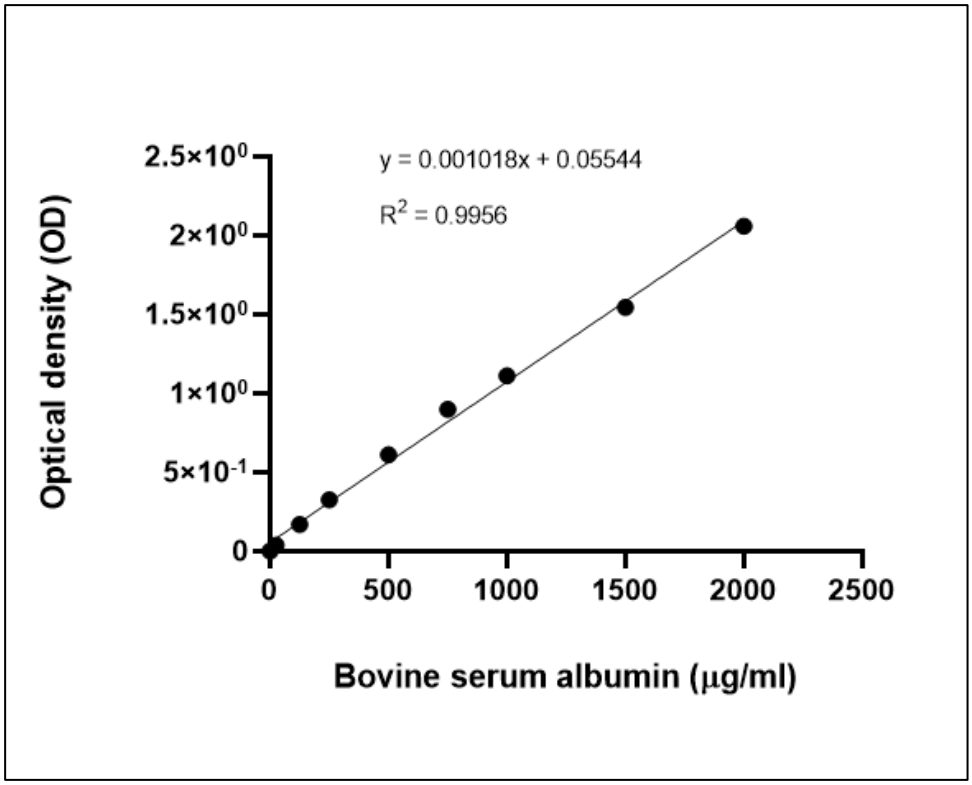


**Figure 6**: **Standard calibration curve using a range of known BSA concentrations to quantify sample protein concentration using the bicinchoninic acid assay.**

## **APPENDIX I:** HOECHST STAINING ASSAY

Hoechst staining assay analyzed live cells, typically measuring the DNA content of cultured cells and assessing mycoplasma contamination. Hoechst 33342 is a permeable blue, fluorescent nucleic dye used in fluorescent microscopy. It binds to adenine-thymine-rich DNA regions in the minor groove, and upon binding, the fluorescence increases. Uncontaminated cells show fluorescent nuclei, whereas mycoplasma-positive cells contain small cocci or filaments. Figure 7 represents the morphology of Hoechst-stained $HepG_2$ cells.

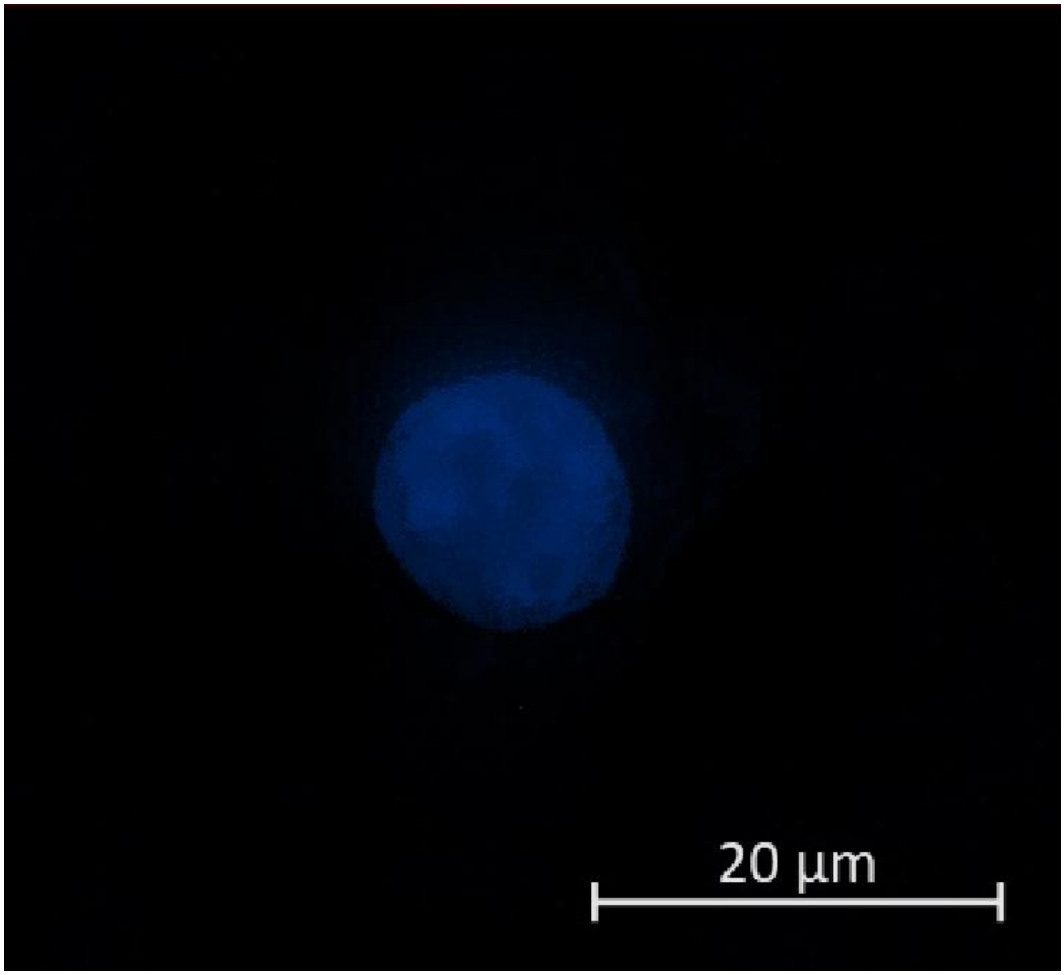


**Figure 7: Hoechst-stained $HepG_2$ cells.** Scale bar of 20 µM, 400x magnification.

**APPENDIX J:** LANGUAGE EDITOR LETTER


## LANGUAGE PRACTITIONER: Anneke-Jean Diesel

BA Communication Science (Corporate and Marketing Communications)*
BA Hons Communication Science (Corporate and Marketing Communications)*
* Cum Laude

17A Innes Avenue
Waverley, Bloemfontein

Tel: 084 244 8961
annekedenobili@gmail.com


July 2023

**DECLARATION**

I, Anneke-Jean Diesel, hereby declare that I did the language editing of the research of MBASAKAZI SAKI (title: *The hepatoprotective effects of Moringa oleifera against antiretroviral-induced cytotoxicity in HepG2 cells*). This research is submitted in fulfilment of the requirements of the degree Master of Medical Science (Physiology) in the Department of Basic Medical Sciences, School of Biomedical Sciences, Faculty of Health Sciences at the University of the Free State. All the suggested changes, including the implementation thereof, were left to the discretion of the student.

**Please note:**

The language editing did not include reference editing/checking or formatting. Also, the editor will not be held accountable for any later additions or changes to the document that the editor did not edit, nor if the student rejects/ignores any of the changes, suggestions or queries, which he/she is free to do. It remains the student's responsibility to ensure that the similarity index is according to the University's regulations. The editor can also not be held responsible for errors in the content of the document or whether or not the student passes or fails. It is the student's responsibility to review the edited document before submitting it for evaluation.

Sincerely

*SATI Registration #: 1003466*

**APPENDIX K:** Qubit™ RNA HS and IQ assay

Qubit™ RNA HS Assay Kit

Catalog number: Q32852

**Contents and storage**

| Component | Cat. No. Q32852 (100 assays) | Cat. No. Q32855 (500 assays) | Concentration | Storage[1] |
|---|---|---|---|---|
| Qubit™ RNA HS Reagent (Component A) | 250 µL | 1.25 mL | 200X in DMSO | 2°C to 8°C 2°C[2] Desiccate Protect from light |
| Qubit™ RNA HS Buffer (Component B) | 50 mL | 250 mL | Not applicable | ≤30°C |
| Qubit™ RNA HS Standard #1 (Component C) | 1 mL | 5 mL | 0 ng/µL in TE buffer | 2°C to 8°C [3] |
| Qubit™ RNA HS Standard #2 (Component D) | 4 × 250 µL | 10 × 500 µL | 10 ng/µL in TE buffer | |

[1] When stored as directed, kits are stable for 6 months.
[2] For long-term storage, the Qubit™ RNA reagent can be stored at ≤–20°C.
[3] For long-term storage, store the RNA standards at ≤–20°C or –70°C.

1. Thaw the RNA (50 µL) samples at room temperature.
2. Set up the required number of Qubit™ tubes for standards and samples. Only label the lid of the tube.
3. Prepare the Qubit™ working solution by diluting the Qubit™ RNA HS reagent 1:200 in Qubit™ RNA HS buffer. Use a clean conical tube each time you prepare Qubit™ working solution.
4. Add Qubit™ working solution to each tube. The final volume of working solution should be 200 µL in each tube. ***Read first the undiluted sample, if the concentration of the sample is too high (out of range), then dilute (1-5 µL).

| | Standard assay tubes | User sample assay tubes |
|---|---|---|
| Volume of working solution | 190 µL | 180–199 µL |
| Volume of standard | 10 µL | – |
| Volume of user sample | – | 1–20 µL |
| Total volume in each assay tube | 200 µL | 200 µL |

**Note:** The final volume in each tube must be 200 µL. Each standard tube requires 190 µL of Qubit™ working solution, and each sample tube requires anywhere from 180–199 µL. Ensure that you have sufficient Qubit™ working solution to accommodate all standards and samples. For example, for 8 samples, prepare enough working solution for the samples and 2 standards: ~200 µL per tube in 10 tubes yields 2 mL of working solution (10 µL of Qubit™ reagent plus 1990 µL of Qubit™ buffer).

**Calculations**

**To make enough working solution for the required number of standards and samples:**

- 2 standards are required.
- 5 tubes (1–5 µL) for each of the 8 samples are required.
- 5 x 8 = 40 tubes + 2 standard tubes = 42 tubes required.
- 42 tubes x 200 µL = 8 400 µL of working solution required.
- 1/200 = 0.005
- 0.005 x 8 400 µL = 42 µL of Qubit™ RNA HS reagent
- 8 400 µL – 42 µL = 8 358 µL of Qubit™ RNA HS buffer.

5. Add 10 µL of each Qubit™ standard to the appropriate tube. Then add 1–5 µL of each user sample to the appropriate tube.

***Each standard tube will have 10 µL of standard + 190 µL of working solution. For Sample tubes (1–5 µL):

- 1 µl sample + 199 µL of working solution

- 2 µl sample + 198 µL of working solution
- 3 µl sample + 197 µL of working solution
- 4 µl sample + 196 µL of working solution
- 5 µl sample + 195 µL of working solution

6. Vigorously vortex for 3–5 seconds.
7. Allow all tubes to incubate at room temperature for 2 minutes, then proceed to read standards and samples with the Qubit™ 4 Fluorometer:
    - Use the RNA high sensitivity programme to measure RNA concentration

Qubit™ RNA IQ Assay

Catalog No. Q33221

**Note:** The Qubit™ RNA IQ assay kit can only be used with the Qubit™ 4 Fluorometer. The RNA IQ assay does not work on the original Qubit™, Qubit™ 2.0, or Qubit™ 3 Fluorometers.

**Table 1.** Contents and storage

| Material | Amount | | Concentration | Storage* |
|---|---|---|---|---|
| | Q33221 (75 assays) | Q33222 (175 assays) | | |
| Qubit™ RNA IQ Reagent (Component A) | 2 × 100 µL | 10 × 100 µL | 200X concentrate in DMSO | • ≤–20°C<br>• Desiccate<br>• Protect from light |
| Qubit™ RNA IQ Buffer (Component B) | 40 mL | 200 mL | N/A | Room temperature |
| Qubit™ RNA IQ Standard #1† (Component C) | 850 µL | 2 × 1.5 mL | 0 ng/µL RNA in 1 mM citrate buffer | ≤–70°C |
| Qubit™ RNA IQ Standard #2† (Component D) | 850 µL | 2 × 1.5 mL | 100 ng/µL small RNA in 1 mM citrate buffer | |
| Qubit™ RNA IQ Standard #3† (Component E) | 4 × 225 µL | 10 × 300 µL | 100 ng/µL large RNA in 1 mM citrate buffer | |

* When stored as directed, the kits are stable for at least 6 months from the date of receipt.
† The RNA IQ assay kit standards are stable for shipment and short-term storage at ≤–20°C; long-term storage at ≤–70°C is recommended.
N/A: Not applicable

The Qubit™ RNA IQ Assay Kit provides a fast, simple method to check whether an RNA sample has degraded using the Qubit™ 4 Fluorometer. Results are presented as an RNA IQ number (RNA IQ#) that indicates the RNA sample integrity and quality, and also as a calculated percent of large and small RNA in the sample. The RNA IQ# is a value from 1 to 10, similar to other RNA quality scores, where a small number indicates that the sample is comprised of mainly small RNA fragments and a larger number indicates that the sample consists of mainly large RNA or RNA with tertiary structure.

1. Thaw the RNA samples prepared for the Qubit™ RNA HS Assay at room temperature.
2. Thaw the Qubit™ RNA IQ Assay solutions at room temperature.

3. Set up the required number of Qubit™ tubes for standards. The Qubit™ RNA IQ Assay requires 3 standards.
4. Label the tube lids.
5. Prepare the Qubit™ working solution by diluting the Qubit™ RNA IQ Reagent 1:200 in Qubit™ RNA IQ Buffer using 50 mL conical tube.

**Note:** The final volume in each tube must be 200 µL.

Calculations:

- 3 standard tubes x 200 µL = 600 µL working solution
- 1/200 = 0.005
- 0.005 x 600 µL = 3 µL reagent
- 600 – 3 = 597 µL buffer

6. Add 190 µL of Qubit™ working solution to each of the tubes used for standards.
7. Add 10 µL of each Qubit™ standard to the appropriate tube, then mix by vortexing 2–3 seconds. Be careful not to create bubbles.
8. Allow all tubes to incubate at room temperature for 2 minutes. Proceed to "Read standards and samples" with the Qubit™ 4 Fluorometer:
    - Use the RNA integrity and quality programme to measure RNA purity. Good RNA quality ranges between 1.6–1.8.

**APPENDIX L:** HIGH SENSITIVITY RESULTS

| **Treatment groups** | **Assay Name** | **Original sample conc.** | **Original sample conc. units** |
|---|---|---|---|
| 24 hour Control | RNA High Sensitivity | 154000 | ng/mL |
| 24 hour Ten | RNA High Sensitivity | 118000 | ng/mL |
| 24 hour MO | RNA High Sensitivity | 78200 | ng/mL |
| 24 hour Ten + MO | RNA High Sensitivity | 27200 | ng/mL |
| 120 hour Control | RNA High Sensitivity | 14140 | ng/mL |
| 120 hour Ten | RNA High Sensitivity | 8960 | ng/mL |
| 120 hour MO | RNA High Sensitivity | 8280 | ng/mL |
| 120 hour Ten + MO | RNA High Sensitivity | 7520 | ng/mL |

## **APPENDIX M:** RAW DATA

a. MTT Assay

| Concentration (mg/ml) | 0 | 0,1 | 0,5 | 1 | 1,5 | 2 | 2,5 | 5 |
|---|---|---|---|---|---|---|---|---|
| | **1** | **2** | **3** | **4** | **5** | **6** | **7** | **8** |
| **A** | 3,88E-01 | 3,71E-01 | 3,20E-01 | 1,99E-01 | 1,08E-01 | 6,82E-02 | 4,59E-02 | 4,12E-02 |
| **B** | 3,94E-01 | 2,10E-01 | 1,28E-01 | 1,96E-01 | 1,84E-01 | 1,55E-01 | 5,07E-02 | 3,96E-02 |
| **C** | 2,72E-01 | 1,84E-01 | 1,11E-01 | 1,98E-01 | 9,41E-02 | 7,24E-02 | 7,04E-02 | 4,18E-02 |

b. TBARS ASSAY

| | 24-hour | | | 120-hour | | | | | |
|---|---|---|---|---|---|---|---|---|---|
| | **1** | **2** | **3** | **4** | **5** | **6** | **7** | **8** | **9** |
| **A** | 1,78E-02 control | 1,91E-02 control | 1,97E-02 control | 1,63E-02 control | 1,92E-02 control | 1,93E-02 control | 5,50E-01 + Control | 5,74E-01 + Control | 5,84E-01 + Control |
| **B** | 2,00E-02 tenofovir | 1,72E-02 tenofovir | 1,65E-02 tenofovir | 2,06E-02 tenofovir | 1,84E-02 tenofovir | 2,23E-02 tenofovir | 2,61E-02 – Control | 2,29E-02 – Control | 2,60E-02 – Control |
| **C** | 1,83E-02 MO | 2,01E-02 MO | 1,99E-02 MO | 2,04E-02 MO | 1,96E-02 MO | 1,59E-02 MO | | | |
| **D** | 1,98E-02 Ten+MO | 1,79E-02 Ten+MO | 2,24E-02 Ten+MO | 1,79E-02 Ten+MO | 1,54E-02 Ten+MO | 1,76E-02 Ten+MO | | | |

c. ELISA: SOD2 activity

| | Standards | | Samples | |
|---|---|---|---|---|
| | **1** | **2** | **3** | **4** |
| **A** | 1,13E-01 | 1,17E-01 | 2,30E-01<br>Control (24hours) | 1,83E-01<br>Control (24hours) |
| **B** | 1,98E-01 | 2,23E-01 | 2,91E-01<br>Tenofovir (24hours) | 2,82E-01<br>Tenofovir (24hours) |
| **C** | 2,72E-01 | 2,82E-01 | 3,02E-01<br>MO (24hours) | 2,50E-01<br>MO (24hours) |
| **D** | 4,54E-01 | 4,32E-01 | 2,23E-01<br>Ten+MO (24hours) | 2,25E-01<br>Ten+MO (24hours) |
| **E** | 6,00E-01 | 7,15E-01 | 2,26E+00<br>Control (120hours) | 1,24E+00<br>Control (120hours) |
| **F** | 1,41E+00 | 1,14E+00 | 2,44E+00<br>Tenofovir (120hours) | 2,07E+00<br>Tenofovir (120hours) |
| **G** | 1,94E+00 | 2,49E+00 | 2,28E+00<br>MO (120hours) | 2,06E+00<br>MO (120hours) |
| **H** | 3,56E+00 | 3,65E+00 | 2,49E+00<br>Ten+MO (120hours) | 2,32E+00<br>Ten+MO (120hours) |

d. ELISA: Catalase activity

| | Standards | | samples | | | High control | | |
|---|---|---|---|---|---|---|---|---|
| | **1** | **2** | **3** | **4** | **5** | **6** | **7** | **8** |
| **A** | 0,04 | 0,04 | 0,08<br>Control (24hours) | 0,08<br>Control (24hours) | 0,08<br>Control (24hours) | 0,12<br>Control (24hours) | 0,11<br>Control (24hours) | 0,10<br>Control (24hours) |
| **B** | 0,07 | 0,07 | 0,09<br>Tenofovir (24hours) | 0,11<br>Tenofovir (24hours) | 0,10<br>Tenofovir (24hours) | 0,16<br>Tenofovir (24hours) | 0,09<br>Tenofovir (24hours) | 0,09<br>Tenofovir (24hours) |
| **C** | 0,08 | 0,09 | 0,10<br>MO (24hours) | 0,16<br>MO (24hours) | 0,10<br>MO (24hours) | 0,12<br>MO (24hours) | 0,19<br>MO (24hour) | 0,11<br>MO (24hours) |
| **D** | 0,10 | 0,14 | 0,10<br>Ten+MO (24hours) | 0,12<br>Ten+MO (24hours) | 0,13<br>Ten+MO (24hours) | 0,12<br>Ten+MO (24hours) | 0,14<br>Ten+MO (24hour) | 0,12<br>Ten+MO (24hours) |
| **E** | 0,10 | 0,18 | 0,10<br>Control (120hours) | 0,10<br>Control (120hours) | 0,12<br>Control (120hours) | 0,16<br>Control (120hours) | 0,14<br>Control (120hour) | 0,12<br>Control (120hours) |
| **F** | 0,14 | 0,10 | 0,15<br>Tenofovir (120hours) | 0,12<br>Tenofovir (120hours) | 0,12<br>Tenofovir (120hours) | 0,16<br>Tenofovir (120hours) | 0,13<br>Tenofovir (120hour) | 0,15<br>Tenofovir (120hours) |
| **G** | 0,09 | 0,13 | 0,12<br>MO (120hours) | 0,13<br>MO (120hours) | 0,12<br>MO (120hours) | 0,16<br>MO (120hours) | 0,16<br>MO (120hour) | 0,16<br>MO (120hours) |
| **H** | 0,06 | 0,05 | 0,09<br>Ten+MO (120hours) | 0,14<br>Ten+MO (120hours) | 0,15<br>Ten+MO (120hours) | 0,15<br>Ten+MO (120hours) | 0,16<br>Ten+MO (120hours) | 0,20<br>Ten+MO (120hours) |

e. qPCR

| PLATE 1: SOD2, GAPDH (57° C) | | | |
|---|---|---|---|
| Well/Set | Description | Gene | C(t) |
| A1 | 24 hr Control | SOD2 | 30,771 |
| A2 | 24 hr Control | SOD2 | 31,076 |
| A3 | 24 hr Control | SOD2 | 31,576 |
| A4 | 120 hr Control | SOD2 | 31,185 |
| A5 | 120 hr Control | SOD2 | 32,359 |
| A6 | 120 hr Control | SOD2 | 35,200 |
| B1 | 24 hr Tenofovir | SOD2 | 30,843 |
| B2 | 24 hr Tenofovir | SOD2 | 31,725 |
| B3 | 24 hr Tenofovir | SOD2 | 33,258 |
| B4 | 120 hr Tenofovir | SOD2 | 33,719 |
| B5 | 120 hr Tenofovir | SOD2 | 32,576 |
| B6 | 120 hr Tenofovir | SOD2 | 35,574 |
| C1 | 24 hr MO | SOD2 | 34,506 |
| C2 | 24 hr MO | SOD2 | 33,784 |
| C3 | 24 hr MO | SOD2 | 32,727 |
| C4 | 120 hr MO | SOD2 | 31,757 |
| C5 | 120 hr MO | SOD2 | 31,152 |
| C6 | 120 hr MO | SOD2 | 32,151 |
| D1 | 24 hr Ten + MO | SOD2 | 30,891 |
| D2 | 24 hr Ten + MO | SOD2 | 32,262 |
| D3 | 24 hr Ten + MO | SOD2 | 31,284 |
| D4 | 120 hr Ten + MO | SOD2 | 32,676 |
| D5 | 120 hr Ten + MO | SOD2 | 31,985 |
| D6 | 120 hr Ten + MO | SOD2 | 32,022 |
| | | | |
| A7 | 24 hr Control | GAPDH | 35,384 |
| A8 | 24 hr Control | GAPDH | 25,095 |
| A9 | 24 hr Control | GAPDH | 25,470 |
| A10 | 120 hr Control | GAPDH | 24,394 |
| A11 | 120 hr Control | GAPDH | 24,397 |
| A12 | 120 hr Control | GAPDH | 24,791 |
| B7 | 24 hr Tenofovir | GAPDH | 0,000 |
| B8 | 24 hr Tenofovir | GAPDH | 0,000 |
| B9 | 24 hr Tenofovir | GAPDH | 23,052 |
| B10 | 120 hr Tenofovir | GAPDH | 24,867 |
| B11 | 120 hr Tenofovir | GAPDH | 24,911 |
| B12 | 120 hr Tenofovir | GAPDH | 25,223 |
| C7 | 24 hr MO | GAPDH | 21,837 |
| C8 | 24 hr MO | GAPDH | 21,900 |

| | | | |
|---|---|---|---|
| C9 | 24 hr MO | GAPDH | 22,081 |
| C10 | 120 hr MO | GAPDH | 26,220 |
| C11 | 120 hr MO | GAPDH | 27,063 |
| C12 | 120 hr MO | GAPDH | 26,287 |
| D7 | 24 hr Ten + MO | GAPDH | 22,035 |
| D8 | 24 hr Ten + MO | GAPDH | 22,031 |
| D9 | 24 hr Ten + MO | GAPDH | 22,019 |
| D10 | 120 hr Ten + MO | GAPDH | 21,657 |
| D11 | 120 hr Ten + MO | GAPDH | 27,183 |
| D12 | 120 hr Ten + MO | GAPDH | 27,873 |
| | | | |
| | | | |
| | | | |
| PLATE 2: Nrf2, Catalase, GAPDH (58°C) | | | |
| Well/Set | Description | Gene | |
| A1 | 24 hr Control | Nrf2 | 31,713 |
| A2 | 24 hr Control | Nrf2 | 31,388 |
| A3 | 24 hr Control | Nrf2 | 30,673 |
| A4 | 120 hr Control | Nrf2 | 32,942 |
| A5 | 120 hr Control | Nrf2 | 33,174 |
| A6 | 120 hr Control | Nrf2 | 34,042 |
| B1 | 24 hr Tenofovir | Nrf2 | 32,544 |
| B2 | 24 hr Tenofovir | Nrf2 | 32,297 |
| B3 | 24 hr Tenofovir | Nrf2 | 31,469 |
| B4 | 120 hr Tenofovir | Nrf2 | 31,785 |
| B5 | 120 hr Tenofovir | Nrf2 | 34,061 |
| B6 | 120 hr Tenofovir | Nrf2 | 35,119 |
| C1 | 24 hr MO | Nrf2 | 32,679 |
| C2 | 24 hr MO | Nrf2 | 33,008 |
| C3 | 24 hr MO | Nrf2 | 32,543 |
| C4 | 120 hr MO | Nrf2 | 33,858 |
| C5 | 120 hr MO | Nrf2 | 34,365 |
| C6 | 120 hr MO | Nrf2 | 33,096 |
| D1 | 24 hr Ten + MO | Nrf2 | 33,287 |
| D2 | 24 hr Ten + MO | Nrf2 | 32,226 |
| D3 | 24 hr Ten + MO | Nrf2 | 32,266 |
| D4 | 120 hr Ten + MO | Nrf2 | 32,736 |
| D5 | 120 hr Ten + MO | Nrf2 | 33,951 |
| D6 | 120 hr Ten + MO | Nrf2 | 32,764 |
| | | | |
| A7 | 24 hr Control | GAPDH | 29,812 |
| A8 | 24 hr Control | GAPDH | 23,679 |
| A9 | 24 hr Control | GAPDH | 22,223 |
| A10 | 120 hr Control | GAPDH | 24,032 |

| | | | |
|---|---|---|---|
| A11 | 120 hr Control | GAPDH | 23,966 |
| A12 | 120 hr Control | GAPDH | 24,429 |
| B7 | 24 hr Tenofovir | GAPDH | 35,542 |
| B8 | 24 hr Tenofovir | GAPDH | 33,656 |
| B9 | 24 hr Tenofovir | GAPDH | 22,743 |
| B10 | 120 hr Tenofovir | GAPDH | 25,698 |
| B11 | 120 hr Tenofovir | GAPDH | 25,682 |
| B12 | 120 hr Tenofovir | GAPDH | 25,781 |
| C7 | 24 hr MO | GAPDH | 23,229 |
| C8 | 24 hr MO | GAPDH | 22,371 |
| C9 | 24 hr MO | GAPDH | 22,996 |
| C10 | 120 hr MO | GAPDH | 26,053 |
| C11 | 120 hr MO | GAPDH | 25,935 |
| C12 | 120 hr MO | GAPDH | 25,966 |
| D7 | 24 hr Ten + MO | GAPDH | 21,338 |
| D8 | 24 hr Ten + MO | GAPDH | 21,511 |
| D9 | 24 hr Ten + MO | GAPDH | 21,551 |
| D10 | 120 hr Ten + MO | GAPDH | 25,863 |
| D11 | 120 hr Ten + MO | GAPDH | 25,769 |
| D12 | 120 hr Ten + MO | GAPDH | 25,438 |
| | | | |
| E1 | 24 hr Control | Catalase | 30,303 |
| E2 | 24 hr Control | Catalase | 31,995 |
| E3 | 24 hr Control | Catalase | 32,051 |
| E4 | 120 hr Control | Catalase | 32,050 |
| E5 | 120 hr Control | Catalase | 32,484 |
| E6 | 120 hr Control | Catalase | 31,727 |
| F1 | 24 hr Tenofovir | Catalase | 32,899 |
| F2 | 24 hr Tenofovir | Catalase | 31,537 |
| F3 | 24 hr Tenofovir | Catalase | 31,528 |
| F4 | 120 hr Tenofovir | Catalase | 33,303 |
| F5 | 120 hr Tenofovir | Catalase | 33,517 |
| F6 | 120 hr Tenofovir | Catalase | 32,412 |
| G1 | 24 hr MO | Catalase | 31,827 |
| G2 | 24 hr MO | Catalase | 31,533 |
| G3 | 24 hr MO | Catalase | 31,867 |
| G4 | 120 hr MO | Catalase | 29,967 |
| G5 | 120 hr MO | Catalase | 29,486 |
| G6 | 120 hr MO | Catalase | 29,987 |
| H1 | 24 hr Ten + MO | Catalase | 30,168 |
| H2 | 24 hr Ten + MO | Catalase | 28,931 |
| H3 | 24 hr Ten + MO | Catalase | 28,831 |
| H4 | 120 hr Ten + MO | Catalase | 29,111 |
| H5 | 120 hr Ten + MO | Catalase | 29,395 |
| H6 | 120 hr Ten + MO | Catalase | 29,228 |

| | | | |
|---|---|---|---|
| | | | |
| PLATE 3: GCLC, GAPDH (59° C) | | | |
| Well/Set | Description | Gene | |
| A1 | 24 hr Control | GCLC | 28,595 |
| A2 | 24 hr Control | GCLC | 28,721 |
| A3 | 24 hr Control | GCLC | 29,088 |
| A4 | 120 hr Control | GCLC | 31,938 |
| A5 | 120 hr Control | GCLC | 33,051 |
| A6 | 120 hr Control | GCLC | 30,585 |
| B1 | 24 hr Tenofovir | GCLC | 28,619 |
| B2 | 24 hr Tenofovir | GCLC | 28,320 |
| B3 | 24 hr Tenofovir | GCLC | 28,862 |
| B4 | 120 hr Tenofovir | GCLC | 30,245 |
| B5 | 120 hr Tenofovir | GCLC | 35,036 |
| B6 | 120 hr Tenofovir | GCLC | 34,516 |
| C1 | 24 hr MO | GCLC | 29,783 |
| C2 | 24 hr MO | GCLC | 30,152 |
| C3 | 24 hr MO | GCLC | 29,987 |
| C4 | 120 hr MO | GCLC | 30,360 |
| C5 | 120 hr MO | GCLC | 29,936 |
| C6 | 120 hr MO | GCLC | 30,974 |
| D1 | 24 hr Ten + MO | GCLC | 29,633 |
| D2 | 24 hr Ten + MO | GCLC | 30,181 |
| D3 | 24 hr Ten + MO | GCLC | 30,078 |
| D4 | 120 hr Ten + MO | GCLC | 31,112 |
| D5 | 120 hr Ten + MO | GCLC | 31,151 |
| D6 | 120 hr Ten + MO | GCLC | 31,954 |
| | | | |
| A7 | 24 hr Control | GAPDH | 21,871 |
| A8 | 24 hr Control | GAPDH | 21,824 |
| A9 | 24 hr Control | GAPDH | 21,198 |
| A10 | 120 hr Control | GAPDH | 23,568 |
| A11 | 120 hr Control | GAPDH | 23,159 |
| A12 | 120 hr Control | GAPDH | 23,649 |
| B7 | 24 hr Tenofovir | GAPDH | 27,690 |
| B8 | 24 hr Tenofovir | GAPDH | 36,616 |
| B9 | 24 hr Tenofovir | GAPDH | 21,681 |
| B10 | 120 hr Tenofovir | GAPDH | 23,521 |
| B11 | 120 hr Tenofovir | GAPDH | 23,195 |
| B12 | 120 hr Tenofovir | GAPDH | 23,654 |
| C7 | 24 hr MO | GAPDH | 21,010 |
| C8 | 24 hr MO | GAPDH | 20,871 |
| C9 | 24 hr MO | GAPDH | 20,924 |

| | | | |
|---|---|---|---|
| C10 | 120 hr MO | GAPDH | 25,467 |
| C11 | 120 hr MO | GAPDH | 24,867 |
| C12 | 120 hr MO | GAPDH | 25,179 |
| D7 | 24 hr Ten + MO | GAPDH | 21,191 |
| D8 | 24 hr Ten + MO | GAPDH | 20,722 |
| D9 | 24 hr Ten + MO | GAPDH | 21,518 |
| D10 | 120 hr Ten + MO | GAPDH | 25,708 |
| D11 | 120 hr Ten + MO | GAPDH | 25,752 |
| D12 | 120 hr Ten + MO | GAPDH | 26,139 |

f. Western blot

Beta-actin raw data:

| Band Label | Adj. Volume (Int) |
|---|---|
| 24-hour control | 21212576 |
| 24-hour ten | 18820122 |
| 24-hour MO | 11681604 |
| 24-hour ten+MO | 9831800 |
| 120-hour control | 6106045 |
| 120-hour ten | 6983600 |
| 120-hour MO | 6645704 |
| 120-hour ten+MO | 10592856 |

SOD2 raw data:

| Band Label | Adj. Volume (Int) |
|---|---|
| 24-hour control | 141984 |
| 24-hour ten | 122716 |
| 24-hour MO | 313600 |
| 24-hour ten+MO | 438250 |
| 120-hour control | 221250 |
| 120-hour ten | 1127150 |
| 120-hour MO | 366991 |
| 120-hour ten+MO | 471954 |

Catalase raw data:

| Band Label | Adj. Volume (Int) |
|---|---|
| 24-hour control | 3112830 |
| 24-hour ten | 1211868 |
| 24-hour MO | 6200550 |
| 24-hour ten+MO | 10788344 |
| 120-hour control | 1935207 |
| 120-hour ten | 1895991 |

| | |
|---|---|
| 120-hour MO | 1977900 |
| 120-hour ten+MO | 3465660 |

NRF2 raw data:

| Band Label | Adj. Volume (Int) |
|---|---|
| 24-hour control | 3037728 |
| 24-hour ten | 1262762 |
| 24-hour MO | 2100758 |
| 24-hour ten+MO | 412560 |
| 120-hour control | 1942596 |
| 120-hour ten | 3537572 |
| 120-hour MO | 1997205 |
| 120-hour ten+MO | 4007104 |

p-NRF2 raw data:

| Band Label | Adj. Volume (Int) |
|---|---|
| 24-hour control | 20553 |
| 24-hour ten | 23192 |
| 24-hour MO | 20160 |
| 24-hour ten+MO | 55641 |
| 120-hour control | 17719 |
| 120-hour ten | 22032 |
| 120-hour MO | 50933 |
| 120-hour ten+MO | 42336 |